2013

INVESTIGATION OF USAGE OF VELOCITY AND PRESSURE DATA WITHIN A WATER DISTRIBUTION LAB MODEL FOR CALIBRATING HYDRAULIC MODELS

Robert Craig Ashby

University of Kentucky, superashby@Insightbb.com

Click here to let us know how access to this document benefits you.

INVESTIGATION OF USAGE OF VELOCITY AND PRESSURE DATA WITHIN A
WATER DISTRIBUTION LAB MODEL FOR CALIBRATING HYDRAULIC
MODELS

THESIS

A thesis submitted in partial fulfillment of the
requirements of the degree of Master of Science in Civil Engineering in the
College of Engineering
at the University of Kentucky

By:

Robert "Craig" Ashby
Lexington, Kentucky

Director: Dr. Scott Yost, Associate Professor of Civil Engineering
Lexington, Kentucky
2013

ABSTRACT OF THESIS

INVESTIGATION OF USAGE OF VELOCITY AND PRESSURE DATA WITHIN A
WATER DISTRIBUTION LAB MODEL FOR CALIBRATING HYDRAULIC
MODELS

Water distribution modeling for hydraulics and water quality is an important tool for managing system performance of water utilities. An important component of a water distribution model is the calibration of a network model with field data in the real world system. The calibration effort requires a protocol or selection criteria for the location of field measurements that best support the calibration effort. A water distribution model was constructed at the University of Kentucky hydraulics lab for the purpose of investigating the performance of water distribution models. The lab model contains numerous hydraulic (pressure, flows) and water quality (concentrations) sensors for measuring system characteristics. This research work utilizes the lab model to compare hydraulic calibration using pressure heads from hydraulic data, velocities from water quality data, and combinations of both as the basis of calibration. It also presents an example of a small experimental system where velocity data as a basis for a calibration effort and pressure based data as a basis doesn't converge to the same solution. The results of the research demonstrate the necessity of using both velocity & pressure data for hydraulic calibration to avoid compensating errors.

KEYWORDS: Hydraulic calibration, water distribution modeling, water distribution calibration, laboratory model hydraulic calibration, water network modeling

 Robert "Craig" Ashby

 5/2/2013

INVESTIGATION OF USAGE OF VELOCITY AND PRESSURE DATA WITHIN A
WATER DISTRIBUTION LAB MODEL FOR CALIBRATING HYDRAULIC
MODELS

By

Robert "Craig" Ashby

Dr. Scott Yost, Associate Professor of Civil Engineering

Director of Thesis

5/2/2013

Dr. Kamyar C. Mahboub, Ph.D., Lawson Professor of Civil Engineering

Director of Graduate Studies

5/2/2013

(DEDICATION)

Table of Contents

List of Tables

List of Figures

Chapter 1.   Introduction

Water distribution modeling is an important tool for the management and optimization of a water utility. A water distribution model can be created using information from construction plan sheets, other documentation on assets, and public information such as elevation data from USGS. Some of the information can be expected to be incomplete in some aspects and may contain errors. Since the ultimate goal of the computer model is to assist in water utility management decisions, a field calibration is typically required during the development of a computer water distribution model. The calibration effort's goal should both test and adjust the computer model to as accurately as possible represent the true field system flow and pressure characteristics during multiple system configurations within the network. The goal of this research is to examine the use of velocity data from tracer studies, pressure data for node measurements, and combination of both data types to examine calibration methodologies using an experimental laboratory scaled model of a water distribution system. Within the controlled laboratory setting, more data can be collected than can be during a field water distribution network calibration.

The hydraulic pipe network and experimental monitoring system utilized in this research was designed and constructed to function as a skeletonized scaled model of a medium-sized water utility. The laboratory model was constructed as a component of the larger NIHS research project (separate from the research presented in this work) to test water distribution computer algorithms ability to replicate network scenarios in multiple configurations in a laboratory model.   In the experimental model, there are a virtually unlimited number of different scenarios and conditions that can be placed upon the model network. In the context of the thesis research goal of examining hydraulic calibration of a network model, both flow and pressure measurements were made in multiple network configurations. In doing so, both hydraulic data from installed sensors and water quality data in the form of an injected conservative tracer were utilized to perform this calibration. In particular, calibration comparisons were made using either exclusively velocity based data from the arrival times of the "plug" from a conservative tracer or pressure based data, or combinations of both data types. The waveform in the time series plot, as measured by the electrical conductivity sensors, determined the arrival time of the tracer to the sensor. The pressure data is obtained by installed pressure sensors at each node.

Any research using experimental work requires an effort to maintain consistency in the methodology and testing techniques. The methodology for analyzing data and ensuring repeatability of experiments will be briefly presented in this report in the context of the primary topic of comparing hydraulic calibration using exclusively hydraulic data and exclusively water quality data.

1

The methods and information presented in this work represent the general guidelines and procedures utilized for maintaining quality and repeatability of experiments within the laboratory. The general procedures are presented briefly to illustrate the procedures used in hydraulic calibration comparison. The methodology does not represent a comprehensive procedure or protocol for every possible experiment that can be conducted using the physical laboratory model.

A brief overview of the physical model setup and components is presented within this work. Also included is a discussion and presentation of the experimental statistical and lab procedures, as well as an overview of the physical model setup used in the experimental work. These components are part of examining the research topic comparing hydraulic calibration using both water quality and hydraulic data. Three different calibrations will then be performed using exclusively measured pressure, measured velocity, or combinations of both. The research goal will then be to compare the results of the three calibrations. The examination will determine if the calibration process to minimize errors between modeled pressures to measured pressures will distort the velocities away from the measured velocity data. The examination will also perform a similar analysis to determine if only using velocity data and attempting to minimize the measured-to-modeled velocities in the network will distort the calculated pressures away from the measured pressures. The hypothesis of the research is that considering both pressure and velocities measurements and the differences between measured and modeled results for both pressures and velocities is necessary to successfully calibrate a network model. Using only pressure or velocity measurements is expected to distort the other feature (i.e., velocities in pressure only based calibration, and vice versa).

To investigate using pressure data as a basis of calibration and velocity data as a basis of calibration, the research used experimental results and simulations using a modeled water distribution system constructed at the University of Kentucky. Two network simulations, a branched and a looped system configuration, are tested and examined in network calibration.

Chapter 2. Literature review

2.1 Introduction

Calibration is the process of fine-tuning a model until it simulates the conditions in network as measured within an acceptable limit. (American Water Works Association, 2005, p. 56). Water distribution network hydraulic calibration is the adjustment of physical pipe resistance parameters (roughness, loss coefficients, and demand adjustments) within a computer model to most closely match a series of pressure, tank level, and/or velocity measurements taken within a real world water distribution model. The need for calibration arises because of statistical uncertainties involved in roughness coefficients from pump performance, valve performance, and pipe aging effects over time. In addition there are epistemic uncertainties involving user demands, the skeletonization process required for reducing a model to computational manageable system, and other unknown features present in the physical system. Estimates for those unknowns are typically assumed during model development based on statistical averages or typical literature values. Topographical errors between the model system and the real world system can create errors in the ability of the model to simulate the real world system. The plans and engineering drawings in the utility's records may not fully represent the final construction of the water system or site elevations. The data on a system required to create a network model may be incomplete, requiring assumptions to create a system model. The process of creating a model from engineering plans can create errors between the real world system due to measurement errors and tolerances between distances on a scaled map and real world distances. (HAESTAD METHODS, 2001) There may be differences between the nominal and actual diameters of a pipe. The differences may vary by manufacturer and construction technique of placement. The diameters may adjust over time from depositing and buildup along the pipe walls and thus may be contingent to the locality, age of the pipe, and the experiences of the system over time. Aggregating and grouping water usage at the junction nodes instead of actual locations produces minor differences between field performance of the network and modeling performance of the network. These possible errors and assumptions necessitate a water distribution model be checked using field data to verify and correct the network model's ability to replicate the true real world system.

The ultimate goal of network calibration is to have the best possible modeling tool for making operational and managerial decisions in the water distribution system. Individual calibration efforts should be targeted to the management issues or problem goal and deal with the challenges mentioned as source of possible error and uncertainty. Lindell and Lingireddy proposed a seven step process for model calibration. (Ormsbee & Lingireddy, "Calibrating hydraulilc network models", 1997)

1. Identify the intended use of the model
2. Determine initial estimates of the model parameters
3. Collect calibration data
4. Evaluate the model results
5. Perform the macro level calibration

3

6. Perform the sensitivity analysis
7. Perform the micro level calibration.

Ormsbee and Lingireddy state that for steady-state analysis of network modeling, calibration can be made using field data collected during different portions of the day. Pipe roughness is measured in the field using fire hydrants either via a parallel pipe method or two-hydrant method. Fire flow testing should be made using at least a drop of *5 psi* and preferable at least *20 psi* drop from the reference hydrant as the other hydrant is turned from the non-flowing to flowing condition. (Ormsbee & Lingireddy, "Calibrating hydraulilc network models", 1997) . The macro level calibration refers to the initial step of examining the data collected and modeled data for anomalies. If these anomalies are widely wrong or erroneously different, it is possible that something such as an improperly closed valve in the field and not closed within the model or other issue must be examined. The issue may need to be corrected prior to using a calibration algorithm and field data to calibrate the network to avoid erroneous calibration results. Otherwise, the micro calibration may be practically impossible or very difficult if the issue is unresolved. This macro calibration must be investigated before selecting the calibration groups using some sensitivity analysis to determine data collection locations. Also calibration groupings should be checked before major roughness parameters to calibrate are selected. In some cases, the initial field data collection may lead to a sensitivity analysis where it is realized that additional data is required before attempting the hydraulic calibration of the network model (micro calibration step).

2.2 Practical considerations for site selection

Many practical problems are noted in M32 manual "Computer Modeling of Water Distribution Systems" from AWWA on the topic of site data collection. Velocity heads cause errors near pumps since the velocity head at a pump flange is converted to pressure in larger pipes leaving a pump station. (American Water Works Association, 2005, p. 59). The measured pressure head at a pump flange must be added to velocity head before comparing with a modeled pressure head at the pump outlet. Another potential problem is that two identical pumps from the same manufacturer may have quite different pump curves contingent to their individual service life experience and in slight variance from a manufacturer's pump curve. (American Water Works Association, 2005, p. 59) Another issue of importance from a calibration perspective is that matching pressure HGLs without considering flows or vice versa is not acceptable. (American Water Works Association, 2005, p. 56) It is important to have both data types because errors can cause incorrect flows in the model to produce correct pressures, and vice versa, as compensating errors. The model would appear to be correctly calibrated in this instance; however it is really not calibrated. Calibration problems are typically under constrained and thus exact best global solutions are difficult to determine. The optimization problem is highly nonlinear and also not well posed. This requires limiting the number of pipe roughness values adjusted to at most the number of measurements made. A simple case is presented by Walski, et. al showing that multiple C-factors can correctly match the pressure drop across a simple two pipe branch if only the total system flow is known, the

total flow in one of the two pipes must be known for a unique calibration solution (HAESTAD METHODS, 2001, p. 204).

Walski notes that for the case of low flows or low pressure drops, field data measurements for roughness may prove useless. (Walski, "Model calibration data: the good, the bad, and the useless", 2000). He presents the case where the errors in flows and pressure drop measurements when combined into a head loss measurement may have a composite error on the same order of magnitude as the total head loss measurement. Avoiding this leads to the ideal testing scenario being done at the highest pressure drop and highest flow demands possible. However in practice it may not be possible to create a high enough pressure drop and flow combination due to the requirements for maintaining safety and service within the water distribution system during field data collection. Walski, after illustrating the problem, presents some best practices for remedying the issue of too low flows or low pressure drops yielding roughness values that are on order of magnitude with the errors involved with the measurements (Walski, "Model calibration data: the good, the bad, and the useless", 2000). Walski recommends using higher quality elevations over the typical *20 ft* USGS contours maps to minimize the elevation errors in calibration. He further recommends using pressure gauges as accurate to *1 psi* or better, using HGL units to compare model and field values over pressure units and flow units, and to avoid pressure measurements near boundary head locations.

2.3 Optimal sampling design for water distribution calibration

As illustrated above, the determination of sites for data collection is a vital component of a calibration effort. The most sensitive locations within the model should be selected so that the data collected can make the greatest contribution to the calibration of the network components not measured. Conversely, the site of data measurement must be stable enough so that volatility in the site combined with a limited sampling size does not bias the calibration of the larger network. There must be some tradeoff between selecting the most sensitive locations for measurement and the need for stability at a location for accurate and precise measurements. Using entropy theory, Do Guen Yoo, found numerically that pipe nodes with a relatively high flow demand tend to have relatively high "giving entropy" (Yoo, Chang, & Jun, 2012). This numerically coincides with Walski's suggestion of high demand locations being the optimal locations for pressure gauge location for calibration and other system management issues (Walski, "Technique for calibrating network model", 1983). Essentially high "giving entropy" for a site means changes in the variation in a time series of the measurements at a site tend to correlate with changes in the time series of measured values at other pipes. A site with high "receiving entropy" has properties that are highly sensitive to neighboring sites properties. If of high quality, measurements at a high "receiving entropy" site can reveal the states of neighboring sites. If of high quality, measurements at high "giving entropy" site can restrict the unknown states of the neighboring sites to a smaller bandwidth of possibilities. Do Guen Yoo thus states that the best locations of pressure gauges are at nodes with both high GE & RE values (giving and receiving entropy) for energy head in

comparison with the other nodes in the network. The approach by Yoo, can be used to both determine the best locations for data collection and identifies "linkages" between junctions and pipes for segmenting pipes into calibration groupings. Other methods, such as D-optimality (FOSM), use a similar theoretical logic of determining the best combinations of sample sites by comparing the covariance of changes in parameter estimates at a node to other different site node changes (Uber & Bush, 1998). The FOSM method essentially develops a parameter covariance matrix from the Jacobean of model predicted values with respect to each independent parameter (Kapelan, Savic, & Walters, "Optimal Sampling Design Methodologies for Water Distribution Model Calibration", 2005). Both approaches use a priori assumption of measurement variance and results from the non-calibrated model. Also both assume that the physical real world nodal relationships (entropy or correlations) are approximately similar to the pre-calibrated system. Thus there is an assumption of statistical analysis of covariance and entropy in the pre-calibrated model relationships between nodes is approximately true for the real system. They also assume a constant variance, which is not contingent on the pressure at a location and does not change very significantly at different pressures at the location.

2.4 Numerical methods for water distribution calibration

The micro calibration step (hydraulic calibration), in the seven step process by Ormsbee, can be done using various numerical methods and techniques to solve the nonlinear optimization problem. Several numerical methods have been investigated for solving the problem of calibrating a network model to fit site specific measurements within the real world system. Ormsbee proposed an explicit method for the solving the matrix of energy and continuity equations relationships between nodes, paths, and loops by converting the nonlinear conservation of energy equations into a linear system of equations using Newton's method. (Ormsbee & Wood, "Explicit Pipe Network Calibration", 1986). Implicit methods have also been developed to estimate parameters of hydraulic network models by Ormsbee (Ormsbee & al, "Implicit Network calibration", 1989) and Lansey (Lansey & al, "Parameter Estimation for Water Distribution Networks", 1991). In the implicit methods, both the current step and following step are related and require iterations which must be solved before the algorithm can be processed into the next step. The next step will also require iterations with the following step. In explicit method the solution of the system of equations is directly solved, in a forward process which is independent of following steps, at least in an approximate sense using linearization techniques. The sum of the error norms between the measured values and model values are minimized in an attempt to find the approximation of best fit in both implicit and explicit methods.

Both implicit methods and explicit methods utilize gradient based approaches to solve the optimization problem. Gradient based methods are generally faster than stochastic methods, but are more difficult to formulate because analytical expressions must be derived or gradient must be approximated (HAESTAD METHODS, 2001, p. 215). A type of stochastic calibration algorithm is the genetic algorithm, and is quite popular in the engineering literature for hydraulic calibration of network models.

Various genetic algorithms are the state–of-the-art for network calibration over older implicit or explicit methods of network calibration in the literature. These algorithms rely on the collective learning process within a population of individuals, each of which represents a search point in the space of potential solutions (Walters, Savic, & Godfrey, 1997). Genetic algorithms attempt to replicate natural selection processes by creating a random assortment of possible solutions for calibration and using a fitness criterion to determine the best solutions for further exploration. The various genetic algorithms also attempt to "breed" solutions together in an attempt to create superior hybrid solutions using the fitness criteria as a basis for determining the probability of how widely a solution "breeds" with other solutions based on the solution's fitness score. The genetic algorithms include a mutation process to randomly adjust a solution's genes as an additional component of iterating to an optimal solution. As stated by Pedro L. Iglesias, the mutation process is a parameter which is not convenient to abuse; since it is both a generating mechanism of diversity, but also it reduces the genetic algorithm to a random search and thus can significantly reduce computational speed if the mutation parameter is too large (Iglesias, Mora, Martinezr, & Fuertes, 2007).

2.5 Objective functions for optimal network calibration

A critical component of micro calibration step (network calibration) is the objective function used for determining the pipe roughness parameters that best fit the physical field measurements of the real system. Regardless of the methodology of the algorithm type used, an objective function must be defined to determine the optimum solution. The gradient based explicit or implicit method, genetic algorithm, or other algorithm approach seeks to find the minimum (or maximum) of the objective function. An objective function as presented by Lansey is a combined least square difference between energy heads of observed and modeled predicted flows; tank levels, and pressures (Lansey, El-Shorbagy, Araujo, & Haan, 2001).

$$J_{min} = \Sigma_{i=1}^{LOAD} \left[\Sigma_{i=1}^{n_p} w_P \left(P_{i,obs} - P_{i,pred} \right)^2 + \Sigma_{i=1}^{n_Q} w_Q (Q_{i,obs} - Q_{i,pred})^2 + \Sigma_{i=1}^{n_T} w_T (T_{i,obs} - T_{i,pred})^2 \right]$$

$$(1)$$

where

J_{min} = Least Squares of the observed and modeled pressures, flows, and tank levels in terms of energy head. w_p =the square of the conversion factor of pressures to pressure head

w_P = the square of the conversion factor of pressures to pressure heads

w_Q = the square of the conversion factor of flows to velocity heads

w_T =the square of the conversion factor of tank levels to tank levels in *ft*.

n_p = number of observed measurements for each pressure head group

n_Q = number of observed measurements for each velocity head group

n_T = number of observed measurements for each tank levels

LOAD = Number of test periods or test simulations that field data has been collected under.

$P_{i,obs}$ = pressure observed at location *i*

$P_{i,pred}$ = pressure modeled at location i
$Q_{i,obs}$ = flow observed at location i
$Q_{i,pred}$ = flow modeled at location i
$T_{i,obs}$ = tank level observed at location i
$T_{i,pred}$ = tank level modeled at location i

      A similar objective function is presented by Zheng as Eq. 2 (Zheng Y. Wu, 2009). The objective function is normalized by two weighting factors. The P_{pnt} term is the hydraulic head per fitness point and Q_{pnt} term is the flow per fitness point.   The terms are used to convert pressure and flow differences into dimensionless values. The P_{pnt} term can be the average pressure for the *NH* points of pressure measurements or the maximum pressure for the *NH* points of measurements for the purposes of converting to a dimensionless measurement value (Zheng Y. Wu, 2009).   The Q_{pnt} term is similar but for flows measurements within the network. The w_i term is an additional weighting term for each of *NP* points of pressure measurements as the ratio of head loss at the ith point and the sum of the head losses at all *NP* points. The *NP* term is the number of observed measurements as stated in Eq. 2. The w_k term is an additional weighting term for each of *NQ* points of flow measurements as the ratio of flow at the kth point and the sum of the flows at all *NQ* points. Equation two presents the objective function in terms of the l_2 norm, sum of the squares, for the difference between observed and model predicted pressure and flow measurements. Zheng also presents an objective function for the l_1 norm, sum of the absolute value, for the difference between observed and model predicted pressure and flow measurements.

$$F(\vec{X}) = \sum_{j=1}^{T}\left[\frac{\sum_{i=1}^{NP}\left[w_i\left(P_{pnt}*(P_{s,i}-P_{o,i})\right)^2\right]+\sum_{k=1}^{NQ}\left[w_k\left(Q_{pnt}*(Q_{s,k}-Q_{o,k})\right)^2\right]}{NP+NQ}\right] \tag{2}$$

where

w_i = the weighting ratio from dividing the measured pressure at location i by the sum of the measured pressures at all locations.
w_k = the weighting ratio from dividing the measured flow at location k by the sum of the measured flows at all locations.
NP = the number of observed measurements for each pressure head group
NQ = the number of observed measurements for each velocity head group
P_{pnt} = the conversion factor required to convert pressures into pressure heads.
P_{pnt} = the conversion factor required to convert flows into velocity heads.
$P_{s,i}$ = the modeled pressure at location i
$P_{o,i}$ = the observed pressure at location i
$Q_{s,k}$ = the modeled flow at location k
$Q_{o,k}$ = the observed flow at location k

The objective function formulation presented in Eq. 3 is normalized similar to the Zheng presented formulation except that the variance of the measurement data at the measurement location is used (Shanmugam, Narasimham, & et-al., 2010). However the measurement types are made dimensionless by dividing by the maximum roughness value for pipe roughness. The pressures are made dimensionless by dividing pressures by the pressure at the source (supply pressure from pump, reservoir). The flows are also made dimensionless by dividing the flows by maximum flow values. The error in the equation is presented in terms of the l_2 norm for the difference between observed and model predicted pressure and flow measurements.

$$\varphi = \sum_{i=1}^{N_p}\left[\frac{(P_{Obs,i}-P_{pred,i})^2}{\sigma_i^2}\right] + \sum_{j=1}^{N_Q}\left[\frac{(Q_{Obs,j}-Q_{pred,j})^2}{\sigma_j^2}\right] + \sum_{k=1}^{N_O}\left[\frac{(O_{Obs,k}-O_{pred,k})^2}{\sigma_k^2}\right] \tag{3}$$

where

σ_x = Standard deviation of the measurement class at site i, j, and k respective measurement points.
$P_{y,i}$ = Pressures observed (y=obs) and model predicted (y=pred) at location i
$Q_{z,j}$ = Flows observed (z=obs) and model predicted (z=pred) at location j
$O_{w,k}$ = Outflow water use demands observed (w=obs) and model predicted (w=pred) at location k.

A slightly different approach for an objective function for calibration of a water network distribution system is presented by Greco, et al. (Greco & Guidice, 1999), as Eq. 4. In this particular approach, instead of minimizing the sum of square errors between observed and modeled measurements, the formulation is presented as minimizing the amount of deviations of pipe roughness values away from typical literature values for pipe roughness. The constraints of the minimization problem are that the modeled and measured pressure at each measurement location is below a maximum tolerance based on the volatility of instrument and estimated experimental errors at each site. Equation4 presents the formulation of the network calibration problem presented by Greco, et al. While the paper presented the calibration routine working only with pressure data, the author stated that flow measurements could be handled in a similar fashion within the same objective function $f(\varepsilon)$ with the flow measurements added to the j inequality constraints.

$$\min f(\varepsilon) = \sum_{i=1}^{N}(\varepsilon_i - \varepsilon_{assumed\ literature\ value\ at\ i})^2 \tag{4}$$

where

$$\left|P_{modeled\ at\ j} - P_{measured\ at\ j}\right| \leq imposed\ maximum\ tolerance\ at\ jth\ point$$

$$\forall j\ measurement\ locations$$

ε_i = roughness value modeled for location i

      Tabesh, et al. presented a formulation of the objective function of the calibration problem that is presented as Eq. 5 (Tabesh, Jamasb, & Moeini, 2011). This formulation, like Eq. 2, is both normalized and made dimensionless. The normalization takes the form of dividing the errors between measurement value and modeled value at the point before squaring. The weighting factors (W_p and W_q) weight the relative individual measured to modeled errors by the relative size of the head loss or flow measured at a location to the total head losses and flows measured, respectively.

$$\min f(x) = \sum_{j=1}^{N_p}\left[W_p\left(\frac{P_{measured\,j}-P_{modeled\,j}}{P_{measured\,j}}\right)^2\right] + \sum_{j=1}^{N_q}\left[W_q\left(\frac{Q_{measured\,j}-Q_{modeled\,j}}{Q_{measured\,j}}\right)^2\right] \quad (5)$$

$$W_p = \frac{H_{measured\,loss,j}}{\sum_{j=1}^{N_p}\left(H_{measured\,loss,j}\right)}$$

$$W_q = \frac{Q_{measured\,loss,j}}{\sum_{j=1}^{N_q}\left(Q_{measured\,loss,j}\right)}$$

where

N_p = number of pressure measurement sites
N_q = number of flow measurement sites
P = Pressure, psi, modeled or measured
Q = Flow, gpm, modeled or measured
W_p = weighted conversion factor for pressures, using the above equation
W_Q = weighted conversion factor for flows, using the equation

      Each of the formulations of the calibration objective functions from the literature review assumes that pressure and flow residual errors can be combined into a single objective function. The assumption is that pressures and velocity/flow errors can be added either as normalized and made dimensionless or by converting the flows and pressure into the same unit head. The literature review does not consider that using the pressure data as a basis of calibration may lead to different calibration results if utilized separately from the flow data or velocity data as a basis of calibration. If the demands are fixed during the calibration procedure and the energy inputs into the system by the reservoirs and pumps are fixed during the calibration procedure, then the system during calibration should have relatively the same energy state. Intuitively from this it can conjectured that discrepancies can develop in velocity heads from adjusting the pressure heads to better correspond to measured pressure values and vice versa. Much research work with calibration algorithms solves calibration problems within networks using only pressure based field data measurements when testing the algorithms.

Chapter 3.   General Laboratory System Information

The pipe network was designed to serve as a rudimentary scaled model of a moderately sized water utility. The network is complete with a water supply reservoir, storage tanks, and demand nodes. The final constructed model consists of approximately *470 feet* of PVC pipe, *10* demand nodes, and *3* storage tanks. The system network is supplied with a *900 gallon* reservoir and *3 horsepower* pump that can deliver up to *120 GPM* to *10* demand nodes and *3* different storage tanks.

The system is also equipped with a DATAQ data acquisition system consisting of *44* different sensors that monitor and record the pressure, flow, conductivity, and water level at various points in the system network.   A brief overview is of the physical components follows.

3.1 Physical components:

3.1.1 Tanks

There are three *110 gallon* tanks located approximately *17 feet* above the laboratory floor. These are used to simulate the actual operation of water storage tanks within a typical water utility system. If they are allowed to fill, they can pressurize and feed the system without the assistance of the pump. When studying particular dynamics or conditions of flow, it is generally useful to try and keep the system in a steady state condition. This can generally be governed by keeping the tank levels constant.

Each tank also possesses an overflow line that will allow water to flow out of the tank and back into the reservoir. The overflow level in each tank is about *32 inches* above the bottom of the tank. This level was monitored carefully when collecting in order to avoid ambiguity about whether or not the tanks are overflowing and whether or not water was physically flowing into or out of the tank lines. Figure 3.1 illustrates the middle tank within the lab model; the overflow line in the tank is visible in the figure.

Figure 3.1 Tank "T3"

3.1.2 Reservoir

The reservoir is located underneath the the pipe network. The reservoir can hold up to *900 gallons* of water. The reservoir level was therefore generally maintained at about 1 foot from its full height *(~5 ft.)* when not in operation. The level of water in the tanks was kept above a *1.5 ft.* minimum depth in order to reduce the possibility of pump cavitation. The reservoir is fed via two collection lines that return water flowing out of the system from the various outlets thus the water volume is fully conserved within the experimental apparatus. Figure 3.2 shows the reservoir for the laboratory model.
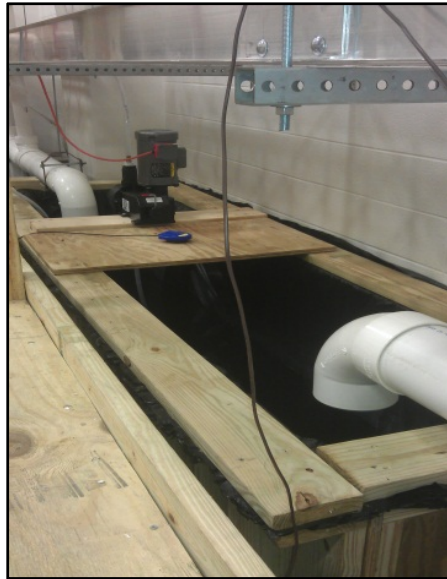
Figure 3.2 Supply reservoir

3.1.3 Pump

The pump used to supply the model distribution system is a three horsepower Grundfos model CR 20. The pump has a rated flow of *102 gpm* and a rated head of *52.8 ft*. The pump is located on the ground adjacent to the reservoir and is connected by approximately *1.5 ft.* section of a *2 in* diameter PVC pipe with flanged connections. Downstream of the pump, there is a *2 in* brass gate valve that can be used to adjust the total amount of flow being fed into the system from the reservoir. There are also two tee joints that can be fitted with sensors or valves for injection or monitoring purposes. The tee joints were both directly upstream and downstream of the pump. The pump is illustrated in Figure 3.3.

Figure 3.3 Network supply recirculating pump

3.1.4 Data acquisition system

The data collection system consists of a series of sensors and meters that monitor pressure, flow, water levels in the tanks and reservoir, and electrical conductivity. Figure 3.4 provides photography of the instruments. All of these instruments and their variables can be monitored and recorded through the Lab View software. All data from every experiment is automatically saved to a test specific text file. The program allowed the experimental team to monitor any parameter of the system using time series plots and tables as the data was collected and continuously written to a text file. The instruments within the laboratory model are presented in Fig. 3.4.

(A)

(B)

(C)

(D)

Figure 3.4 Various sensors: (a) Water level meter; (b) Conductivity sensor; (c) Flow meter; (d) Pressure sensor.

3.1.5 Control valves

Ball valves provide a simple means of opening and closing a pipe segment. They are useful for establishing different conditions and flow patterns within the system, as well as rerouting water away from sections of the network.

The network was constructed with *10* different demand nodes and *3* tanks, each of which contains a flow meter and a gate valve. Each gate valve allows the user to adjust the amount of flow passing through a pipe, and hence act as the primary flow control within the network. During the course of the experiments, the turn settings as the number of full turns and number of *1/8th* turns from fully open was recorded in the experiment's notes.

3.1.6 Injection check valve

A check valve's basic functionality allows flow to proceed in one direction through it. The particular check valve in the model used for injection experiments involving the Omni injection pump is illustrated in Fig. 3.5. This three-way valve was equipped with two hoses; the vertical hose attached to the top provides the injecting fluid from the Omni pump while the other hose protruding from the side serves as the release. The purpose of this configuration is to get water all the way to the injection point prior to beginning the experiment so that the actual injection into the system and the collection of data can be as exactly as possible synchronized in time. This will be accomplished by directing the injecting fluid to the release hose first so that the fluid can fill the line completely and once redirected, can immediately begin feeding into the actual system. Figure 3.5 illustrates the injection check valve as it is located near the main distribution line in the laboratory model.

Figure 3.5 Injection line flow control valve

3.1.7 Injection pump

One of the primary purposes of this research is to trace and study the flow of contaminants within a pipe network and use this data for better hydraulic calibration of a network model. The pump selected to inject conservative contaminants for the research project is an Omni Mechanical Diaphragm Metering Pump, model DC5C2PP. This pump has been installed on the top of the reservoir and has the ability to pump approximately *1.45 gpm* against a pressure of about *90 psi*. It operates using a reciprocating diaphragm that draws water in from a source (usually a bucket of metered tracer solution water) with a "Suction Stroke" and pushes it out and into the system with the diaphragm arm striking the collection chamber on a "Discharge Stroke." The length and strength of the stroke can be adjusted according to how much injection is required for a particular experiment. Figure 3.6 illustrates the injection pump setup above the water reservoir.
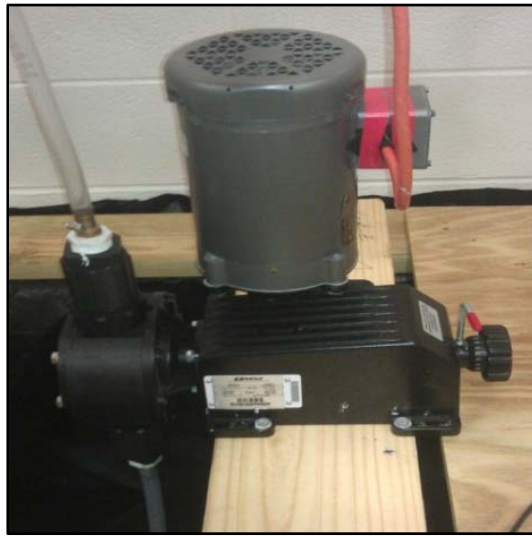

Figure 3.6 Tracer injection pump

The general protocol for experimental data collection will be detailed and briefly discussed. The methods presented here have evolved directly from the experience and empirical knowledge of the experimental research team. This procedure was followed for examining hydraulic data and water quality data in network calibration within this research. The procedures represent the initial experimental network setup and the procedures for reaching steady state equilibrium in the network.

1) The computer and data acquisition system were first turned on. The current reading in lab view was checked so that the instruments read the correct value of below *~0.20 mA* while system is not in use.
2) The water level in the reservoir was adjusted to the adequate level for the experiment and in addition the water level was checked so that it was above the *1.5 ft.* minimum depth of water above the pump inlet elevation.
3) There are *6* conductivity meters and *12* possible conductivity meter locations. The conductivity meters valves are placed in their appropriate positions as determined for the experimental setup. The remaining six locations were inspected to insure that stainless steel plugs were installed wherever there was an empty monitoring position.
4) Assuming the tank levels were filled prior to the experiment, the demand gate valves were adjusted to the appropriate settings for the experiment. In addition, the ball valves were set to their desired position prior to turning on the pump. The tank supply lines were adjusted after the pump was turned on.
5) During the tank filling step of the process, one person was directly at the computer work station. A second individual was stationed at the model so that she could adjust the tank flow lines. All other demand lines were closed, thus the pump exclusively supplied the tanks.   The two individuals used radios to communicate and coordinate the tank filling effort.
6) Once the tank levels had been filled to slightly above the levels required for the experiment, the remaining system gate valves at the demand line locations were adjusted to the specific settings required for the experiment. This procedure was done as swiftly as possible to prevent the tank lines from deviating away from targeted values for the specific experiment.
7) The final step for initial setup was to turn on the pump at the circuit breaker box.
8) The experimental setup model was then allowed to run for a few hours to reach as close as possible the targeted steady state equilibrium while the network was monitored in the lab view program.
9) The experimental notes and individual valve settings were recorded in the text file in the experimental folder structure.

3.2.1 Procedure for injection testing of a tracer

The conservative tracer used for injection testing was Calcium Chloride Dihydrate ($CaCl_2*2H_2O$), a hydrate which is *75.5%* $CaCl_2$ salt by weight. This procedure describes the appropriate method and steps involved in performing an injection experiment. This procedure involves the Omni injection pump, the three way valve, a supply of calcium chloride dihydrate, a liter-sized graduated cylinder, at least two *5 gallon* buckets, stopwatch, *2-3 radios*, *3 persons*, and two stoppers or clamps for pump hoses.

1) The network should be at steady state equilibrium before attempting an injection test.
2) A measured portion of $CaCl_2$ hydrate for mixing a solution of $CaCl_2$ was collected. The portions were made with the understanding that injections using the pump typically require concentrations of at least about *0.75 g/L* $CaCl_2$ (*1 g/L* of dihydrate salt) to be detected by the electrical conductivity sensors.
3) The solution was mixed in the graduated cylinder with the desired measured amount of water. The quantities were recorded and poured into a bucket container for supplying the injection pump.
4) One empty bucket was carried to the injection point tee connection near the outlet of main network pump.
5) One person was located at the Omni pump, one person was located at the injection point with a stopwatch, and the third member stationed at the computer. Communication was made by radios between the three team members.
6) The Configuration of the three-way injection valve was initially such that any flow from the injection pump would be directed through the release hose into the empty bucket.
7) The Omni pump's inlet hose was then submerged into the bucket of premixed $CaCl_2$ solution.
8) The person at the pump initiates the injection process by turning on the pump. Initially, as stated, the injected solution is released to the empty bucket by the injection valve.
9) Once the injection hose has been fully filled with solution, the person at the injection valve began a countdown via radio communication. At the end of his countdown, he started the stopwatch at the same time the three-way lever was turned from release to injection. While the person at the computer began collecting data in lab view at the end of the countdown. Switching the lever forced the injected solution into the network.
10) The injection was continued for a standard *80 seconds* time period from the countdown.
11) Once the experiment was ready to conclude as determine by the stopwatch, the injection pump was turned off, and the three-way lever switched to the release position.
12) The amount of fluid in the release bucket and any amount of fluid that still remained in the pump line and solution bucket were measured to determine the

quantity of solution injected within the *990 seconds* standard time period and the average injected flow rate calculated.

13) In lab view, data would be collected until experimenters were satisfied with the amount of data collected and/or the network reached a new average conductivity background level.

14) A text file was created describing the experiment, participants, and system conditions (number of turns on each valve, water levels, conductivity meter positions, etc.). The amount of injected solution volume and concentration level was recorded. The injection flow rate and time was also recorded.

Chapter 4.   Experimental Calibration Cases

4.1 Introduction

This section of the report will very briefly describe and summarize the looped and branched networks with the laboratory model. The focus will describe the laboratory processes and procedures of setting up the experimental tests. The section will also summarize the findings of each experiment and the data collected during Case A, Case B, and Case C. The difference between the three cases will be presented.

4.2 Case A & B, Looped Scenarios

4.2.1 Description of Cases A and B experiments

The experimental water distribution network, at the start of the experiment, was initially dry and empty throughout with full reservoir. Prior to the test, the tanks were filled by closing off the demand valve with the pump exclusively supplying the tanks. After the tanks were filled to an approximate desired level, the demand nodes would be set to create a steady-state operation of the network model.

The pump was running throughout as described in the experimental procedures. The network was set in a looped configuration with all the appropriate pipe ball valves in the network open and associated pipes within the network allowed to flow.

The test was then run with the tanks partially full throughout the steady-state test. The data was acquired after steady state equilibrium was reached. The gate valves were set in an attempt to create flow throughout the remainder of the network above the minimum detectable flow (*0.8 gpm*) for the flow meters.

The injection process was followed as described in the Injection testing procedure protocols in section 3.2.1. During case A, one of the EC meters failed to collect data during the simulation. The test was repeated after moving the EC meter to a new location, CM location 2 in case B. For inject 1, over the course of *80 seconds* standard time length, *6.68 Liters* of solutions were injected into the network. The average flow rate into the network is *1.32 gpm* over the course of the tracer testing period for third injection test. For third injection test, over the course of *80 seconds* standard time length, *6.93 Liters* of solutions were injected into the network. The average flow rate into the network is *1.37 gpm* over the course of the tracer testing period for Inject 3 test. Table 4.1 presents the gate value settings for the Case A and Case B test scenario. Table 4.2 presents the electrical conductivity meter settings within the network.

Table 4.1 Case A & Case B gate value settings

Valve	Number of Turns from Open
J-4180	4 and 7/8 turns
J-5921	4 and 1/4 turns
J-2689	4 and 3/8 turns
J-3999	4 and 3/4 turns
J-4	3 and 1/8 turns
J-809	4 and 3/8 turns

Table 4.2 Case B electrical conductivity locations

LABVIEW EC instrument ID	KYPIPE Measurement location
CURRENT 5	CM 8 LOCATION
CURRENT 6	CM 6 LOCATION
CURRENT 7	CM 7 LOCATION
CURRENT 8	CM 12 LOCATION
CURRENT 9	CM 4 LOCATION
CURRENT 10	CM 11 LOCATION

The six instruments in Table 4.2 indicate the six EC physical locations in the network as indicated by KYPIPE measurement locations using the KYPIPE project files node number scheme within the computer model. The Lab view EC instrument ID numbers are the instrument measurement numbers within the Labview program with identifies the datastream by which channel of the pinned circuit board the instrument is wired into at the data acquisition system. Since during each EC instrument can be moved to different locations with the physical model, tables such as Table 4.2 were created for each experiment to insure and keep track of where each of the EC meters (numbered *5* thru *10*) are physically located in the laboratory model and where that point represents in the computer KYPIPE network model.

The network was allowed to run for an extended period of time before collecting data within lab view and before the conservative tracer injection procedure. Each of the demand flows for Case A was sufficiently above the *0.8 gpm* minimum detectable as indicated in Table 4.3. Table 4.3 summarizes the hydraulic data statistics collected during the injection test for Case A.

Table 4.3 has four principal columns for each row of the table. The first column is the instrument or meter identification. The second column is the average of the total amount of data collected over the time period of the experiment for each instrument. The

third column is the standard deviation of the data collected for the instrument over the steady state test. If the instrument was measuring perfectly and the system was completely in steady state equilibrium, the standard deviations would be zero. However there are minor statistical fluctuations in the instruments as represented by the standard deviations. The fourth column is the standard deviation for the instrument divided by the average of instrument over the experimental test duration. The fourth column can be thought of as the relative volatility about the measured average values in terms of percentage of the average. It can be seen from investigating Table 4.3 that the each of the instruments is operating within at most plus/minus 3.5%. This indicates the experimental data collection is operating under very good control.

Table 4.3 Case A experimental data summary

	Instrument	EXPERIMENT AVG (psi)	Experiment STD Dev.	STD DEV to AVG Ratio
TANK MEASURES	RIGHT TANK (T-2)	23.724	0.025	**0.11%**
	CENTER TANK (T-3)	27.469	0.043	**0.16%**
	RESERVOIR (R-1)	43.517	0.076	**0.17%**
	LEFT TANK (T-1)	13.505	0.05	**0.37%**
FLOW MEASURES SUMMARY	P-38 (Transmission)	60.536	0.748	**1.23%**
	P-34 (Transmission)	49.639	0.652	**1.31%**
	P-22 (T-3)	0	0.039	**N/A**
	P-23 (T-1)	0	0.028	**N/A**
	J-2689	4.206	0.074	**1.76%**
	J-809	4.692	0.081	**1.72%**
	J-4180	1.783	0.058	**3.24%**
	J-3999	2.469	0.062	**2.51%**
	J-5253	6.803	0.094	**1.38%**
	J-3896	31.615	0.303	**0.96%**
	J-4071	14.686	0.155	**1.06%**
	J-4069	25.948	0.27	**1.04%**
	P-24 (T-2)	0	0.026	**N/A**
	J-5421	5.893	0.107	**1.82%**
	J-4	17.893	0.191	**1.06%**

Table 4.3 Case A experimental data summary (Continued)

	Instrument	EXPERIMENT AVG (psi)	Experiment STD Dev.	STD DEV to AVG Ratio
PRESSURE SUMMARY	J-3884	3.4	0.062	**1.83%**
	J-4090	17.796	0.288	**1.62%**
	J-5253	3.918	0.068	**1.74%**
	J-4	3.795	0.081	**2.12%**
	J-2418	3.506	0.027	**0.76%**
	J-5582	2.915	0.031	**1.06%**
	J-4180	5.414	0.117	**2.16%**
	J-809	2.988	0.029	**0.97%**
	J-2689	2.937	0.026	**0.87%**
	J-5421	3.518	0.066	**1.87%**
	J-3893	3.367	0.064	**1.89%**
	J-4186	4.099	0.032	**0.77%**
	J-3832	4.234	0.09	**2.12%**
	J-4181	4.56	0.089	**1.96%**
	J-4069	4.713	0.153	**3.25%**
	J-3999	4.421	0.067	**1.51%**
	J-3896	3.834	0.039	**1.01%**
	J-4071	6.78	0.181	**2.66%**
	J-5580	3.004	0.022	**0.72%**
	PUMP	20.078	0.27	**1.35%**

Table 4.4 presents the data collected thru the network during the Case B test. The Case A test was repeated after moving the EC meter to a new location, CM location 2 as Case B. There are slight differences in pressures, flows, and tank level measurements during Case B from Case A as indicated within Table 4.4. However the average and standard deviations collected during the Case B are nearly identically to the Case A values. In fact, using an ANOVA test with the Data Analysis package within excel indicates that the Case A and Case B measured values are not statistically significantly different. They represent mildly different experimental errors present during each test.

Table 4.4 Case B experimental data summary

	Instrument	EXPERIMENT AVG (psi)	Experiment STD Dev.	STD DEV to AVG Ratio
TANK MEASURES	RIGHT TANK (T-2)	23.206	0.049	**0.21%**
	CENTER TANK (T-3)	26.504	0.056	**0.21%**
	RESERVOIR (R-1)	44.293	0.093	**0.21%**
	LEFT TANK (T-1)	12.385	0.068	**0.55%**
FLOW MEASURES SUMMARY	P-38 (Transmission)	60.29	0.758	**1.26%**
	P-34 (Transmission)	49.965	0.623	**1.25%**
	P-22 (T-3)	0	0.043	**N/A**
	P-23 (T-1)	0	0.022	**N/A**
	J-2689	3.733	0.108	**2.89%**
	J-809	5.979	0.302	**5.05%**
	J-4180	1.743	0.065	**3.74%**
	J-3999	2.768	0.068	**2.46%**
	J-5253	6.928	0.096	**1.38%**
	J-3896	31.581	0.309	**0.98%**
	J-4071	15.14	0.159	**1.05%**
	J-4069	25.888	0.277	**1.07%**
	P-24 (T-2)	0	0.022	**N/A**
	J-5421	6.246	0.101	**1.61%**
	J-4	17.889	0.188	**1.05%**

Table 4.4 Case B experimental data summary (Continued)

	Instrument	EXPERIMENT AVG (psi)	Experiment STD Dev.	STD DEV to AVG Ratio
PRESSURE SUMMARY	J-3884	3.383	0.051	**1.50%**
	J-4090	17.864	0.291	**1.63%**
	J-5253	3.885	0.069	**1.77%**
	J-4	3.781	0.034	**0.90%**
	J-2418	3.472	0.027	**0.79%**
	J-5582	2.873	0.017	**0.59%**
	J-4180	5.398	0.116	**2.15%**
	J-809	2.957	0.024	**0.80%**
	J-2689	2.916	0.023	**0.79%**
	J-5421	3.478	0.072	**2.06%**
	J-3893	3.346	0.049	**1.46%**
	J-4186	4.08	0.015	**0.36%**
	J-3832	4.214	0.087	**2.06%**
	J-4181	4.542	0.078	**1.72%**
	J-4069	4.715	0.15	**3.18%**
	J-3999	4.407	0.055	**1.25%**
	J-3896	3.792	0.02	**0.53%**
	J-4071	6.713	0.179	**2.67%**
	J-5580	2.968	0.015	**0.51%**
	PUMP	20.075	0.27	**1.34%**

Figure 4.1 illustrates the network configuration within the KYPIPE computer model. The KYPIPE model present in the figure also shows the distribution of the electrical conductivity meters for measuring the conservative tracer during the Case A and Case B experimental tests.
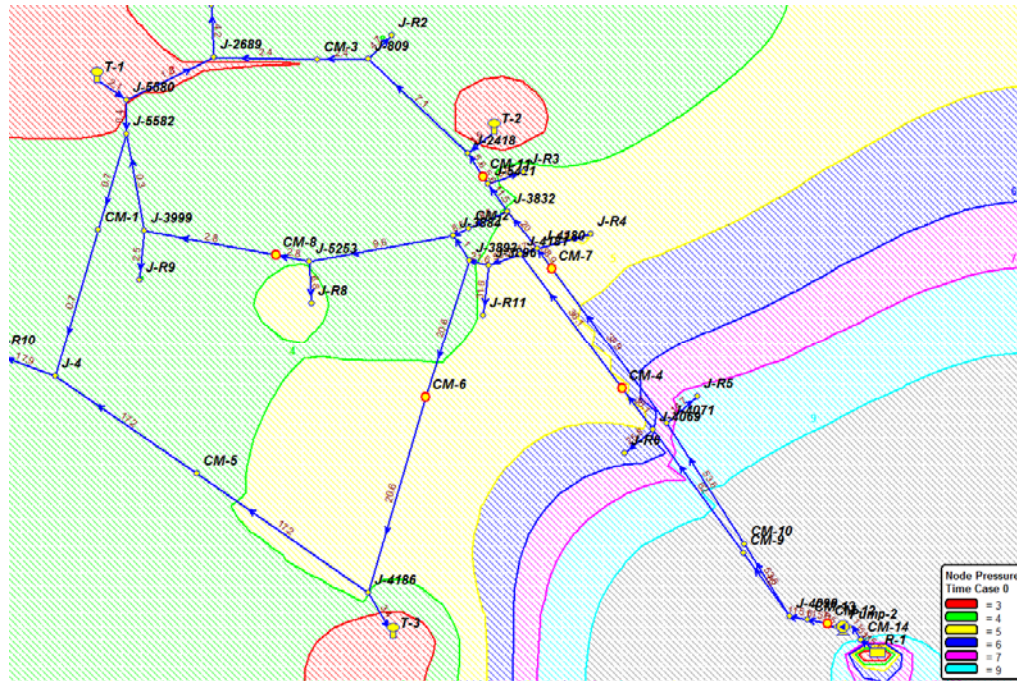
Figure 4.1: Network diagram for cases A & B

The results of the conservative tracer experiments are presented in table 4.5. The measured time from injection start time was obtained by examining the time series for the electrical conductivity sensors and determining the arrival time of the plug of concentrated tracer at the sensor location. Table 4.5 and Table 4.6 represent the velocity measurement from the injection site location to either four or five measured locations within the physical model network.

Table 4.5 Case A velocity results from tracer

CASE A LOCATION	MEASURED TIME, seconds	MEASURED LENGTH, ft. from injection point	AVG PATH Velocity	Measured V2/(2g), ft.
CM 7	19.14	148.55	7.76	0.936
CM 6	28.26	151.93	5.38	0.449
CM 11	30.26	184.72	6.1	0.579
CM 8	52.76	218.79	4.15	0.267

Table 4.6 Case B velocity results from tracer

CASE B LOCATION	MEASURED TIME, seconds	MEASURED LENGTH, ft. from injection point	AVG PATH Velocity	Measured $V2/(2g)$, ft.
CM 7	20.89	148.55	7.11	0.79
CM 6	27.49	151.93	5.53	0.48
CM 11	29.49	184.72	6.26	0.61
CM 8	51.87	218.79	4.22	0.28
CM 2	32.09	190.21	5.93	0.55

Figures 4.2 and 4.3 present the time series plot of the electrical conductivity sensors. The Y axis represents the concentration of ions within the water at the measurement site within the network model. The measurement of concentration is indirectly measured as the resistance provided by the water around the electrical conductivity to current traveling thru the electrical conductivity meter. The X axis represents the time from the initial injection of the conservative tracer of calcium chloride solution (time zero). The points in the time series were the amount of ions within water start to increase represent the point in time when the calcium chloride solution begins to arrive at the measurement location. It must be noted that that the CM 7 meter exhibits odd behavior in the time series plot in Figure 4.2. The electrical conductivity indicates that the dissolved concentration of ions in water around the meter after the conservative tracer arrival somehow drops below the initial background level in the network before the injection process. This is not physically possible and represents some faulty performance of the CM7 meter during the Case A experiment. However, the issue is not of significance for the purpose of this research since each of the three injections for this network configuration (Case A, Case B, and a replication of the Case A test) show that the travel time of the conservative tracer arrival at the CM7 site consistently between *19 and 22.50 seconds* from the initial injection for the tracer into the network. The travel times for the tracer from the injection site to the measurement sites presented Table 4.5 and Table 4.6 are the only information being used within the research
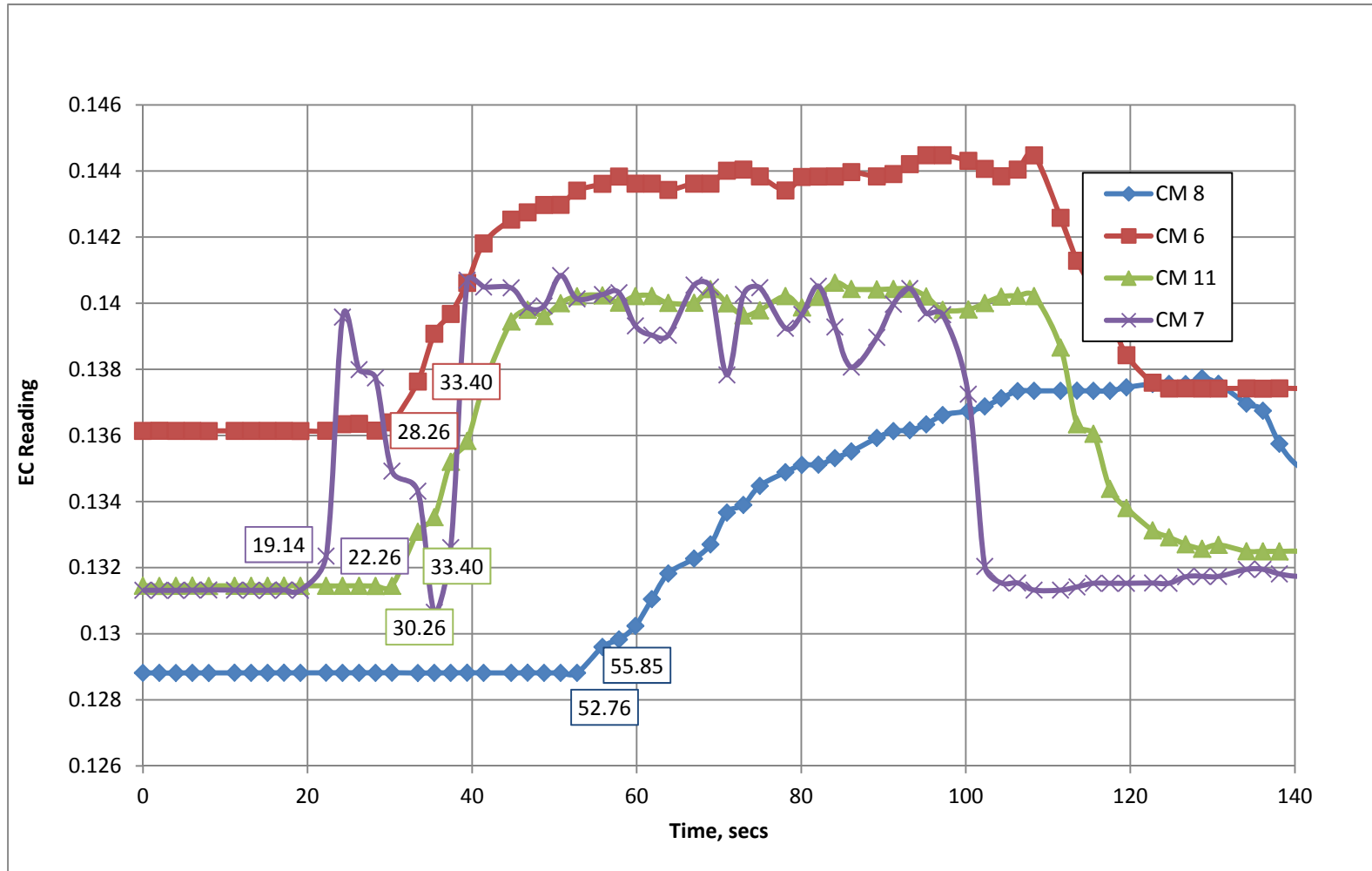
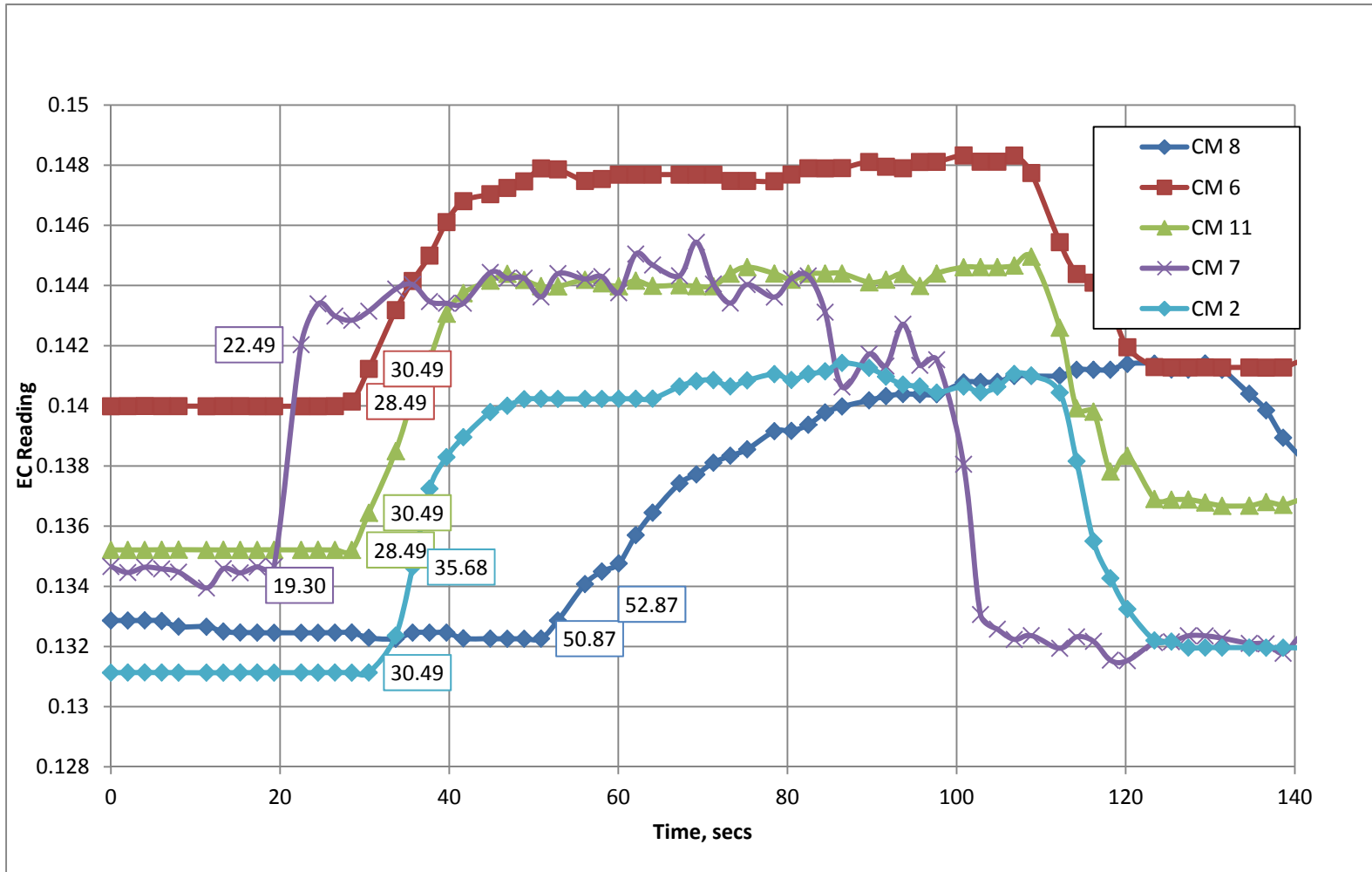Figure 4.2: Case A: electrical conductivity time lag from initial injection time

Figure 4.3: Case B: electrical conductivity time lag from initial injection time

4.3 Case C: Branched scenario

4.3.1 Description of case C experiment

The experimental water distribution network, at the start of the experiment, was initially dry and empty throughout with full reservoir. Prior to the test, the tanks were filled by closing off the demand valve with the pump exclusively supplying the tanks. After the tanks were filled to an approximate desired level, the demand nodes were set to the settings indicated by Table 4.7. The pump was running throughout as described in the experimental procedures. The network was set in a branched configuration with all the appropriate pipe ball valves in the network closed off to restrict flow within the network at one location to exclusively follow a single path within the network.

The test was then run with the tanks partially full throughout the steady state test and data acquired after some time was allowed for steady state equilibrium to be reached. The gate valves were set in an attempt to create flow throughout the remainder of the network above the minimum detectable flow (*0.8 gpm*). Table 4.7 summarizes the gate valve settings prior to the test. The network was allowed to run for an extended period of time before collecting data within lab view and before the conservative tracer injection procedure.

The injection process was followed as described in Section 3.2.1 injection testing procedure. Over the course of *80 seconds* standard time length, *6.0 Liters* of solutions were injected into the network. The average flow rate into the network is *1.19 gpm* over the course of the tracer testing period. Table 4.8 indicates the EC meters testing locations in the network for the branched configuration scenario of Case C.

Table 4.7 Case C Gate value settings

Valve	Number of Turns from Open
J-4069	3 and 1/2 turns
J-4071	3 and 3/4 turns
J-4180	4 and 1/2 turns
J-3896	4 and 1/4 turns
J-5421	4 turns
J-809	3 turns
J-2689	3 turns
J-3999	4 and 1/2 turns
J-5253	4 and 1/2 turns
J-4	0 turns

Table 4.8 Case C Test locations

LABVIEW EC instrument ID	KYPIPE MEASURE LOCATION
CURRENT 5	CM 8 (INSTRUMENT #26)
CURRENT 6	CM 9 (INSTRUMENT #17)
CURRENT 7	CM 5 (INSTRUMENT #19)
CURRENT 8	CM 11 UPSTREAM PUMP
CURRENT 9	CM 3 (INSTRUMENT #29)
CURRENT 10	CM 7 (INSTRUMENT #12)

Each of the demand flows was sufficiently above the *0.8 gpm* minimum detectable as indicated in Table 4.9. Table 4.9 summarizes the hydraulic data statistics collected during the injection test. The network pressures, flows, and tank levels are significantly different from the two previous looped scenarios of Case A and Case B.

Table 4.9 has four principal columns for each row of the table exactly as presented previously in Table 4.3 within section 4.1. The first column is the instrument or meter identification. The second column is the average of the total amount of data collected over the time period of the experiment for each instrument. The third column is the standard deviation of the data collected for the instrument over the steady-state test. If the instrument was measuring perfectly and the system was completely in steady state equilibrium, the standard deviations would be zero. However there are minor statistical fluctuations in the instruments as represented by the standard deviations. The fourth column is the standard deviation for the instrument divided by the average of instrument over the experimental test duration. The fourth column can be thought of as the relative volatilities about the measured average values in terms of percentage of the average. It can be seen from investigating Table 4.9 that each of the instruments is operating within plus/minus at most 3.5% of the average measured values. The order of magnitudes of the relative volatilities about the measured average values are on the same order of magnitude of the Case A and Case B scenarios. This indicates the experimental data collection is operating under very good experimental control.

Table 4.9 Case C summary table

	Instrument	EXPERIMENT AVG (psi)	Experiment STD Dev.	STD DEV to AVG Ratio
TANK MEASURES	RIGHT TANK (T-2)	23.724	0.025	**0.11%**
	CENTER TANK (T-3)	27.469	0.043	**0.16%**
	RESERVOIR (R-1)	43.517	0.076	**0.17%**
	LEFT TANK (T-1)	13.505	0.05	**0.37%**
FLOW MEASURES SUMMARY	Instrument	EXPERIMENT AVG (psi)	Experiment STD Dev.	STD DEV to AVG Ratio
	P-38 (Transmission)	60.536	0.748	**1.23%**
	P-34 (Transmission)	49.639	0.652	**1.31%**
	P-22 (T-3)	0	0.039	**N/A**
	P-23 (T-1)	0	0.028	**N/A**
	J-2689	4.206	0.074	**1.76%**
	J-809	4.692	0.081	**1.72%**
	J-4180	1.783	0.058	**3.24%**
	J-3999	2.469	0.062	**2.51%**
	J-5253	6.803	0.094	**1.38%**
	J-3896	31.615	0.303	**0.96%**
	J-4071	14.686	0.155	**1.06%**
	J-4069	25.948	0.27	**1.04%**
	P-24 (T-2)	0	0.026	**N/A**
	J-5421	5.893	0.107	**1.82%**
	J-4	17.893	0.191	**1.06%**

Table 4.9 Case C summary table (Continued)

	Instrument	EXPERIMENT AVG (psi)	Experiment STD Dev.	STD DEV to AVG Ratio
PRESSURE SUMMARY	J-3884	3.4	0.062	**1.83%**
	J-4090	17.796	0.288	**1.62%**
	J-5253	3.918	0.068	**1.74%**
	J-4	3.795	0.081	**2.12%**
	J-2418	3.506	0.027	**0.76%**
	J-5582	2.915	0.031	**1.06%**
	J-4180	5.414	0.117	**2.16%**
	J-809	2.988	0.029	**0.97%**
	J-2689	2.937	0.026	**0.87%**
	J-5421	3.518	0.066	**1.87%**
	J-3893	3.367	0.064	**1.89%**
	J-4186	4.099	0.032	**0.77%**
	J-3832	4.234	0.09	**2.12%**
	J-4181	4.56	0.089	**1.96%**
	J-4069	4.713	0.153	**3.25%**
	J-3999	4.421	0.067	**1.51%**
	J-3896	3.834	0.039	**1.01%**
	J-4071	6.78	0.181	**2.66%**
	J-5580	3.004	0.022	**0.72%**
	PUMP	20.078	0.27	**1.35%**

Figure 4.4 Case C Network Diagram for Branched System

Figure 4.4 illustrates the network configuration within the KYPIPE computer model for Case C. The KYPIPE model present in the figure also shows the distribution of the electrical conductivity meters for measuring the conservative tracer for Case C. The difference between the looped cases of Case A and Case B and the branched network of Case C is also clearly visible in the figure.

The results of the conservative tracer experiments are presented in Table 4.10 for the locations of the five electrical conductivity locations for the branched system configuration. The measured time from injection start time was obtained by examining the time series for the electrical conductivity sensors and determining the arrival time of the plug of concentrated tracer at the sensor location. Figure 4.5 presents the time series plot of the electrical conductivity sensors measurements during the experiment with the arrival times indicated on the figure. Table 4.10 presents the results of the tracer test for Case C with the arrival times from Figure 4.5 as the second column of the table.

34

Table 4.10 Case C velocity results from tracer

CASE C LOCATION	MEASURED TIME, seconds	MEASURED LENGTH, ft. From injection point	AVG PATH Velocity	Measured $V^2/(2g)$, ft.
CM 3	40.86	232.26	5.68	0.50
CM 5	43.44	223.23	5.14	0.41
CM 7	21.05	148.55	7.06	0.77
CM 8	32.26	153.45	4.76	0.35
CM 9	4	35.75	8.94	1.24
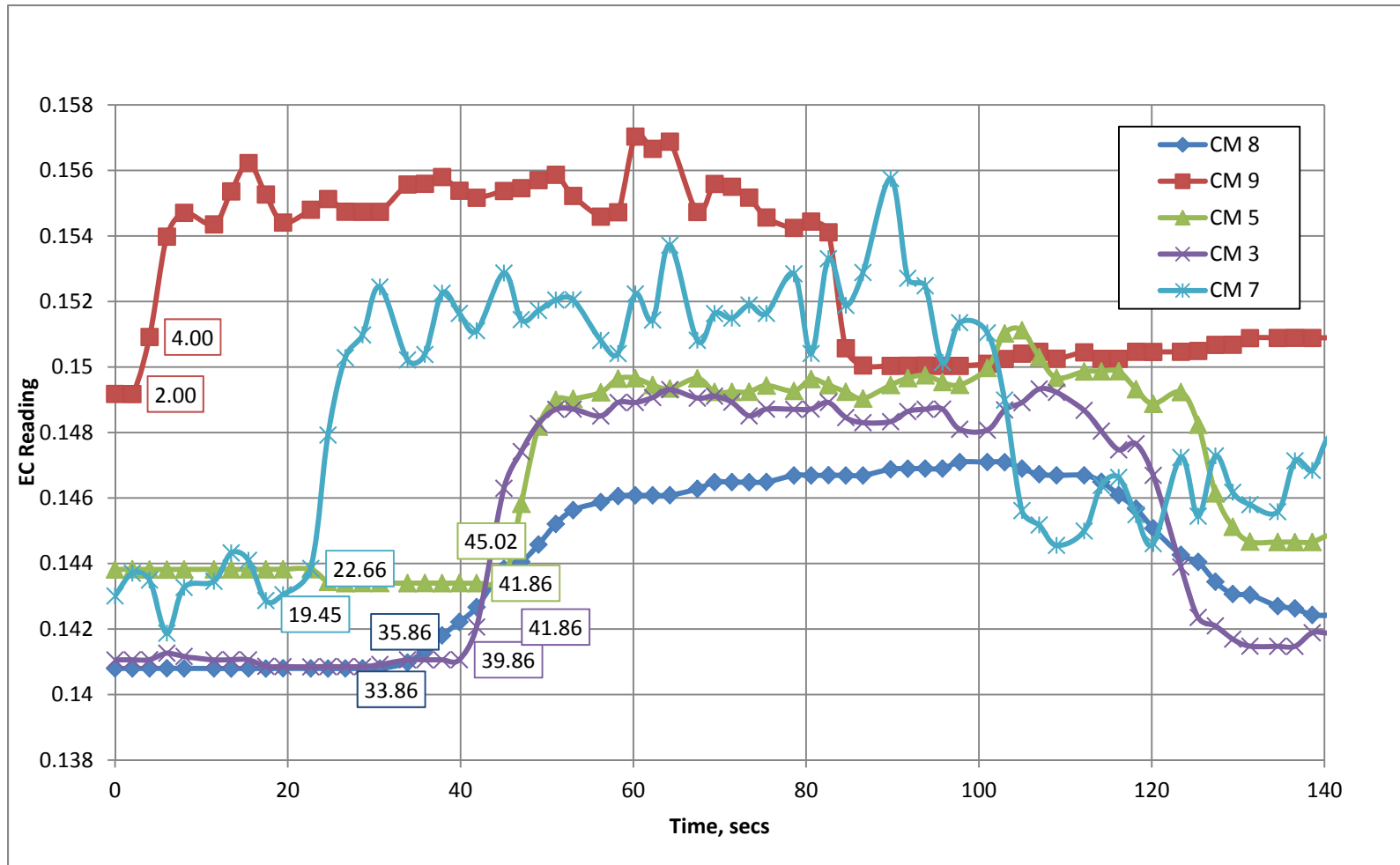
Figure 4.5 Case C electrical conductivity time lag from initial injection time

Chapter 5.   Statistical Analysis of Data

5.1 Introduction

The goal of the research was to examine the use of water quality and hydraulic data as a basis for hydraulic calibration of a network model. The objective of the research requires reviewing and analyzing experimental data collected during an experimental test scenario. When analyzing experimental data it is important to consider errors within the data and within the experiment. It is important to determine if the measurements from the instruments are operating within the established specifications from the manufacturers. In addition it is important to determine the degree of confidence in measurements and for the determination that the experiment is operating within the steady-state, or very near steady-state, equilibrium.

This section of the research report will briefly discuss the procedures and methods utilized in the experimental data statistical analysis portion of the hydraulic calibration of the model. The test methodology for determining normality in the data, de-trending the data, and analyzing non-constant variance in the experiment will be briefly discussed. The focus of this section is the necessary tests to insure quality control for the three tracer tests presented in tables 4.3, 4.4, and 4.9.   Tables 4.3, 4.4, and 4.9 are the post processed results after performing the statistical quality control procedures discussed within this chapter.

5.2 Testing for trends in experiments (verifying steady-state)

The time series for each of the instrument classes (pressure, flow, and tank level meters) was analyzed for trends in the data. Ideally, the network scenario should be in steady-state equilibrium during a test. However, it found from working with the physical model network there were typically very mild but statistical significant trends in most of the instruments during a test scenario. The basis for determining the presence of a trend in a time series was the Fisher test statistic, given here

$$F = \frac{MSR}{MSE} = \frac{\sum(y_{predicted}-\overline{y_{Average}})^2/(number\ of\ dep\ variables)}{\sum(y_{predicted}-y_{measured})^2/(number\ of\ samples-2)} \tag{6}$$

where

y =dependent variable (specific instruments time series of measurements)

$y_{predicted}$ = dependent variable based on regression as function of dependent variables

$y_{measured}$ = dependent variable measured with associated dependent variables measured

The test is a comparison between the square of the difference between predictions and measured values and the square of the error between predictions and the average value on the x-y plane. The only independent variable is time and the

dependent variables with function of time represented by the time series of data collected by each instrument. The divisors in the two sums of the Eq. 6 represent the respective degrees of freedom for the regression. Since the only dependent variable of interest is time, the number of dependent variables is one in the numerator. The number of sample points varies from test to test. The minus two represents the fact that it takes at minimum of three points to distinguish between the presence of a very mild linear relationship with a dependent variable versus a constant value with some unknown perturbed amount (plus or minus all unknown random errors) and no relationship with a dependent variable. Hence, two points are lost in the degrees of freedom for sum of the errors term. The hypothesis test for the determining the lack of a trend is that the slope (B_0) for the regression line is zero or very near zero and is presented as equation seven. The F in Eq. 7 refers back to Eq. 6.

$$H_0: B_0 = 0$$

$$H_a: B_o \neq 0$$

$$Reject\ H_0\ if\ F > F(\alpha; 1, n-2)\ \ Do\ not\ Reject\ H_0\ if\ F \leq F(\alpha; 1, n-2) \quad (7)$$

B_0 = Slope of linear regression that minimizes the square error residuals

Equation 7 represents the decision tree for the fisher test statistic. The alpha in Eq. 7 is the level of confidence for the test, where an α value represents the accepted error of the test. The selected level of confidence for the purpose of the research was 95% and thus alpha was 5%. The test was performed within an excel spreadsheet using the FDIST function command for each time series and for each test. When analyzing the data for the experiments, there tended to be mild trends present in most data sets.

Any trends for each retrospective data series were removed from the individual time series by adjusting the dataset based on the linear trend slope and the distance from the average value for each time series. This was done so that the data and statistics from the experiment could be compared with future experiments, for example comparing statistical properties such as standard deviations and normalized standard deviations and testing for constant statistic properties in each measurement type. This will make comparisons more relatable since each "steady-state" will tend to have very slightly mild trends present in each experiment and unique to that experiment. In addition, removing the trends from the dataset reduces the standard deviations of the adjusted datasets and reduces any biases in the tests for normality represented from larger standard deviations. The results of the experimental measures are after removing the mild trends are presented in tables 4.3, 4.4, and 4.9.

5.3 Testing for normality (verifying normal operation of sensors)

Normality in the data was determined by examining the standardized residuals, which are the measured data points minus the regression predicted data points as a function of time and then divided by the standard deviation of the dataset.

If the data is approximately normal, then 68% of the standard residuals should be between -1 and 1. Also if the data is approximately normal then about 95% of the data should between -2 and 2. This was found be true for the de-trended flow data, tank level data, and pressure measurements and each appeared to meet the normality assumption with two exceptions.

The basis of testing normality was the regression line for the de-trended time series. Ideally, after de-trending the dataset for any upward or downward trend in the almost fully steady-state equilibrium, the slope will be zero or very near zero. For case A, the instruments variance around the average values of the experiment was found to be operating as a normal dataset with the exception of the J-4071 and J-4069 junction flow meters. This is mainly due to some outlier measurements around *11 seconds* to *26 seconds* time interval from the start of the experiment data collection were the instrument defaulted to zero measurement. There was a similar problem for case C when the J-809 pressure meter defaulted to a zero measurement. Removing the outlier points correctly shows all flow data to be normally distributed about its average value during the injection test data interval. Non-normality in a dataset can indicate poor performance in an instrument or that the network still has some disequilibrium away from steady-state. In this case it represents some initial instability created from switching the injection pump flow into the network on and from adjusting the injection pump check value to allow flow from the injection pump.

5.4 Testing for non-constant variance

Ideally if the physical network is in steady state equilibrium, the time series of data for an instrument should be a constant value about the average value. The presence of non-constant variance in a time series most likely indicates some disequilibrium in the network and deviation from a true steady-state network conditions around the section of the network near the instrument. Non-constant variance in an instrument is potentially a problem since it will skew statistic tests and add greater uncertainty to measured averages for given experiment, and hence bias the hydraulic calibration.

A check was made to determine if there existed a non-constant error variance over time. There are several statistical tests for non-constant variance. The one used in the research was the Szroeter test (Eq. 8). Allowing for a longer time period for a steady-state to be reached greatly increased the performance for both normality and non-constant variance in a given experiment's data. Experiments in which the network was allowed to reach steady-state over the course of a few hours, such as the case A test scenario developed for hydraulic calibration, were not found to meet the test statistic for rejecting the constant variance assumption. Therefore the variance can be said to not be increasing over time for the majority of instruments with a constant variance about the mean for Case A thru Case C time series of data collection during the experiments.

$$S = \left(\frac{6*n}{n^2-1}\right)^{1/2} \left(h - \frac{(n+1)}{2}\right) \tag{8}$$

with

$n = \quad$ *the number of data points for timeseries*

$h = \dfrac{\sum_{i=0}^{n}\left(i \times \hat{e_i}^2\right)}{\sum_{i=0}^{n}\left(\hat{e_i}^2\right)}$

$\hat{e_i}^2 = (\text{predicted value} - \text{measured value})^2$

$\qquad\qquad\qquad S =$ the szroeter test statistic

Utilizing Eq. 8 from Dielman (Dielman, 2005, p. 225), requires ordering the data in increasing ranks for the dependent variable. The data series is already naturally ranked in order of increasing time and thus no ordering was necessary. The sum of the squares of the residuals multiplied by the rank in order of increasing explanatory value divided by the sum of squares of the residuals is the value for h. If there is non-constant variances in the residuals, then h will become sufficiently large enough such that S will be larger than If the S test statistic is outside the boundaries of the Z values from a standard normal table with upper area alpha for either side of the normal curve, then the assumption of constant variance can be rejected. The Z values are the ordinates for the standard normal distribution (mean of 0 and standard deviation of 1) with a given probability within the ordinates. The Z values for *99.99%* confidence are *-3.719* and *3.719* respectively, with *99.99%* of the standard normal distribution within those bounds. If the S value is within that range, the hypothesis of a constant variance cannot be rejected. Outside those bounds, the data can be assumed non-constant with *99.99%* confidence. The percentage degree of confidence in constant variance assumption is *100%* minus how low the probability must be lowered for the Z value in a standard normal table to be smaller than the Q value.

Chapter 6.   Hydraulic Calibration Procedures

6.1 KYPIPE baseline model

The hydraulic calibration effort requires a comparison against a baseline. The KYPIPE baseline model and analysis utilized minor loss values and pipe roughness values derived from a literature.   Several source materials were investigated and some variation was found in the standard reference materials. The various reference materials presented in Table 6.1 represent the typical minor loss values for the various components within the network. The typical pipe roughness literature value of 150 and the minor losses presented in Munson text were used as the baseline model for pipe calibration. The pipes in the network are constructed of a uniform PVC material in three pipe sizes of *1 in*, *1.5 in,* and *2.0 in* diameter PVC pipe.

Table 6.1 Minor loss components literature values

	Value utilized research	Gupta	Mayes	Munson et, al
Ball Valve	0.05	-	-	0.05
90' Elbow, Long	0.2	0.3	0.21 to 0.3	0.2
45' Elbow, Long	0.2	0.3	0.2	0.2
Coupling	0.02	-	-	-
Reducer(2"-1")	0.5	-	-	-
Reducer(1.5"-1")	0.2	-	-	-
flow meter	0.1	-	-	-
gate valve (fully open)	0.19	0.19	0.07 to 0.14	0.15
Tee-flanged (thru flow)	0.2	0.2	0.1 to 0.6	0.2
manifold	1	-	-	-
1" U-Bend (4 90' Long Elbow)	0.8	1.2	0.63 to 0.90	0.8
1.5" U-Bend (2 90' Long Elbow)	0.4	0.6	0.42 to 0.6	0.4
2" U-Bend (2 90' Long elbow)	0.4	0.6	0.42 to 0.6	0.4

(Gupta, 2008, p. 673) (Mays, 2011, pp. 98-99) (Munson, 2009, pp. 421-422)

6.2 Pressure head Calibration

The hydraulic calibration effort using pressure data was performed on the basis of comparing a model's sum of square errors between the average nodal pressure heads as measured in comparison between the modeled results. The goal of the calibration effort is to determine the best C-Value for each pipe that minimizes

Eq. 9. This represents the pressure objective function developed from reviewing the various different objective functions found thru the literature review. The formulation is in terms of relative errors similar to the Tabesh formulation (Eq. 5). The formulation in Eq. 9 doesn't include the W_p weighting turn in the Tabesh equation (Eq. 5).

$$PSSE = \sum_{i=1}^{20} \left(\frac{w_p*(P_{obs,i} - P_{pred,i})}{w_p*P_{obs,i}} \right)^2 \qquad (9)$$

where

W_p = conversion factor from pressure in *psi* to pressure head in *ft*.

$P_{obs,i}$ = observed pressure measured at location *i* , *psi*.

$P_{pred,i}$ = model predicted pressure measured at location *i*, *psi*.

The initial calibration model was created by setting uniform C-Values for the three pipe sizes at a specific setting; the model was then run and analyzed for multiple C-Value settings. Figure 6.1 illustrates the initial uniform adjustment all pipes sizes. The minimum sum of the square errors between modeled to measured pressures created when all three pipes C-Values are set to the same uniform setting for the value of *155* was found to be the best performing value for a uniform C-factor that minimized Eq. 9 as displayed by Figure 6.1.
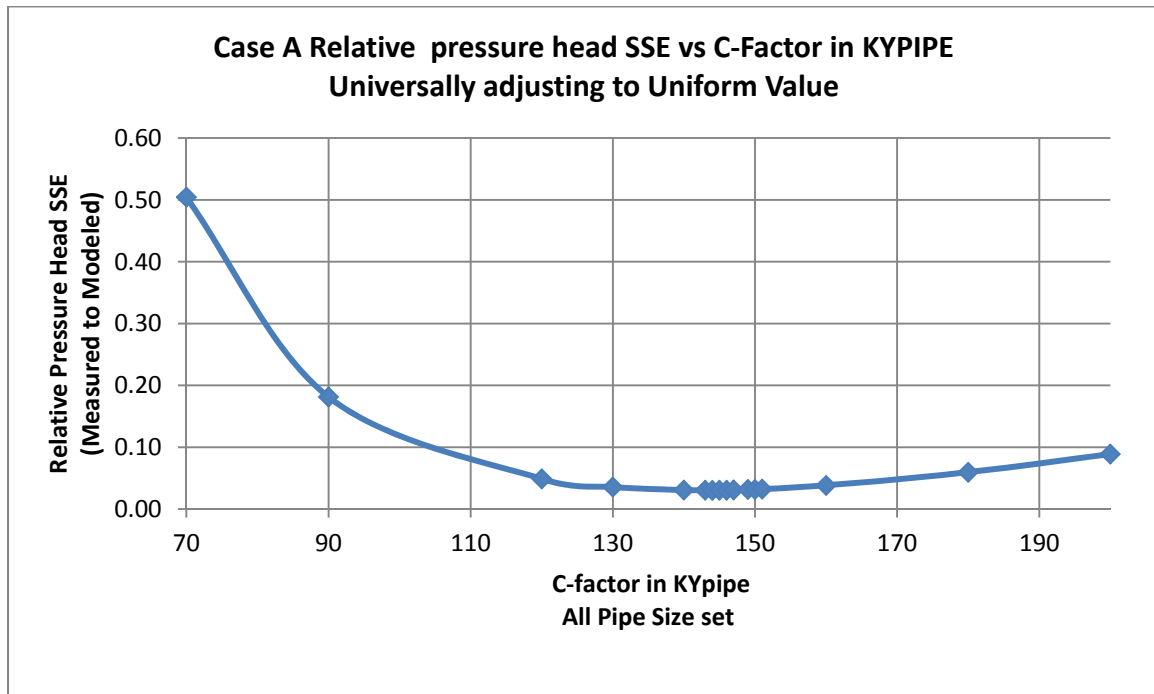
Figure 6.1: Case A: pressure calibration, initial C-Factor adjustment

After the initial adjustment of all pipes sizes to the best uniform C-value, a value of *144* in Case A, each of the three pipe sizes were adjusted individually to the C-value that produced the lowest sum of square errors while keeping the other pipe sizes C-value constant. Figure 6.2 illustrates the sum of squares errors (Eq. 9) created by adjusting the C-values for the *1.5 in* pipes with all other pipe sizes held constant at a roughness of *144*. The C-value of *154* for the *1.5 in* pipes and all other pipe sizes set to *144* created a lower sum of square errors than for the *1.5inch* pipes set to *144* with all other pipes and thus is a better calibration result. The red line in Fig. 6.2 represents the error level from Fig. 6.1 with all pipes at *144*.
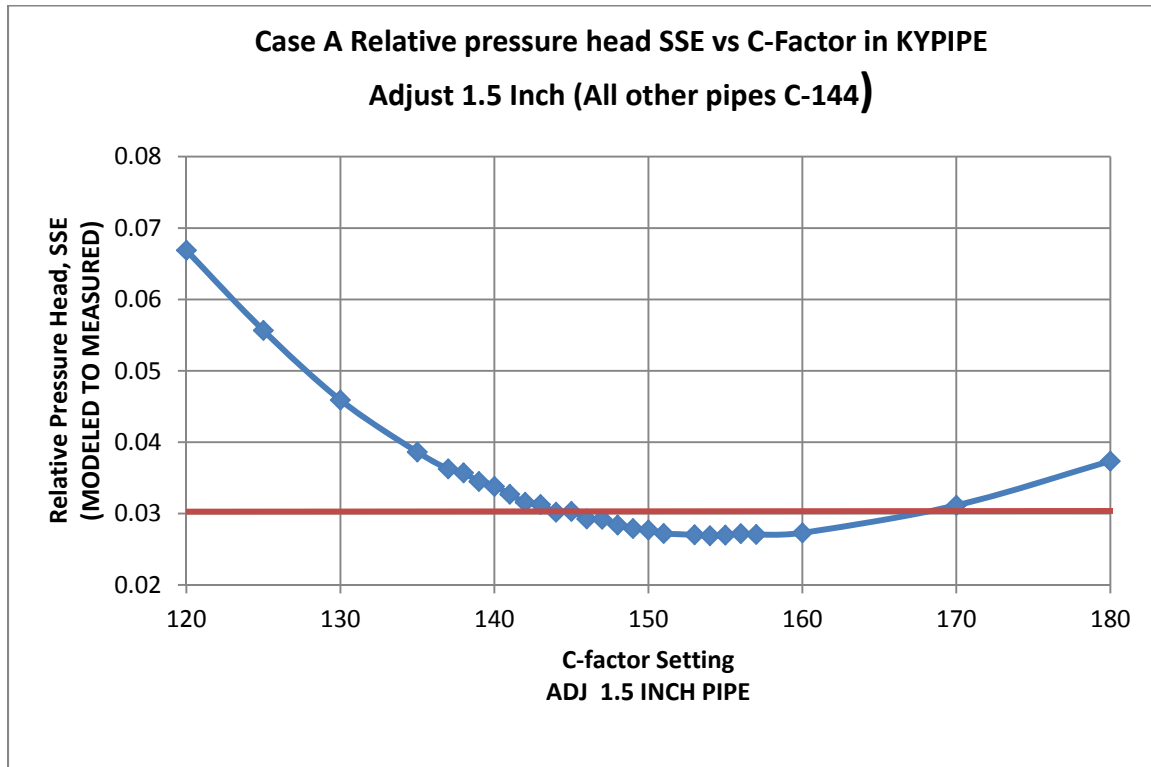
Figure 6.2: Case A: pressure calibration, adjusting 1.5 pipe settings

Finally, Fig. 6.3 illustrates the process of adjusting the *2.0 in* pipe sizes with the *1.0 in* pipes set to a constant C-value of *144* and the *1.5 in* pipes set to a constant C-value of *154*. The *2.0 in* pipe set to a value of *100* creates the lowest PSSE in Eq. 9. The red line in Fig. 6.3 represents the error level from the previous step (Fig. 6.2). The calibration at this point is the *1.0 in* pipes C-values set to *155*, the *1.5 in* pipes set to *141*, and the *2.0 in* pipes set to *100*.
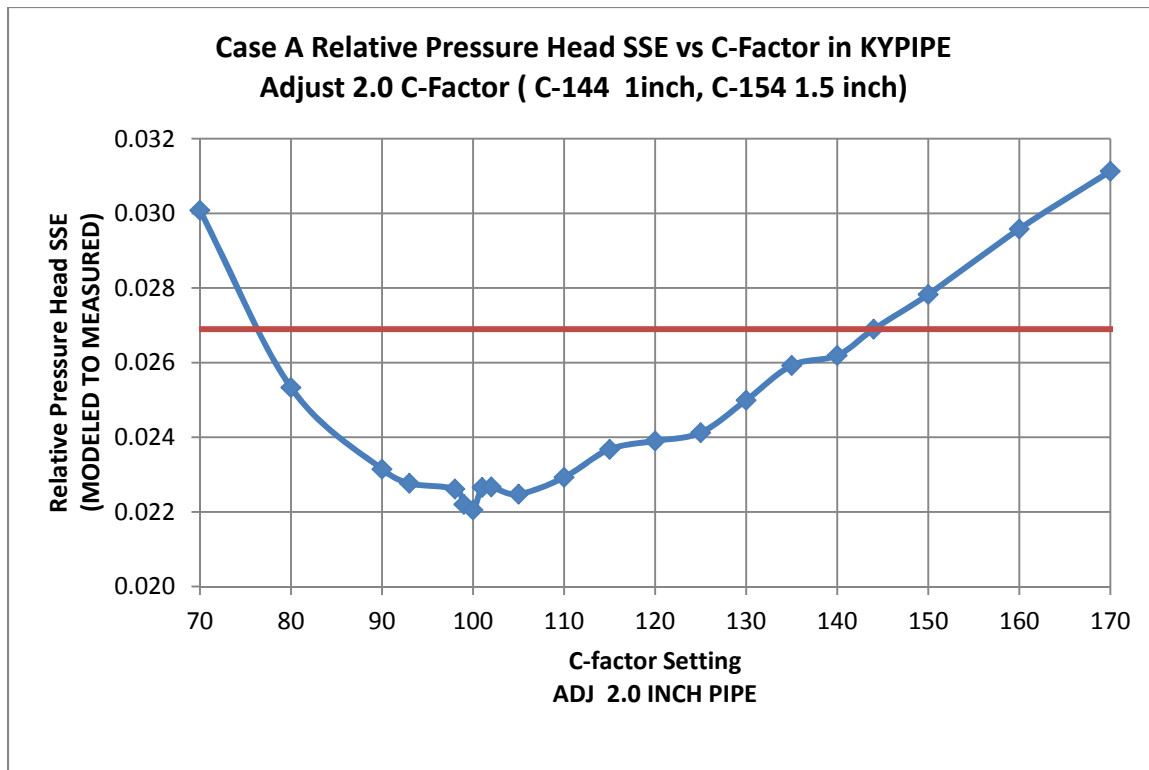
Figure 6.3: Case A: pressure calibration, adjusting 2.0 pipe settings

The process of individually adjusting each pipe size (the *1.0, 1.5*, and *2.0 in* pipes) while maintaining the other two pipes size's C-Value constant was carried out thru two further iterations. If a point was reached where the calibration could not be improved thru further refinement, the calibration effort was ended. The Sum of square errors between the measured pressure head values and the modeled pressure head values at the specific C-values was calculated for each pipe setting. The value that minimized the PSSE at each step was assigned to the respective pipe size being adjusted during that step. The process of adjusting the C-factors for each pipe size individually in Case A is presented in graphical form in appendices A. The process of adjusting the C-factors for each pipe size individually in Case A thru Case C are presented in graphical form in appendices A thru C. The final results for Case A is 103 for the 1.0 in pipe, 151 for the 1.5 in pipe, and 123 for the 2 inch pipe. The results of the pressure calibration for all three cases are presented in Table 6.2.

Table 6.2 Pressure calibration for Case A thru Case C

CALIBRATION TYPE	TEST SCENARIO	C FACTOR for pipe		
		1 inch pipe	1.5 inch pipe	2 inch pipe
PRESSURE CALIBRATION	CASE A	103	151	123
	CASE B	115	151	114
	CASE C	149	162	139

6.3 Velocity head calibration

The velocity head based calibration was performed in a similar manner to the pressure head based calibration. Average velocity measurements for flow moving thru a series of pipes to the locations of conductivity meters were estimated from the waveforms present in the measured conductivity time series from the measured times and known lengths of pipe materials. Figures 4.2, 4.3, and 4.5 in chapter 4 display the travel times to each meter from the injection at time zero for the three cases. Equation 10 is the sum of squares error equation that is to be minimized by adjusting the C-Values for the three pipe diameters. This represents the velocity objective function developed from reviewing the various different objective functions found thru the literature review. The formulation is in terms of relative errors similar to the Tabesh formulation (Eq. 5). The formulation in Eq. 10 doesn't include the W_p weighting turn in the Tabesh equation (Eq. 5).

$$VSSE = \sum_{i=1}^{NV} \left(\frac{w_v*(V_{obs,i}-V_{pred,i})}{w_v*(V_{obs,i})} \right)^2 \qquad (10)$$

where
W_v = conversion factor from velocity in *ft/s* to velocity head in *ft*.
$V_{obs,i}$ = observed average velocity measured from travel time of conservative injection location to point i
$V_{pred,,i}$ = model predicted average velocity measured from travel time of conservative injection location to point i
NV = the number of electrical conductivity meters and tank level meters.

The initial model in each case (case A, B, and C) was determined from uniformly adjusting all pipe roughness values. After the initial adjustment of all pipes sizes to the uniform C-value, each of the three pipe sizes were adjusted individually to the C-value that produces the lowest VSSE in Eq. 10 while keeping the other pipe diameter C-values constant. This process was carried out for two iterations.

For Case A, initially all pipe sizes where adjusted to the same roughness value. The C value that produced the lowest sum of errors in Eq. 10 was *135* as displayed in Fig. 6.4.
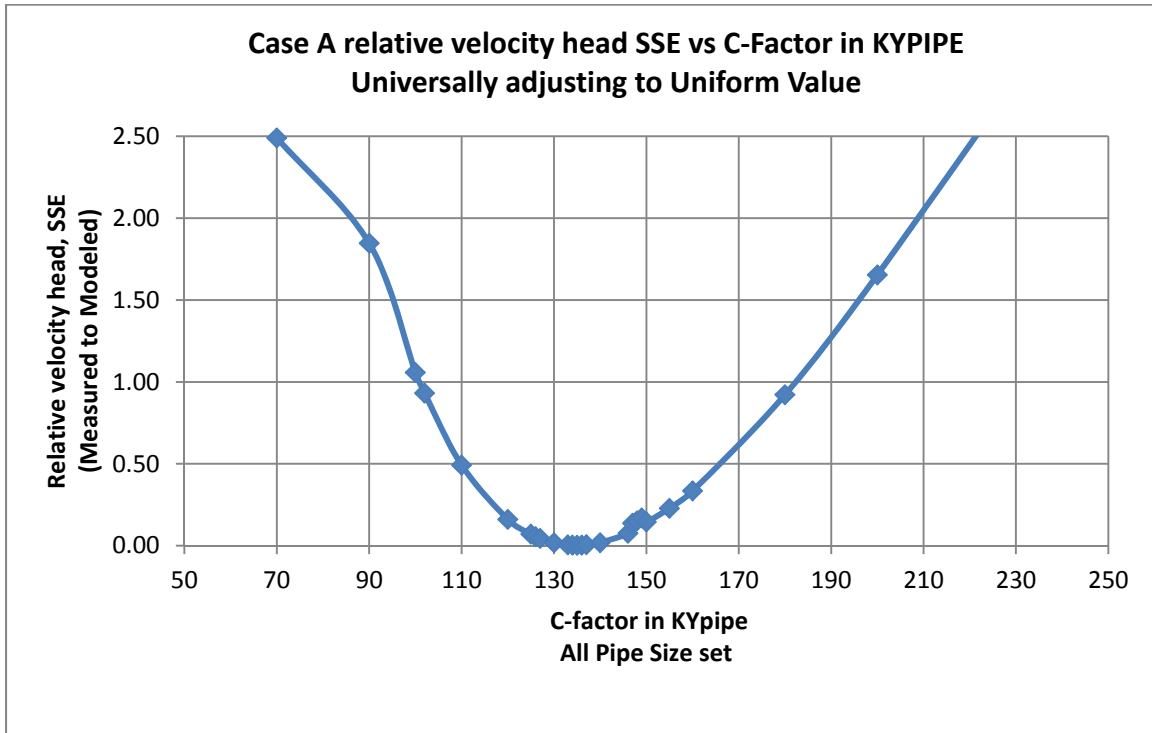
Figure 6.4: Case A: velocity calibration, initial C-Factor adjustment

The *1.5 in* pipes were adjusted while all other pipe sizes C values were set constant at *135* while calculating the error value produced of Eq. 10. The C-value that produced the lowest error was *135*, as shown in Fig. 6.5.
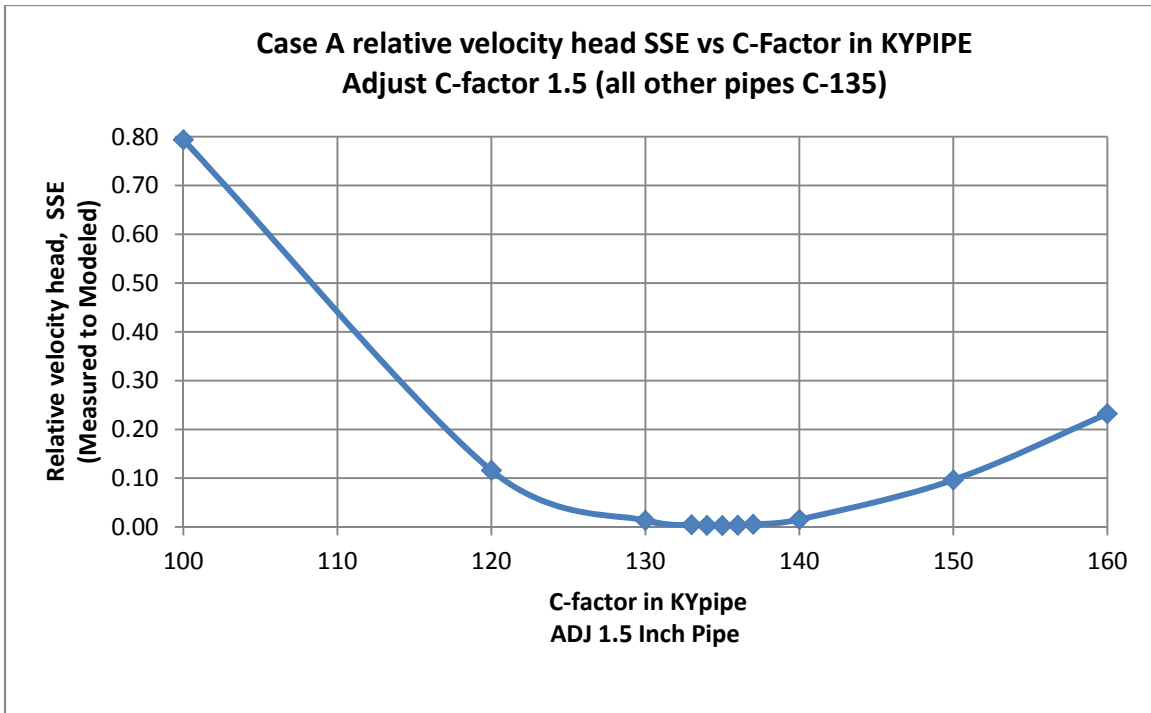
Figure 6.5: Case A velocity Calibration, 1.5 pipe Adjustment

The C-values were adjusted for the *2.0 in* pipes while keeping the *1.0 in* pipes C-value constant at *135* and *1.5 in* pipes constant at *135*. The value that produced the lowest error in Eqn. 10 was a C-value of *133* as illustrated in Fig. 6.6.
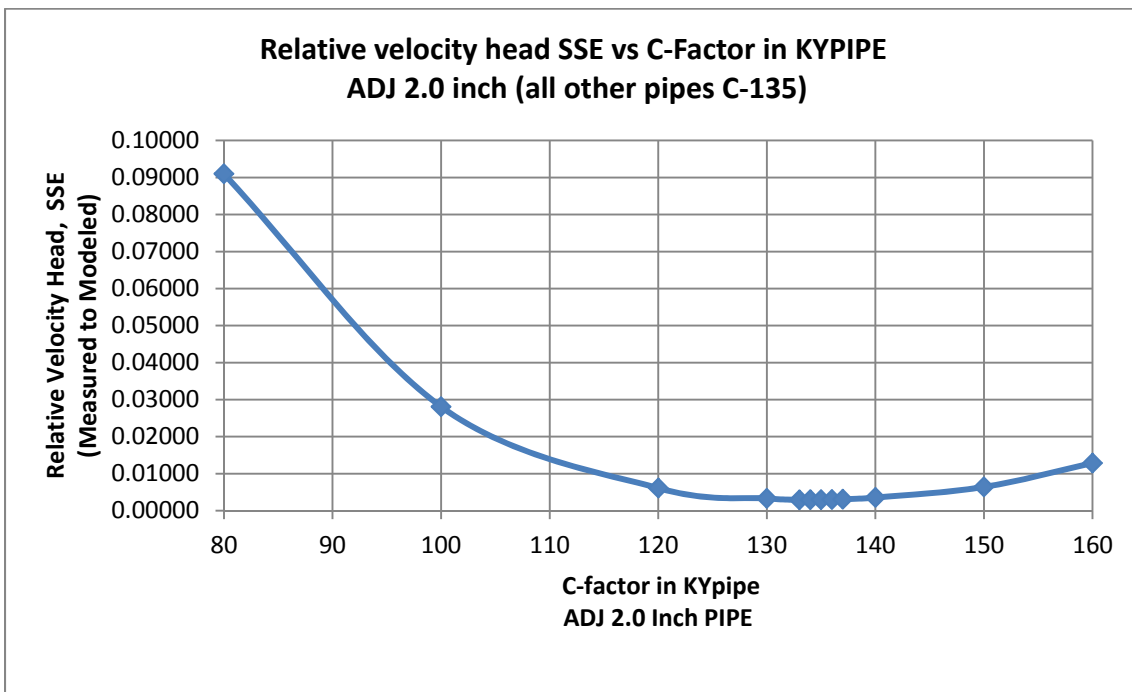
Figure 6.6: Case A velocity Calibration, 2.0 pipe Adjustment

The process of adjusting the *1.0 in* pipes, *1.5 in* pipes, and *2.0 in* pipes C-value individually while keeping the other pipes C-values constant and searching for the lowest possible error from Eq. 10 was repeated thru two iterations or until no error reduction in the Eq. 10 could be made. The final results for Case A velocity calibration are the *1.0 in* pipes *135*, the *1.5 in* pipes *135*, and the *2 in* pipes being *133*. The results of the velocity calibration for all three cases are presented as Table 6.3. The process of individually adjusting each pipe sizes C-factor independently from each case A thru C are presented in graphical form in appendices A thru C. The unrealistic value in Case B for the *2 in* pipe of *192*, seems to be from adding the of the CM 2 velocity measurements into the calibration.

Table 6.3 Velocity calibration for Case A thru Case C

CALIBRATION TYPE	TEST SCENARIO	C FACTOR for pipe		
		1 inch pipe	1.5 inch pipe	2 inch pipe
VELOCITY CALIBRATION	CASE A	135	135	133
	CASE B	134	146	192
	CASE C	151	151	129

6.4 Pressure & velocity head Calibration

The pressure and velocity head based calibration was performed in a similar manner to the pressure head calibration and velocity head based calibration. The two equations for the pressure and velocity head sum of square errors (Eq. 9 and Eq. 10) were combined into the same equation, Eq. 11. The units for both equations were dimensionless. Hence the units for Eq. 11 are also unit less. The initial model was determined from uniformly adjusting all pipe roughness values. After the initial adjustment of all pipes sizes to the uniform C-value, each of the three pipe sizes were adjusted individually to the C-value that produces the lowest sum of square errors while keep the other pipe sizes constant. This process was carried out thru two iterations. The process of individually adjusting each pipe sizes C-factor independently from each the case A, case B, and case C test are presented in graphical form in appendices A thru C. The final results of the pressure and velocity calibration for the three cases are presented as Table 6.4.

$$PVSSE = \sum_{i=1}^{20} \left(\frac{w_p*(P_{obs,i}-P_{pred,i})}{w_p*(P_{obs,i})} \right)^2 + \sum_{i=1}^{NV} \left(\frac{w_v*(V_{obs,i}-V_{pred,i})}{w_v*(V_{obs,i})} \right)^2 \qquad (11)$$

where

W_v = conversion factor from velocity in *ft/s* to velocity head in ft.

$V_{obs,i}$ = observed average velocity measured from travel time of conservative injection location to point i

$V_{pred,i}$ = model predicted average velocity measured from travel time of conservative injection location to point i

NV = the number of electrical conductivity meters and tank level meters.

W_p = conversion factor from pressure in psi to pressure head in ft.

$P_{obs,i}$ = observed pressure measured at location i , psi.

$P_{pred,i}$ = model predicted pressure measured at location i, psi.

Table 6.4 Pressure & Velocity calibration for Case A thru Case C

CALIBRATION TYPE	TEST SCENARIO	C FACTOR for pipe		
		1 inch pipe	1.5 inch pipe	2 inch pipe
PRESSURE & VELOCITY CALIBRATION	CASE A	120	139	111
	CASE B	125	149	163
	CASE C	149	153	134

6.5 Comparison between calibration methods

Equation 12 presents the general form for the adjusted R squared equation which served as the basis for determining if either the velocity head or pressure head measurements calibration efforts are an improvement over the baseline model. Each of the two calibration efforts, velocity head and pressure head based, will be compared using an adjusted R squared approach. Each of the resulting discrepancies, in the velocity head SSE from a purely pressure head based calibration effort and in the pressure head SSE from a purely velocity head based calibration effort was compared using an adjusted R square approach. Also the composite of both velocity head and pressure head SSE, using either the pressure head calibration C-Values or the velocity head calibration C-Values was developed for comparison. The comparisons were made against the baseline value using C-value of *150* for each pipe size roughness coefficients.

$$R^2{}_{ADJ} = 1 - \left(\frac{SSE/(n - K - 1)}{SST/(n - 1)}\right)$$

$$SSE = \sum (y_{predicted} - y_{measured})^2$$

$$SST = \sum (y_{measured} - y_{avg})^2$$

<div align="right">(12)</div>

where

n = number of measurement locations
K = the number of explanatory variables (for pressure or velocity calibration = 1. If both then = 2)

Chapter 7.   Results & Conclusions

7.1 Introduction

As Table 7.1 thru 7.3 will illustrate, the optimum calibration results from velocity head basis created a discrepancy in terms of the pressure heads basis in two of the three cases.   Using the pressure head basis created a discrepancy in terms the velocity heads in two of the three cases. The pressure head based calibrations tended to distort the velocity heads from the measured velocity head more than other way around. The problem was less prevalent in the branched case, Case C. This is due to possibly different configurations within a loop flow orientation being able better correlate with pressure measurement but heavily distort flow velocities in the network. These issues will be discussed in more detail in the next section. The three tables are presented with line numbers for easy reference during the discussion of the results and conclusions of the research.

7.2 Results & Conclusions Analysis

Table 7.1 presents the calibration results for Case A. As an example of the distortion phenomenon, and as Table 7.1 illustrates on line 4, the pressure head calibration improved the correspondence of measured to modeled pressure values by about *0.18* percentage points over the baseline (C values of *150* for all pipes roughness). The *0.18* percentage increase represents the pressure regression improving from *99.57%* (line 1) to *99.75%* (line 4). This represents a modest improvement of the ability of the model to represent pressures as measured. However the pressure head based calibration (again on line 4), distorts the correspondence between velocity measurements to velocity modeled results by *8.55* percentage points from the baseline. This represents the velocity regression decreasing from *95.10%* (line 2) to *86.55%* (line 4). The velocity head based calibration improves the correspondence between velocity measurements to modeled velocities by *4.51* percentage points. This *4.51* percentage improvement is from the regression changing from *95.10%* (line 2) to *99.44%* (line 5). However the velocity based calibration distorts the correspondence between pressure measurements to modeled pressures by *0.25* percentage points. Using the velocity measurement information in the calibration would be much superior to using the pressure measurement information to insuring the computer model approximates the real world behavior of the physical system for both velocities and pressures better than using exclusively pressure based data. However using just velocities or pressures to calibrate a model, tends to distort the other data type's modeled to measured correspondence. As lines 8 thru 10 illustrate, using both pressures and velocities in the calibration tends to increase the correspondence in both pressures and velocities over the baseline.

Table 7.1 Case A: calibration results

LINE NUMBER	CALIBRATION DESCRIPTION	R^2 adj	ΔR^2 adj	R^2 adj for other dataset	ΔR^2 adj
1	BASE LINE PRESSURE HEAD ONLY (C-150 for all pipe sizes)	99.57%			
2	BASE LINE VELOCITY HEAD ONLY (C-150 for all pipe sizes)	95.10%			
3	BASE LINE VELOCITY & PRESSURE HEAD (C-150 for all pipe sizes)	99.65%			
4	PRESSURE HEAD ONLY CALIBRATION (C-103 1 inch, C-151 1.5 inch, C-123 2.0 inch)	99.75%	0.18%	86.55%	**-8.55%**
5	VELOCITY HEAD ONLY CALIBRATION (C-135 1 inch, C-135 1.5 inch, C-133 2.0 inch)	99.44%	4.34%	99.32%	**-0.25%**
6	VELOCITY & PRESSURE HEAD (Using Pressure Head only Calibration) (C-103 1 inch, C-151 1.5 inch, C-123 2.0 inch)	99.81%	0.16%		
7	VELOCITY & PRESSURE HEAD (Using Velocity Head only Calibration) (C-135 1 inch, C-135 1.5 inch, C-133 2.0 inch)	99.48%	**-0.17%**		
8	PRESSURE & VELOCITY CALIBRATION (Using Velocity Head & Pressure Head data) (C-120 1 inch, C-139 1.5 inch, C-111 2.0 inch)	99.69%	0.04%		
9	PRESURE HEADS ONLY (Using PRESSURE & VELOCITY CALIBRATION) (C-120 1 inch, C-139 1.5 inch, C-111 2.0 inch)	99.81%	0.24%		
10	Velocity HEADS ONLY (Using PRESSURE & VELOCITY CALIBRATION) (C-120 1 inch, C-139 1.5 inch, C-111 2.0 inch)	98.96%	3.86%		

Table 7.2, on the next page, presents the calibration results for Case B. As a further example of the phenomenon and as Table 7.2 illustrates for Case B, the pressure head calibration improved the correspondence of measured to modeled pressure values by about 0.16 percentage points over the baseline. This *0.16%* improvement in the ability of the model to represent measured pressures is from *99.60%* (line 1 of Table 7.2) to *99.76%* (line 4). However the pressure head based calibration, distorts the correspondence between velocity measurements to velocity modeled results by *0.85* percentage points from the baseline. The velocity head regression goes from *98.14%* (line 2) to *97.29%* (line 4) using the pressure head calibration. The velocity head based calibration improves the correspondence between velocity measurements to modeled velocities by *1.73* percentage points. However the velocity based calibration distorts the correspondence between pressure measurements to modeled pressures by *0.02* percentage points. Using the velocity measurement information in the calibration would be much superior to using the pressure measurement information to insuring the computer model approximates the real world behavior of the physical system for both velocities and pressures. However using just velocities or pressures to calibrate a model in Case B, tends to distort the other data type's modeled to measured correspondence just as with Case A. As lines 8 thru 10 of Table 7.2 illustrate, using both pressures and velocities in the calibration tends to increase the correspondence in the velocities but not the pressures in the network.

Table 7.2 Case B calibration results

LINE NUMBER	CALIBRATION DESCRIPTION	R^2 adj	ΔR^2 adj	R^2 adj for other dataset	ΔR^2 adj
1	BASE LINE PRESSURE HEAD ONLY (C-150 for all pipe sizes)	99.60%			
2	BASE LINE VELOCITY HEAD ONLY (C-150 for all pipe sizes)	98.14%			
3	BASE LINE VELOCITY & PRESSURE HEAD (C-150 for all pipe sizes)	99.55%			
4	PRESSURE HEAD ONLY CALIBRATION (C-115 1 inch, C-151 1.5 inch, C-114 2.0 inch)	99.76%	0.16%	97.29%	**-0.85%**
5	VELOCITY HEAD ONLY CALIBRATION (C-134 1 inch, C-146 1.5 inch, C-192 2.0 inch)	99.87%	1.73%	99.58%	**-0.02%**
6	VELOCITY & PRESSURE HEAD (Using Pressure Head only Calibration) (C-115 1 inch, C-151 1.5 inch, C-114 2.0 inch)	99.82%	0.27%		
7	VELOCITY & PRESSURE HEAD (Using Velocity Head only Calibration) (C-134 1 inch, C-146 1.5 inch, C-192 2.0 inch)	99.69%	0.14%		
8	PRESSURE & VELOCITY CALIBRATION (Using Velocity Head & Pressure Head data) (C-125 1 inch, C-149 1.5 inch, C-163 2.0 inch)	99.74%	0.19%		
9	PRESURE HEADS ONLY (Using PRESSURE & VELOCITY CALIBRATION) (C-125 1 inch, C-149 1.5 inch, C-163 2.0 inch)	96.65%	**-2.95%**		
10	Velocity HEADS ONLY (Using PRESSURE & VELOCITY CALIBRATION) (C-125 1 inch, C-149 1.5 inch, C-163 2.0 inch)	99.41%	1.27%		

Table 7.3 on the following page presents the calibration results for Case C. Case C is the branched network case for calibration. As a further example of the phenomenon, and as Table 7.3 illustrates for Case C, the pressure head calibration decreases the correspondence of measured to modeled pressure values by about *0.23* percentage points over the baseline. This *0.23* percentage decrease in R^2 is from *99.47%* (line 1) to *99.24%* (line 4). This decrease is due to the R^2 measurements being based on the absolute square of errors in pressure head measured to modeled, but the calibration is based relative pressure head measured to modeled errors. The only way to lower the pressure head relative errors tends to distort the pump pressure absolute errors very heavily. For the branched case the pressure head based calibration distorts the correspondence between velocity measurements to velocity modeled results by *1.84* percentage points. The *1.84* percentage change is from the regression adjusting from *94.67%* (line 2) to *93.83%* (line 4). The velocity head based calibration improves the correspondence between velocity measurements to modeled velocities by *0.58* percentage points. The *0.58* percentage change is from *95.67%* (line 2) adjusting to *96.25%* (line 5).The velocity based calibration improves the correspondence between pressure measurements to modeled pressures by *0.01* percentage points. Like the looped network cases A and B, using the velocity measurement information in the calibration would be more superior to using the pressure measurement information to insuring the computer model approximates the real world behavior of the physical system for both velocities and pressures. However using just velocities or pressures to calibrate a model in Case C tends to distort the other data type's modeled to measured correspondence just as with Case A and Case B.

Table 7.3 Case C calibration results

LINE NUMBER	CALIBRATION DESCRIPTION	R^2 adj	ΔR^2 adj	R^2 adj for other dataset	ΔR^2 adj
1	BASE LINE PRESSURE HEAD ONLY (C-150 for all pipe sizes)	99.47%			
2	BASE LINE VELOCITY HEAD ONLY (C-150 for all pipe sizes)	95.67%			
3	BASE LINE VELOCITY & PRESSURE HEAD (C-150 for all pipe sizes)	99.60%			
4	PRESSURE HEAD ONLY CALIBRATION (C-149 1 inch, C-162 1.5 inch, C-139 2.0 inch)	99.24%	**-0.23%**	93.83%	**-1.84%**
5	VELOCITY HEAD ONLY CALIBRATION (C-151 1 inch, C-151 1.5 inch, C-129 2.0 inch)	96.25%	0.58%	99.48%	0.01%
6	VELOCITY & PRESSURE HEAD (Using Pressure Head only Calibration) (C-149 1 inch, C-162 1.5 inch, C-139 2.0 inch)	99.42%	**-0.18%**		
7	VELOCITY & PRESSURE HEAD (Using Velocity Head only Calibration) (C-151 1 inch, C-151 1.5 inch, C-129 2.0 inch)	99.60%	0.00%		
8	PRESSURE & VELOCITY CALIBRATION (Using Velocity Head & Pressure Head data) (C-149 1 inch, C-153 1.5 inch, C-134 2.0 inch)	99.60%	0.00%		
9	PRESURE HEADS ONLY (Using PRESSURE & VELOCITY CALIBRATION) (C-149 1 inch, C-153 1.5 inch, C-134 2.0 inch)	99.50%	0.03%		
10	Velocity HEADS ONLY (Using PRESSURE & VELOCITY CALIBRATION) (C-149 1 inch, C-153 1.5 inch, C-154 2.0 inch)	98.85%	3.18%		

In all three cases (case A thru C) the velocity data based calibration is superior to both pressure data based calibration since it both optimizes the correspondence between the model and measured basis of data while minimizing the distortion in the other basis of data. Using the pressure data tends to distort the velocities in the network significantly from measured results.   This is true in the other direction as well; using only velocity based data tends to distort the pressures in the network from measured results. From the standpoint of system management, a hydraulic calibration should both provide both an optimal velocity and an optimal pressure representation. If the goal is to both calibrate the model to best represent both pressures and velocity, it is important to realize that calibrations using exclusively pressure data will distort the velocity correspondence between model to measured velocities and vice versa.   The problem can be expected to be worse in more looped networks than branched networks as the experimental cases demonstrate. Utilizing the pressure head calibration as the basis without consideration of velocity heads as measured in the system, would greatly reduce the effectiveness of the model to approximate velocities within the physical system due to compensating errors. In conclusion, both data types are necessary for proper calibration.

The error in the pressure measurement devices is listed as *+/-0.50%* of the full scale of measurement range (*0* to *30 psi*). This translates into an approximate maximum plus or minus error of *0.35 ft.* for each pressure head measurement before accounting other experimental random errors and noise. While the errors in the velocity heads vary from measurement to measurement, it can be see that the time measurements for the plug of the conservative tracer have a maximum error of *+/- 2 seconds* of about *0.18 ft.* for any velocity head measurement. Thus the better performance of velocity head calibration may be due to greater accuracy in measurement data for velocity head measurements over pressure head measurements. An additional issue with the measured pressures was that the pressure measured at the pump was higher than modeled pressure at the location. The pump measurement location was placed at the inlet side of the pump housing as illustrated in Chapter 3. The difference between the baseline modeled pressure head and the measured pressure head was off by about one velocity head. This represents the approximate amount of energy lost from friction of the flow against the impeller blade before the energy (in terms of flow and pressure) is supplied into the water distribution system. Despite these issues, it has been shown that empirical and experimental that both velocity head measurements and pressure head measurements are required to fully calibrate a looped system to avoid compensating errors during real world calibration work. This follows from the discussion in the preceding paragraphs.

The calibration values for the three tests are presented in Table 7.4. While both the looped simulations (case A and case B) reduced to almost identical C-Factor calibrations using the pressure data. The velocity based data for both case A and case B had quite different calibration solutions. The branched (Case A & Case B) and

looped configuration (Case C) had quite different calibration results. This is in spite of the data being taken within the same laboratory network model with the only change being the opening or closing of connection pipes in the model and the selection of velocity head measurement locations. The results presented in Table 7-4 show the critical important of performing calibration using multiple test scenarios since the calibration from one configuration may be quite different from another configuration, even within a simple laboratory model with only a slight change in location of measurement sites.   Extrapolating to real world network calibration work, multiple day scenarios or time scenarios are necessary to insure that the calibration data collection and calibration of network parameters applies to the greatest possible configurations of demands and network reservoir levels.

Table 7.4 Case A thru Case C calibration results summary

CALIBRATION TYPE	TEST SCENARIO	C FACTOR for pipe		
		1 inch pipe	1.5 inch pipe	2 inch pipe
PRESSURE CALIBRATION	CASE A	103	151	123
	CASE B	115	151	114
	CASE C	149	162	139
VELOCITY CALIBRATION	CASE A	135	135	133
	CASE B	134	146	192
	CASE C	151	151	129
PRESSURE & VELOCITY CALIBRATION	CASE A	120	139	111
	CASE B	125	149	163
	CASE C	149	153	134

The case studies presented in this research relates to the general outstanding question of the possibility of creating a global general calibration standard for providing calibration of network models. The experimental scenario presents cases using a simple laboratory model where calibration doesn't converge to the same solution during different experimental setups. It also shows that calibration data selection locations can be quite critical to calibration solutions and that both flow and pressure data should be used for the best calibration solution. It also shows that a looped configuration and a branch configuration can reduce to quite different calibration results even within a very small network. The only different in the cases presented are a few values being either closed or open and slight differences between tank and reservoir levels. The work also shows the wide range of calibration parameters within a very simple laboratory model calibration effects under different network configurations, and thus the importance of using multiple network system configurations during network calibration.

In reference to real systems, it is important to realize that an optimum calibration using one set of data and one possible state of a network may not be the

optimum calibration using a different set of data and a different network state. In addition, the selection of data measurement locations may quite radically change the solution results of calibration parameters. The research also demonstrates the necessity of using both velocity and pressure measurements to insure the calibration effect both optimizes the velocity and pressure correspondence in the model to the true field system since the use of one source of data in this case study distorts the correspondence in the other source of data.

Some results oriented engineering judgment, above purely quantitative basis, was required for optimal system calibration based on the discrepancy created in the velocity basis errors from the pressure basis calibration, and vice versa. Both types of data were required for best calibration of the network model, whereas much calibration work in the literature is based exclusively on the use of the pressure data for model calibration. The errors in the pressure data tend to be balanced by inverse errors in the velocity head data to some extent. It was shown in the discussion of the results of the three cases, that pressure only based calibration tended to distort velocities over the baseline and velocity only based calibrations tended to distort pressures over the baseline. However when the two measurement classes are combined, a better calibration was able to be made were both pressures and velocities could be improved over the baseline.

Finally, the literature review on sampling design for network calibration made the assumption that a variance or standard deviation could be assumed a priori to the calibration effort. The referenced articles from Yoo (Yoo, Chang, & Jun, 2012)and Uber (Uber & Bush, 1998) utilized an assumption of a known constant a priori variance estimate. This assumption on variance was made so that an optimal sampling design for pressure or flow measurements in the water distribution system for calibration purposes could be made. However, it will be shown the standard deviance or variance is functionally contingent on the level of pressure or the level of flow being measured. The data for the three cases presented in Tables 4.3, 4.4, and 4.9 were analyzed to test the assumption of a constant standard deviation or variance independent of the measured average for a time series of data collected during the steady state. Other steady-state scenarios data sets using the same laboratory model were also tested. The results are presented in figures 7.1 and 7.2. Each of the points in the two figures represents a node measured average pressure or flow and standard deviation for the time series of pressure or flow data at a measurement site. Each measurement in figures 7.1 and 7.2 were made using the same type/brand of instrument.
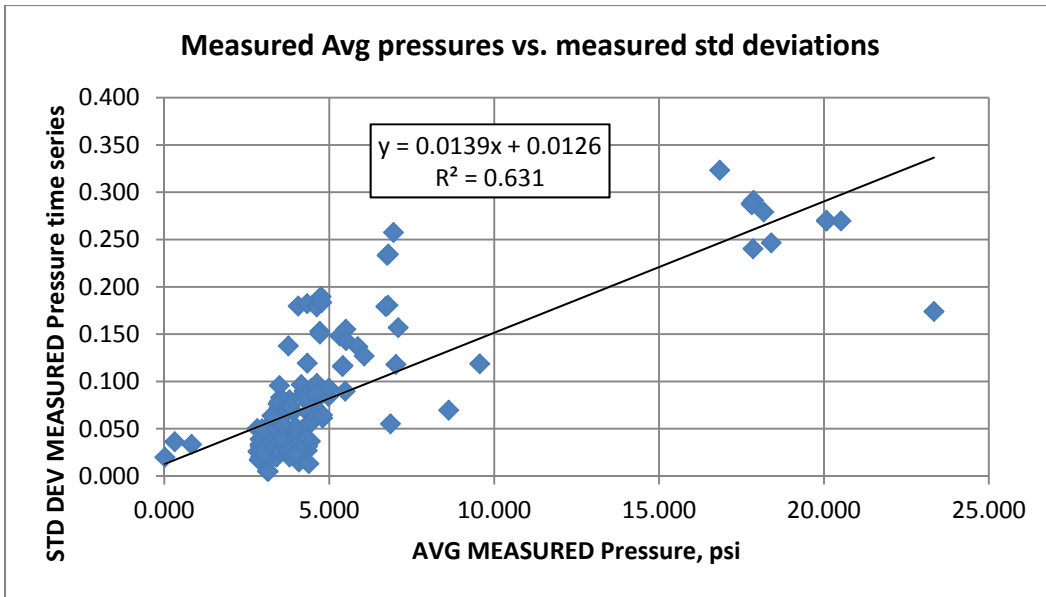
Figure 7.1: Comparison of collected average pressures vs. standard deviation during measurement of average pressure
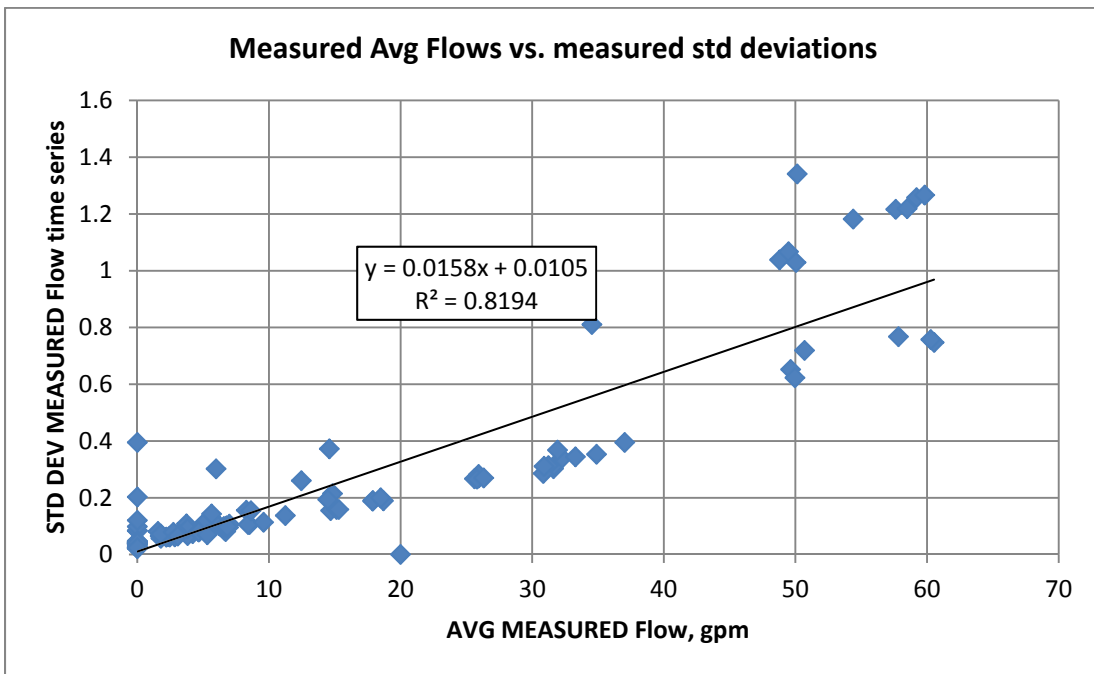
Figure 7.2: Comparison of collected average flow vs. standard deviation of during measurement of average flow

As Figure 7.1 and 7.2 illustrate, the standard deviation of measured values at a measurement site is an increasing function of the relative measurement value using an R squared criteria. Visually inspecting figures 7-1 and 7.2 shows that as the size of the relative measured pressure or flow increases the measured standard deviation also increases. In addition, the range of possible standard deviation/ variances also

increases. Appendix 4 presents the results of a Fisher tests for a zero slope in both regressions. The Fisher tests (Eq. 7) within excel show that the variance/ standard deviation increases at least linearly as the function of the measurement value. In addition, the range of possible variance/ standard deviation about the average increases, so the assumption of constant variance cannot be made using the Szroeter test statistic (Eq. 8). Thus it can be seen experimentally that using measurement instruments within a simple lab model to measure flow and pressure is linearly dependent on the measurement level and has a variance range that is dependent on the measurement level. It can be expected that both of these problems will also occur in real world data collection in a water distribution system. It can be expected that these increase to a greater degree than in the laboratory model for real world distribution system measurements. Some experimental errors are contingent on the scale of pressure or flow within the network and the physical volatility about a steady-state can be expected to oscillate increasingly as the energy level within a network increases. Optimal sampling designs made on the basis of an assumption of a constant known variance of measurement that ignores these issues can lead to false confidence in the sampling design and suboptimal sampling designs. Thus a quality control or verification step should be included after data is collected using an optimal sampling design to verify any expected measurement variance assumptions following data collection. The challenge is that collecting sufficient data in the field to verify variance assumptions can be difficult or impossible due to practical considerations.

As Figs. 4.2, 4.3, and 4.5 illustrate, there was a gradual arrival of the contaminant over time. Figure 4.5 is reprinted on the following page as Fig. 7-3 for the purpose of the discussion on this phenomenon. This indicates that there is some amount of diffusion of chemical concentration traveling faster than the turbulent fluid flow of the "plug" of the conservative tracer which occurred in all three tests and at all measured locations. In essence, the higher concentration of tracer is moving independent of the fluid flow into regime into regimes of lower concentration. If the conservative tracer were moving fully by convection, the concentration as represented by electrical conductivity would remain unchanged until being changed instantly to the concentration of the fluid flow of injected material reached the location were the measurement is taken. (Farlex, 2013) While the diffusion of a chemical agents occurs in addition to convection of the chemical traveling with the flow thru the water distribution model is recognized in the engineering literature, most software for representing contaminant travel in a water distribution network assume dispersion is negligible as a computational simplification. (Basha & al., 2007). Thus experimentally the research demonstrates the presence and importance of diffusion of chemical concentrations are an important component to fully represent the travel of chemical concentrations throughout a water distribution network in both branched and looped networks. The rate of diffusion is expected to be fully independent or very nearly so to fluid flow, whereas convection is dependent on fluid flow. The longer it takes for a fluid flow to reach a point, the more gradual will be the slope of the concentration as a function of time. A more gradual increase in

concentration over time is visual for the most distant measurement locations that are the farthest from the injection location (temporally and/or spatially).
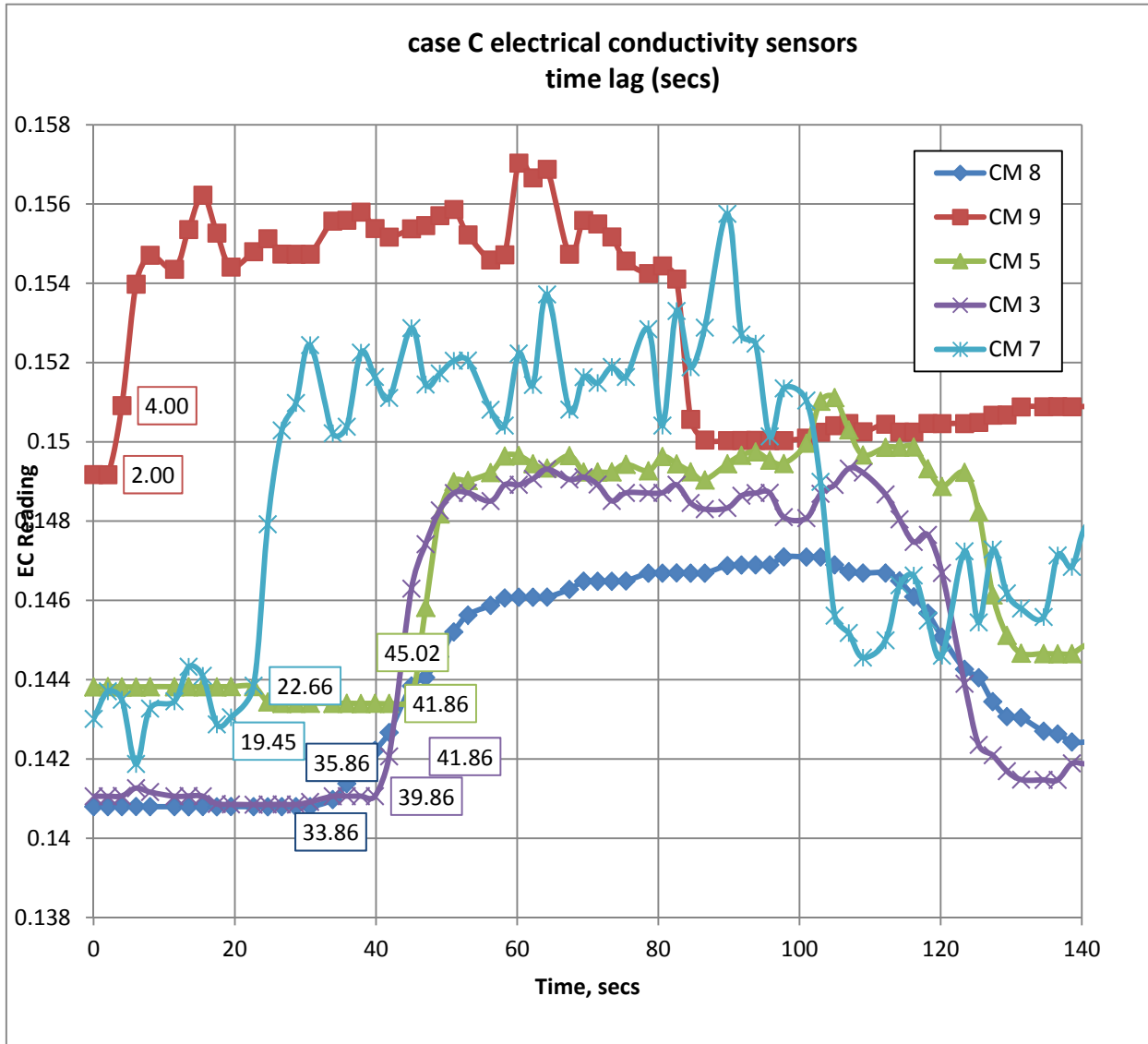
Figure 7.3: Case C EC sensor plot illustrating diffusion within the laboratory model

The most important finding of the research is the experimental demonstration of diffusion occurring within the scenarios studied of the conservative tracer.   As mentioned previously, the effect of diffusion as a component of contaminant traveling is recognized by H.A. Basha and others in the engineering literature but most commercial software applications ignore diffusion as a computational simplification. Research should be conducted of when and under what circumstances that this simplification is an acceptable practice.   In addition while advection of different contaminants will be the same since the contaminant particles are traveling with the fluid flow, it can reasonably be expected that different types of contaminants will have different rates of diffusion throughout a network.   The study of diffusion rates for commonly expected contaminants into a water distribution network, the development of new commercial software routines that include diffusion as a component, study of the current practice of ignoring diffusion, and a study for when and where ignoring diffusion is acceptable are the four areas of possible future research work.

The development of an optimal sampling design procedure for network calibration that includes a nonconstant variance over a constant variance assumption is viewed as necessary by the author. To optimally perform a sampling design of data collection locations it is necessary to consider the dependance of expected measurement level on variance. The a priora assumption of a constant measurement variance is not empirically valid and requires a verification step be added to optimal design procedures.   This step would verify the a priora assumptions made while selecting data collection locations is necessary before a general optimal design procedure for network calibration is accepted as a practice in the opinion of the author as developed will performing this research work. Future research can be made to verify and test if this is truelly an issue of great import for optimal sampling design or it is an acceptable simplification under various conditions and types of networks.

The research demonstrated experimentally that multiple calibration scenarios are required in water distribution systems. This is due to quite different calibration parameter results that can occur even under a very simple laboratory model. Adding a single velocity measurement site quite radically changed the ideal calibration parameters to best respresent the network under the identical scenario.   Future research work can be made to more objectively and numerically determine the number and types of calibration scenarios that are required for a robust calibration that represents physical water distribution model as realistically as possible under numerous scenarios for the best management tool.   In addition, it was found that both velocity and pressure measurements were required to avoid compensating errors occuring as result of the calibration. For example, using only pressure measurements as a basis to calibrate a network tended to distort velocities in the network as measured and vice versa. This phenomenon was worst in the looped network versus a branched network. Future research could be geared toward determining the degree

of "loopness" where compensating errors can be a real problem. Future research can also be geared toward determining the amount of pressure and velocity measurements which should be made to avoid compensating errors which create a calibration that represents the pressures very well but not the velocities in the network very well and vice versa.

Appendix A Case A calibration plots
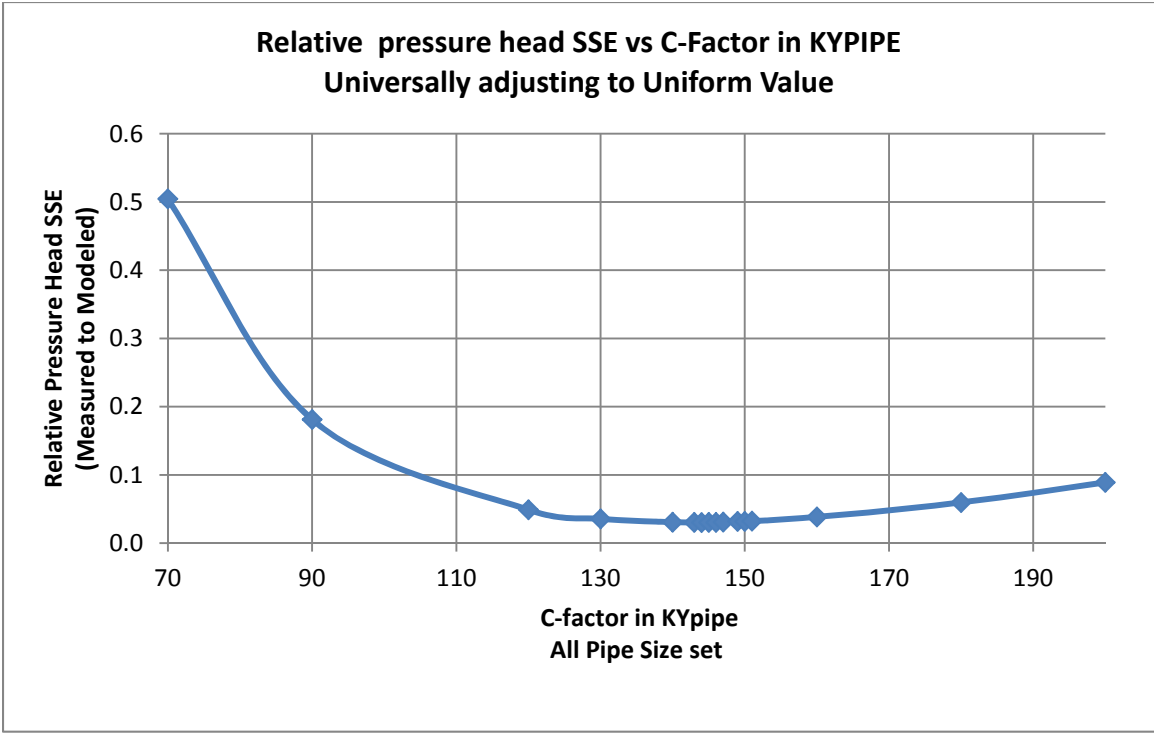
Figure A.1: Case A pressure head calibration, universal adjust of all pipe sizes
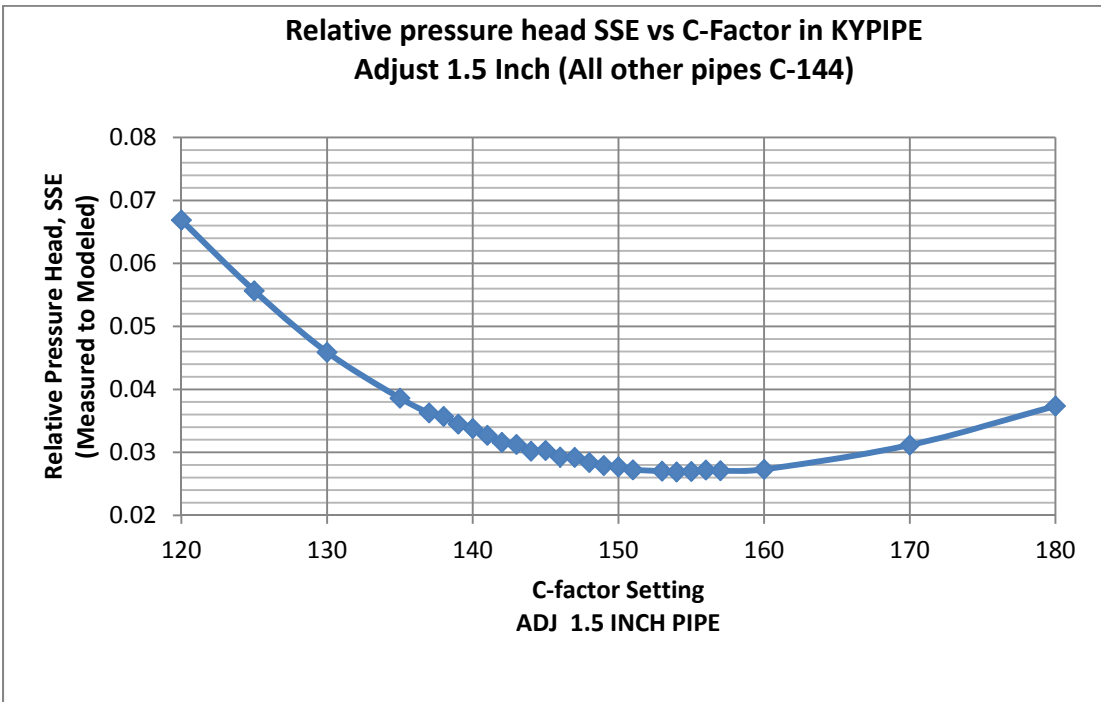
Figure A.2: Case A pressure head calibration, 1.5 inch pipe adjustment
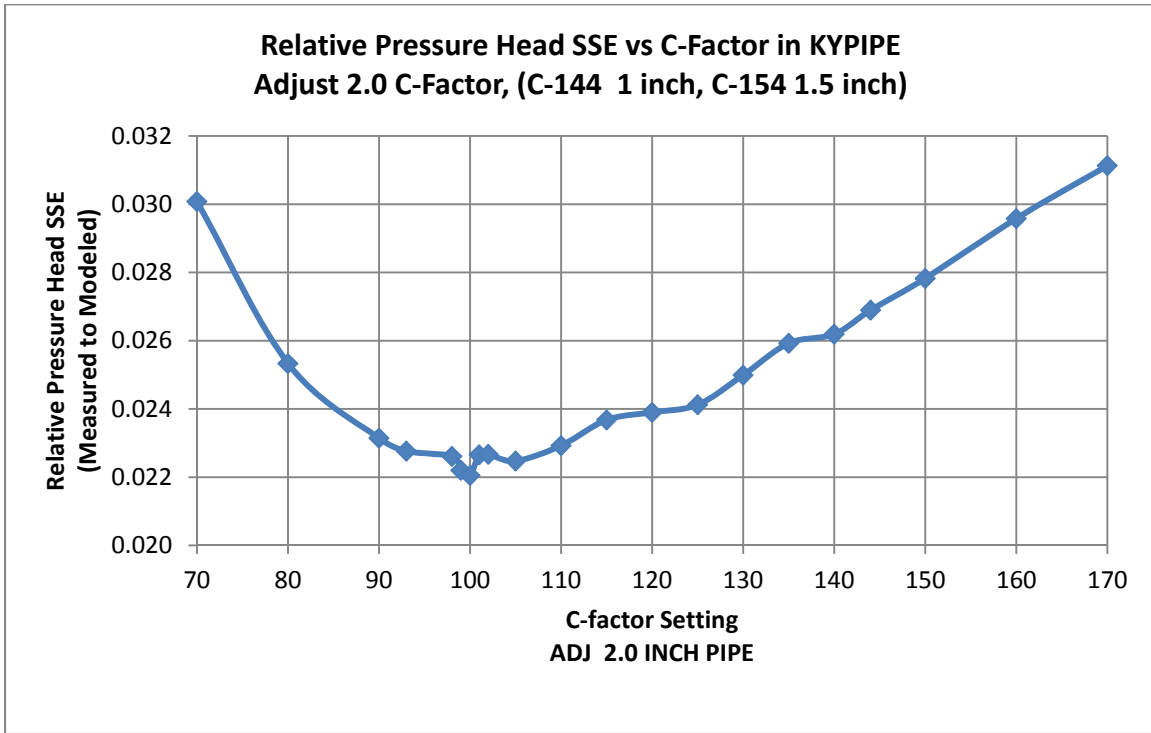
Figure A.3: Case A pressure head, 2.0 inch pipe adjustment
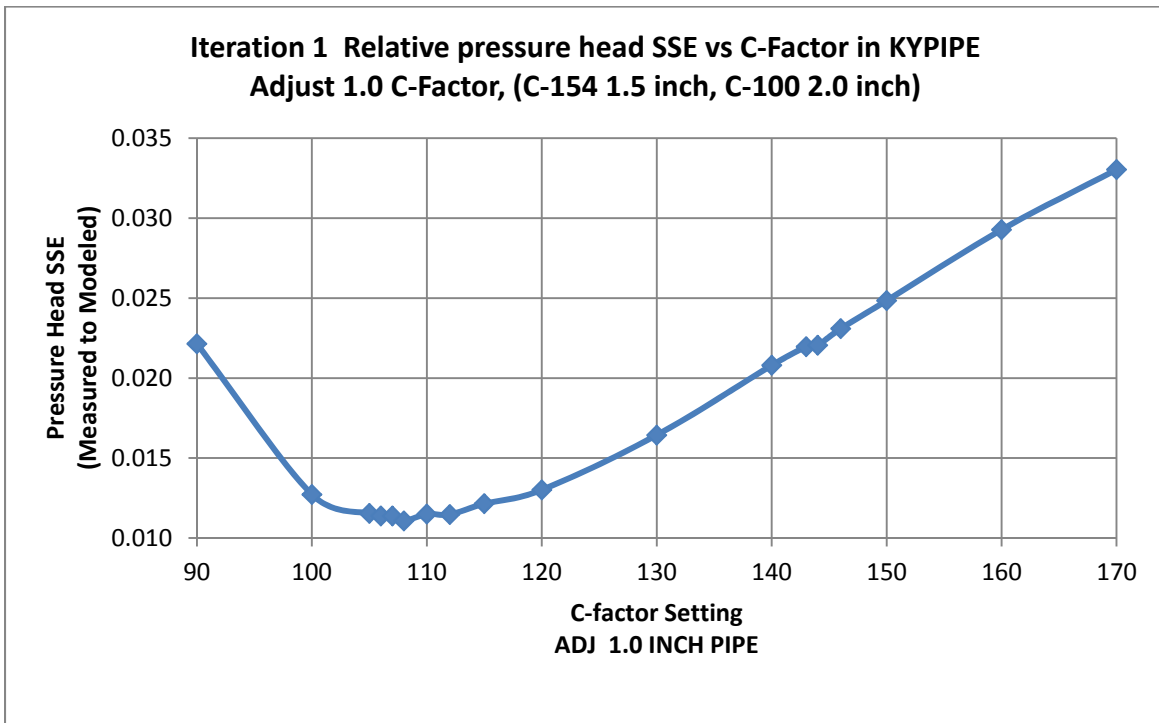
Figure A.4: Case A pressure head, Iteration one, 1.0 inch pipe adjustment
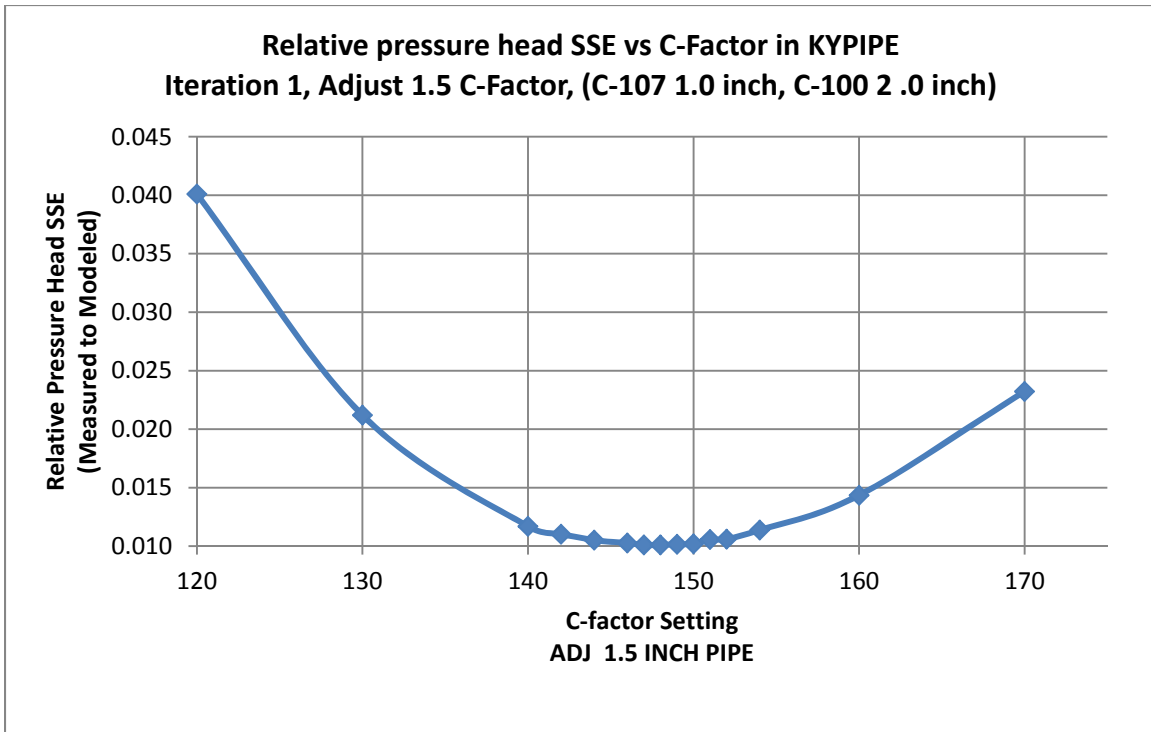
Figure A.5: Case A pressure head calibration, Iteration one, 1.5 inch pipe adjustment
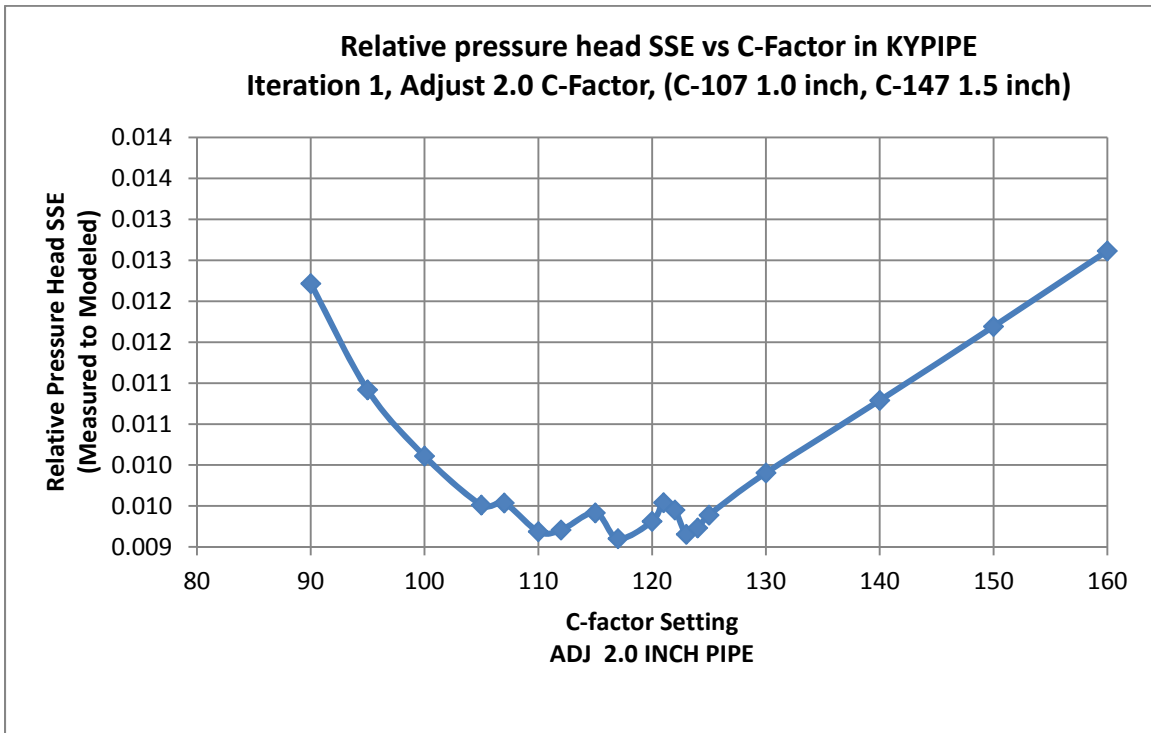
Figure A.6: Case A pressure head calibration, Iteration one, 2.0 inch pipe adjustment

68
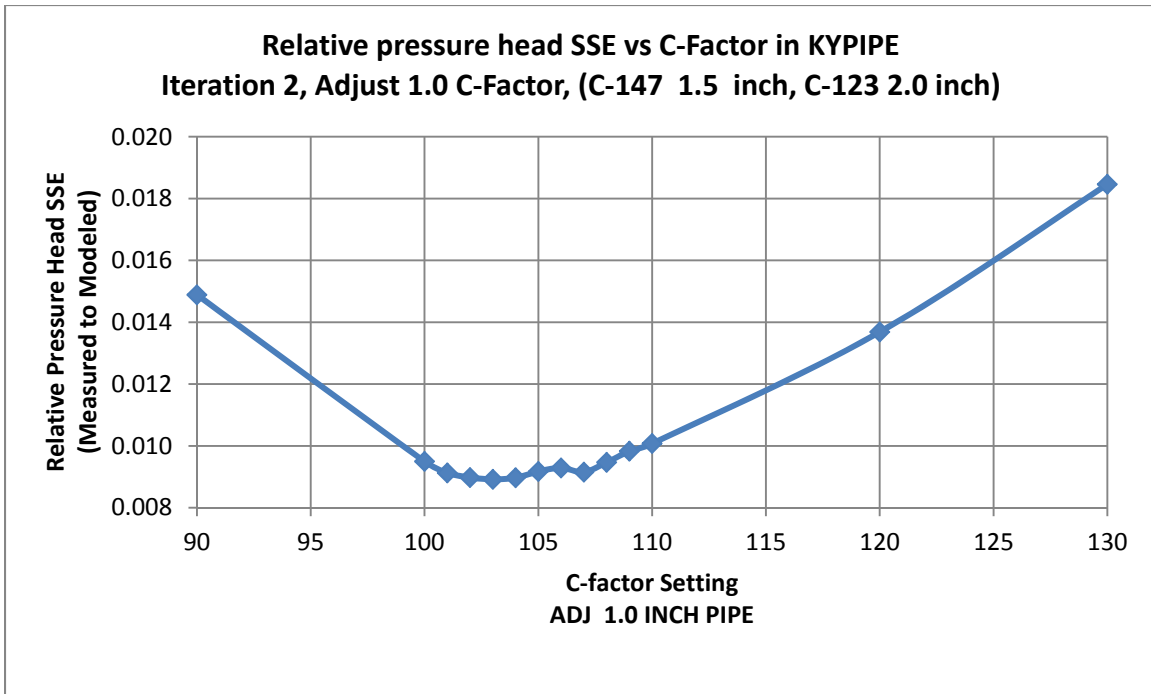
Figure A.7: Case A pressure head calibration, Iteration two, 1.0 inch pipe adjustment
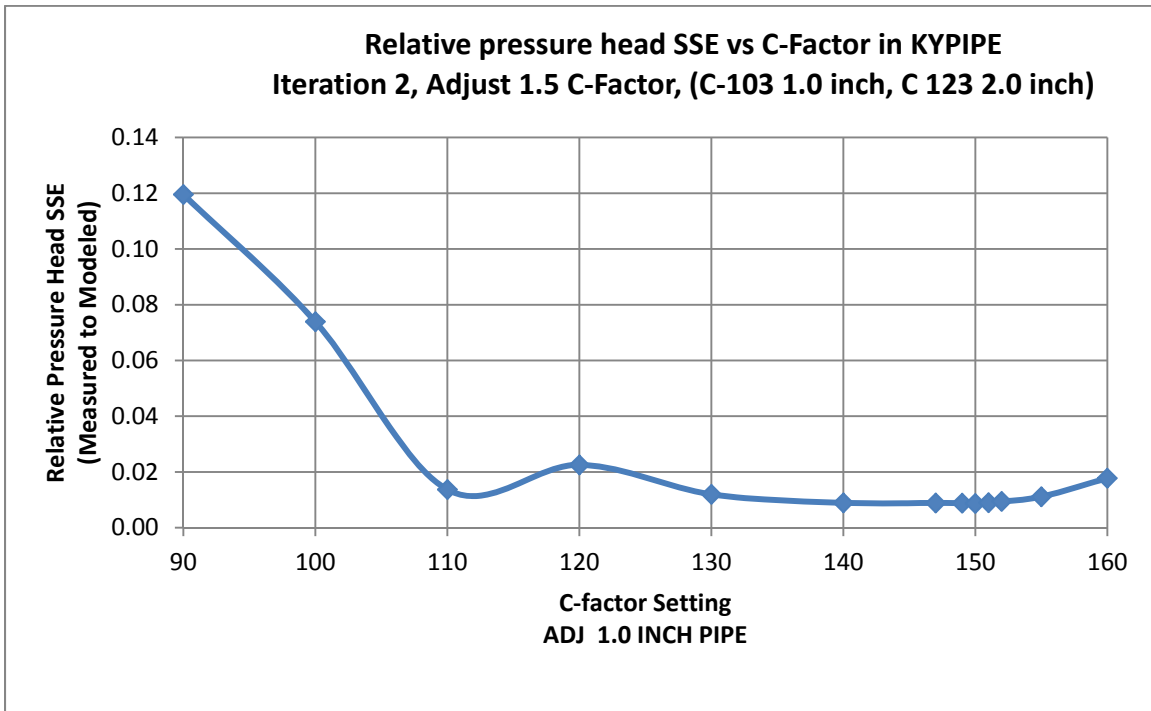
Figure A.8: Case A pressure head calibration, Iteration two, 1.5 inch pipe adjustment
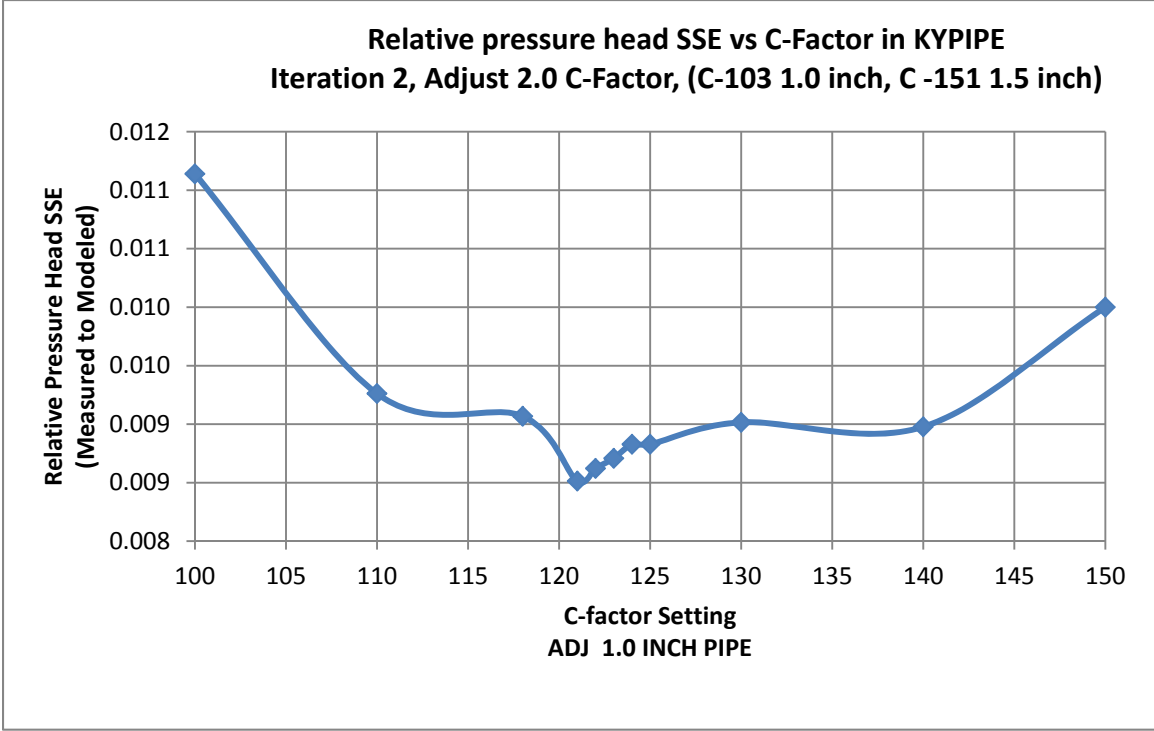
Figure A.8: Case A pressure head calibration, Iteration two, 2.0 inch pipe
Final adjustment
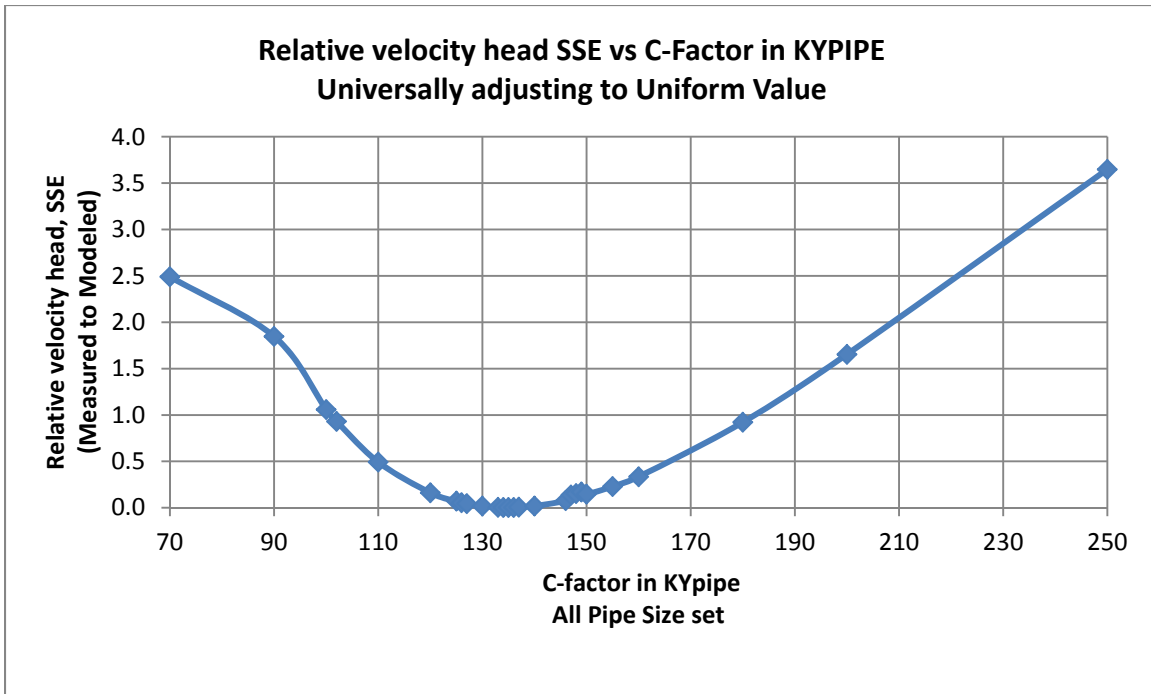
Figure A.9: Case A velocity head calibration, universal adjust of all pipe sizes
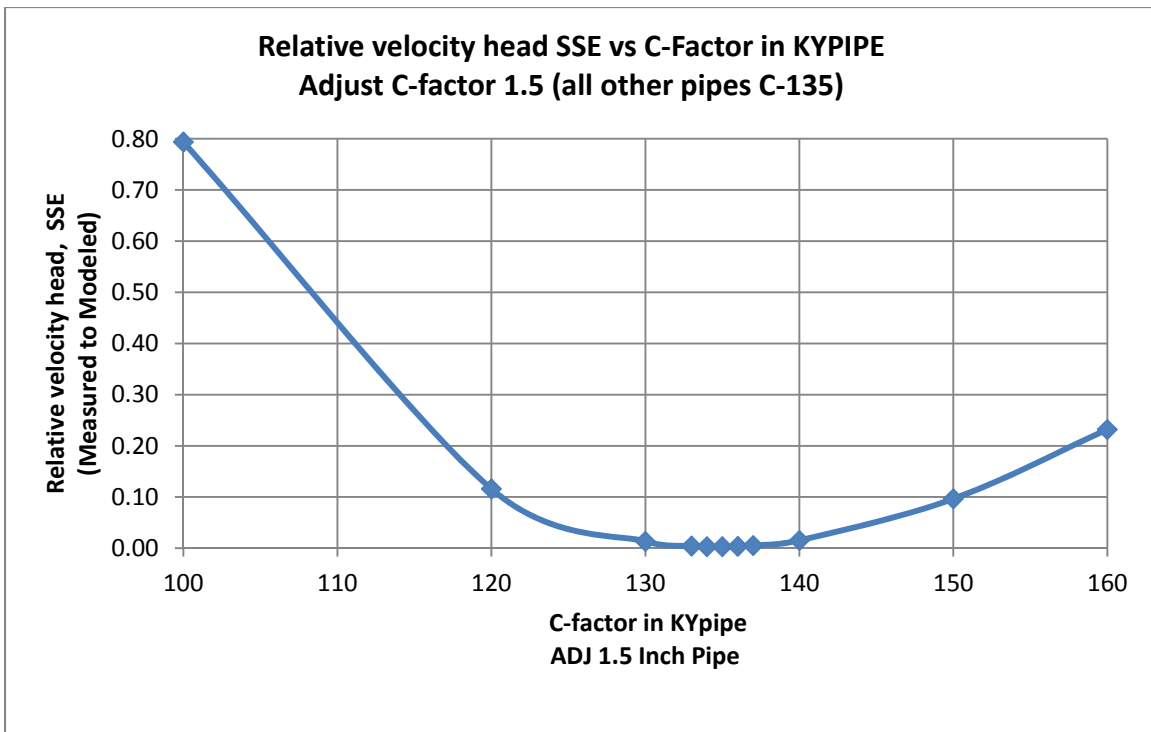
Figure A.10: Case A velocity head calibration, 1.5 inch pipe adjustment
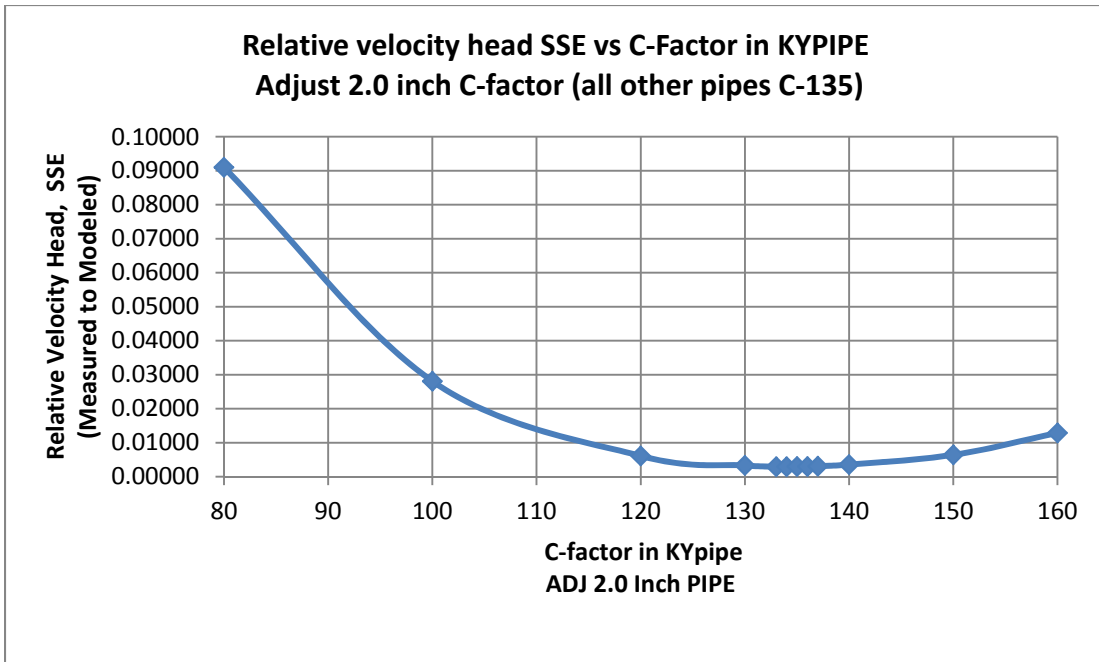
Figure A.11: Case A velocity head calibration, 2.0 inch pipe adjustment
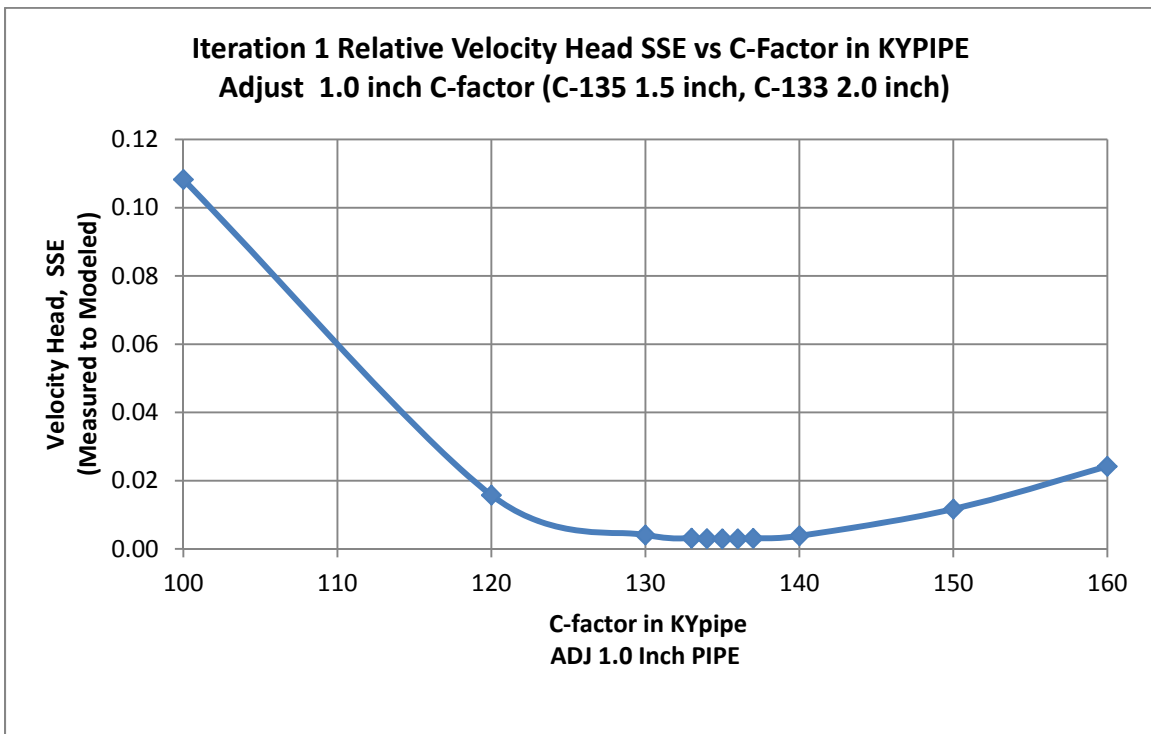
Figure A.12: Case A velocity head calibration, Iteration one, 1.0 inch pipe adjustment
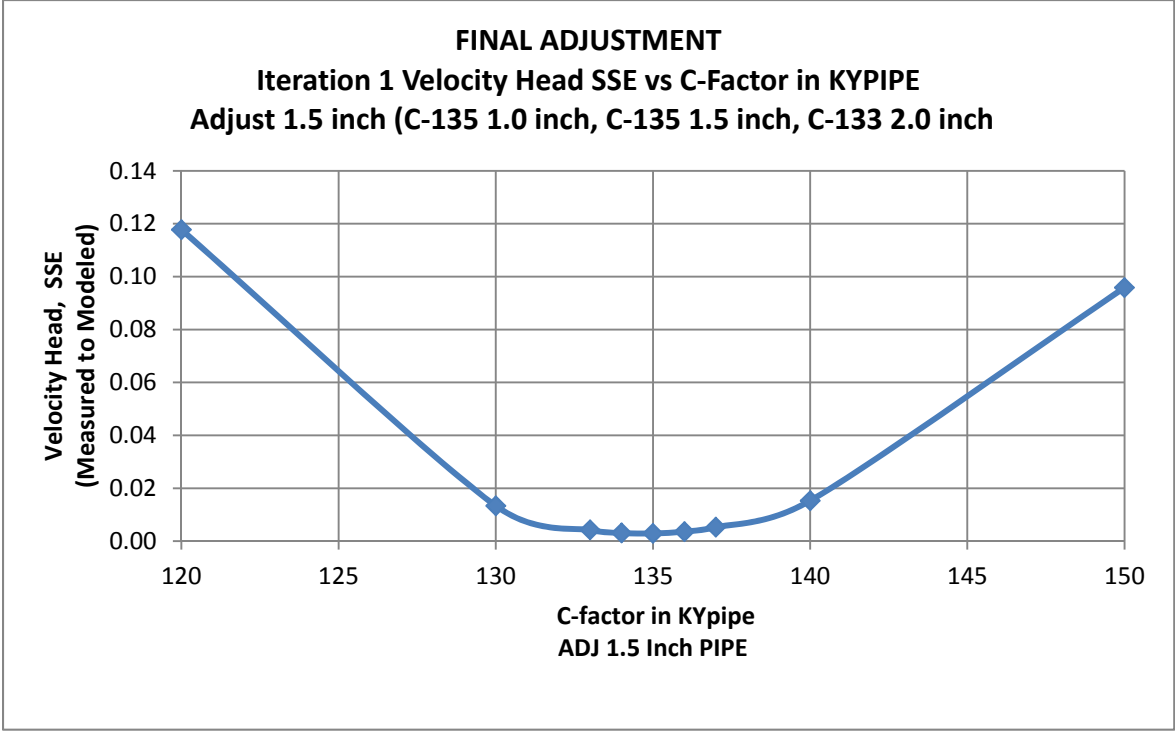
Figure A.13: Case A velocity head calibration, Iteration one, 1.5 inch pipe final adjustment
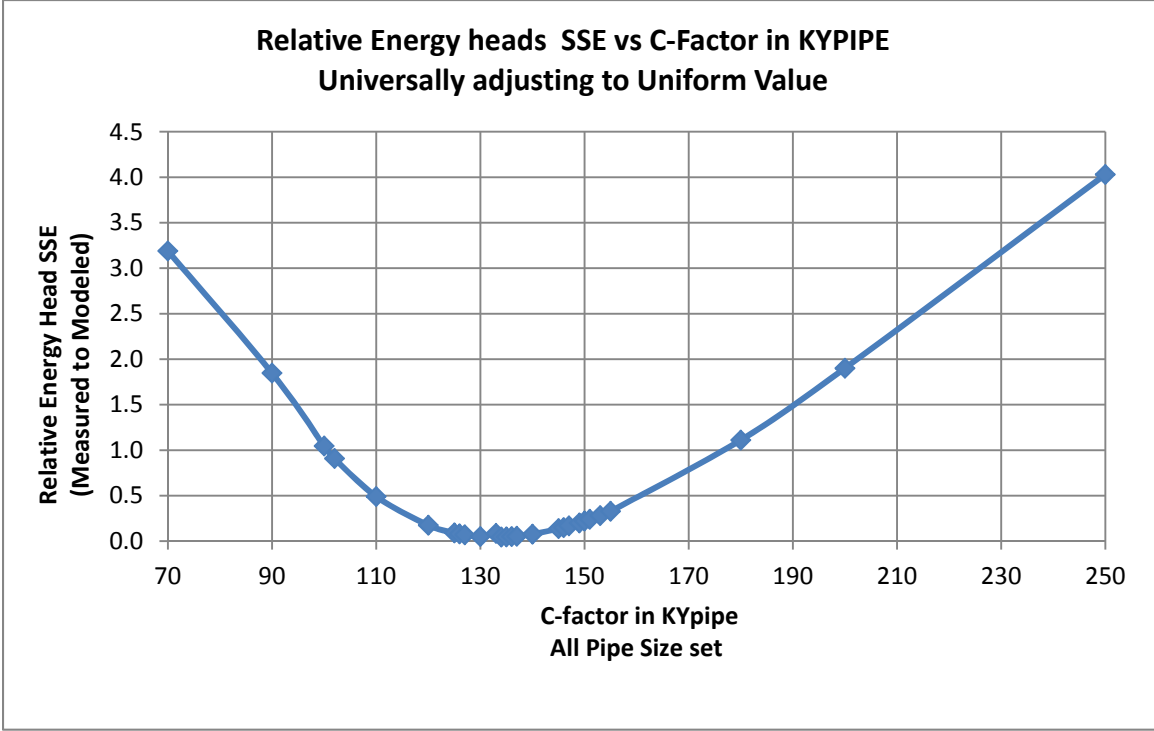
Figure A.14: Case A energy head calibration, universal adjust of all pipe sizes
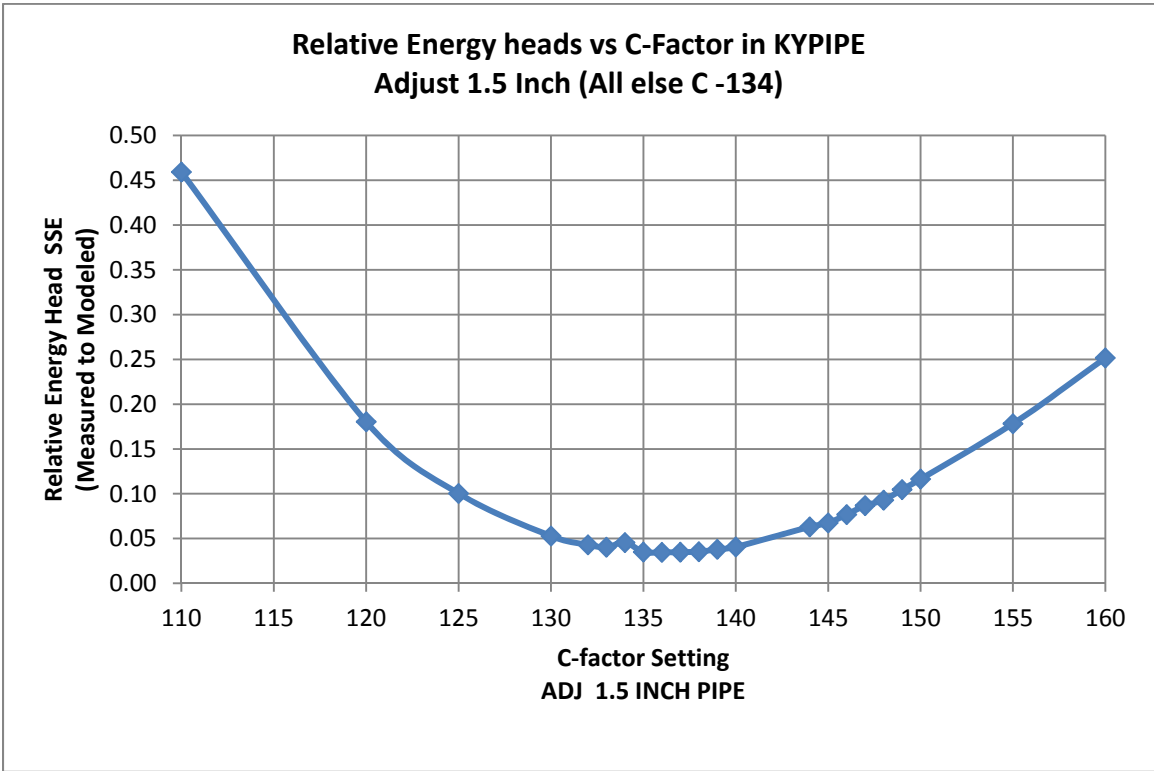
Figure A.15: Case A energy head calibration, 1.5 pipe adjustment
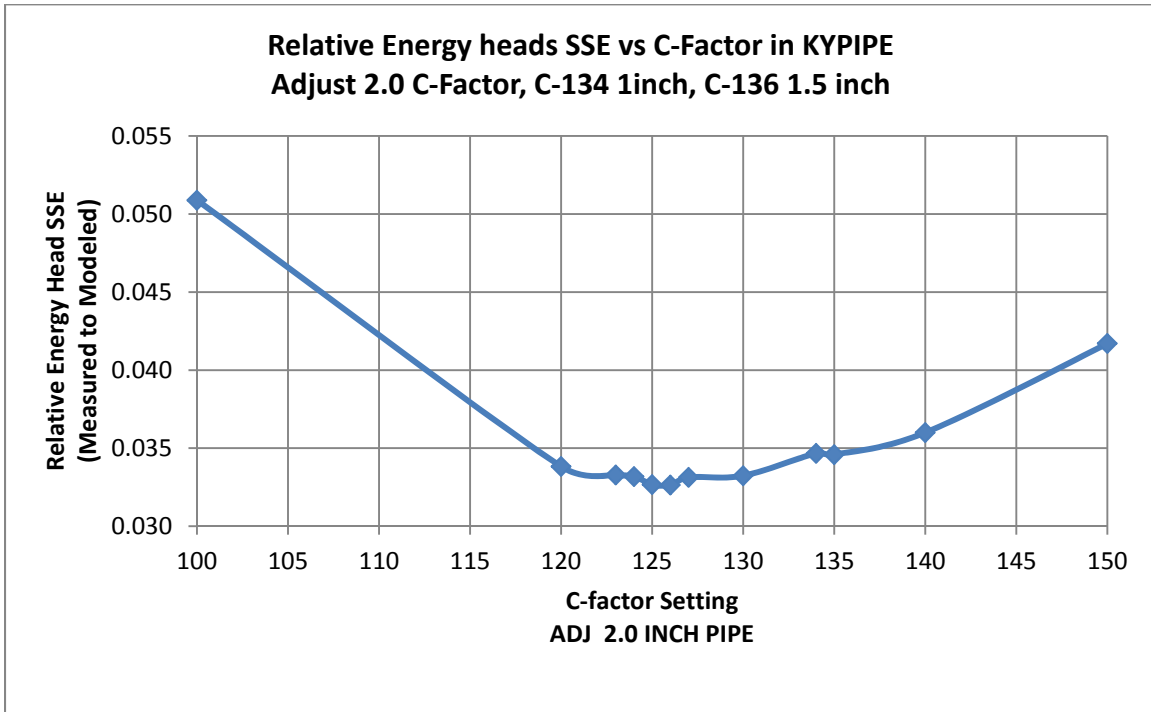
Figure A.16: Case A energy head calibration, 2.0 pipe adjustment
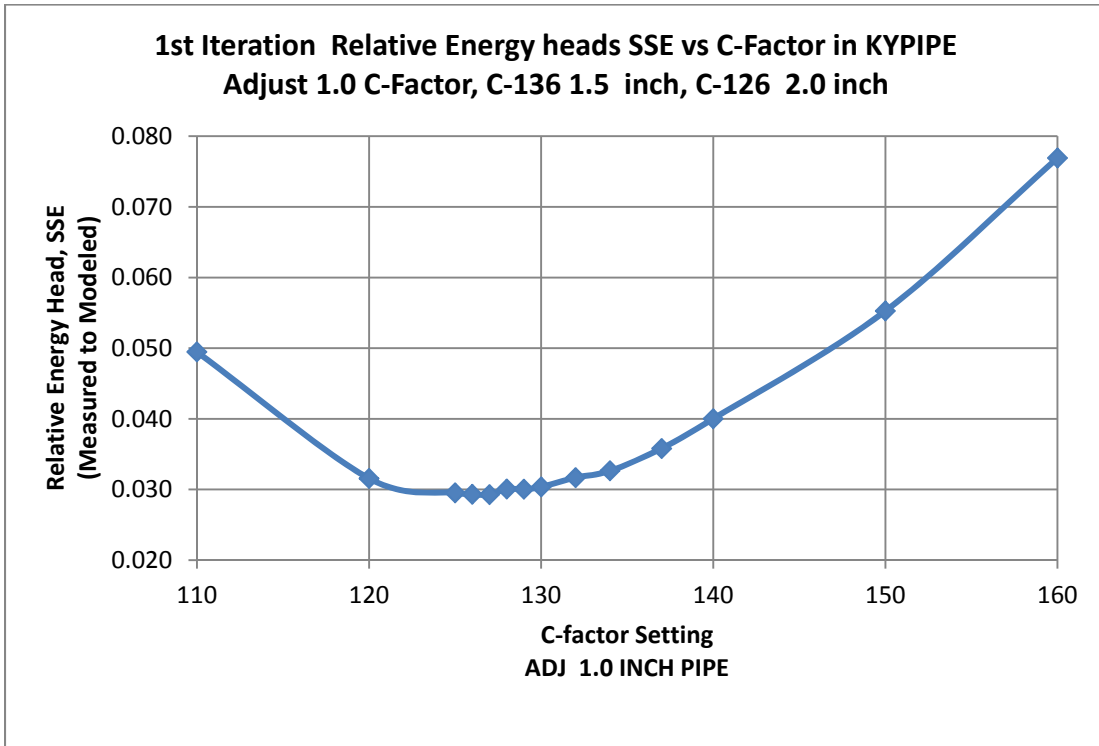
Figure A.17: Case A energy head calibration, Iteration one, 1.0 pipe adjustment
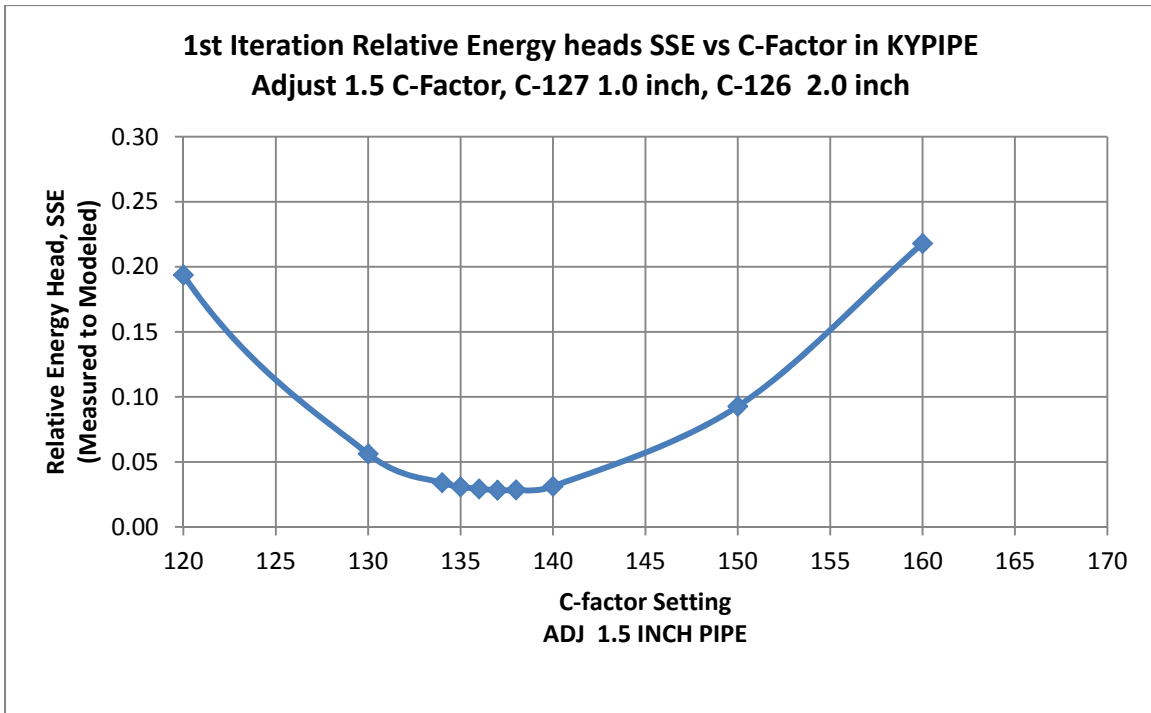
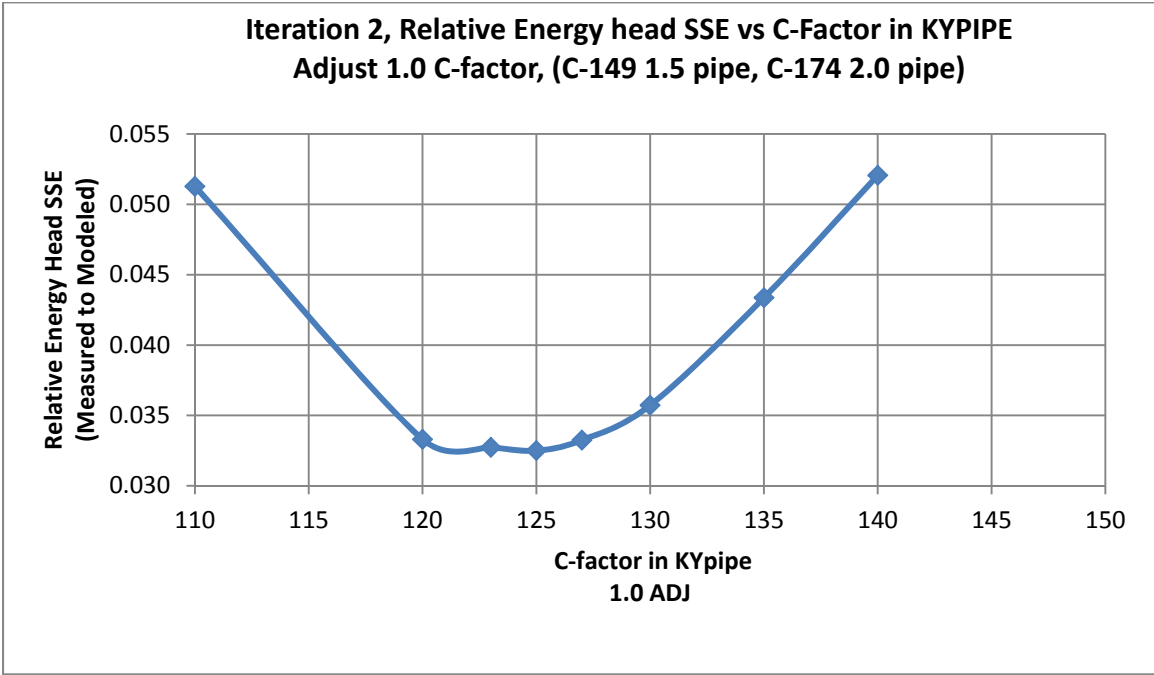Figure A.18: Case A energy head calibration, Iteration one, 1.5 pipe adjustment
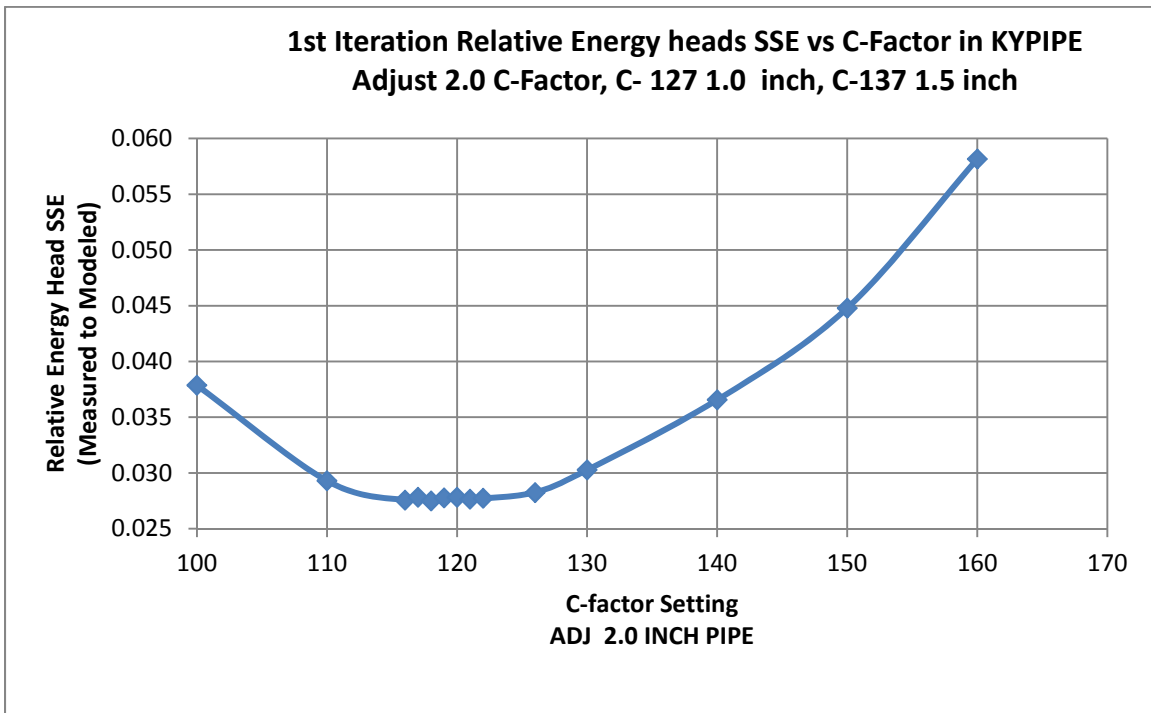
Figure A.19: Case A energy head calibration, Iteration one, 2.0 pipe adjustment
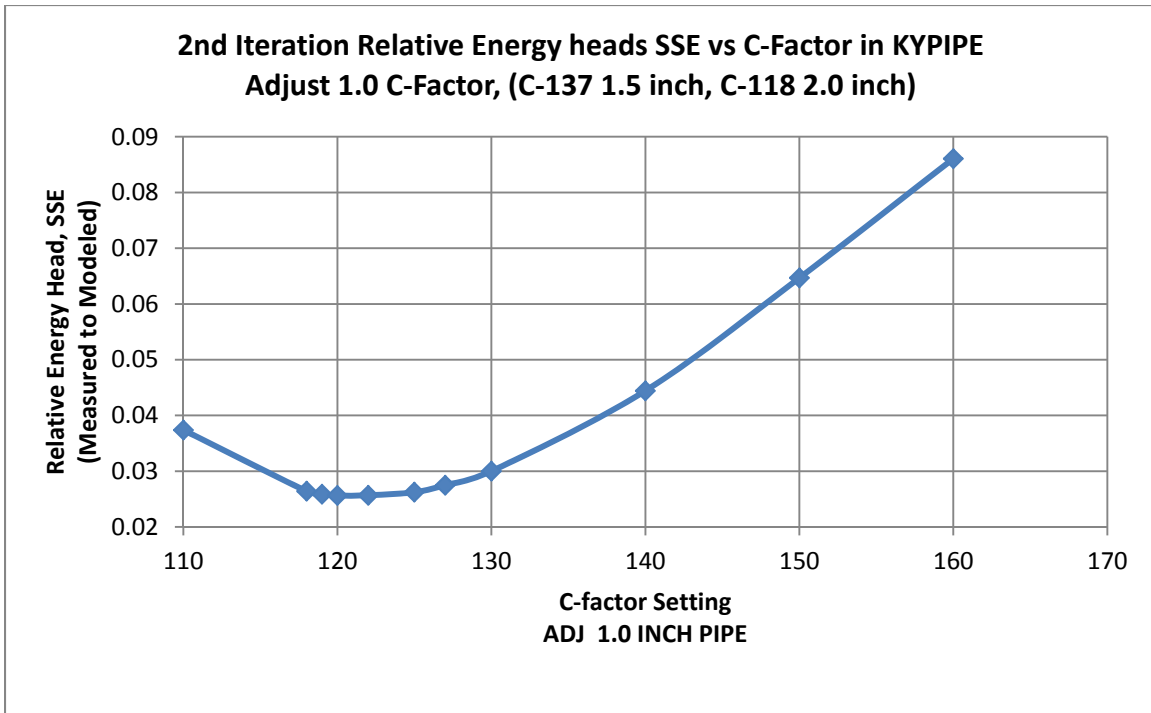
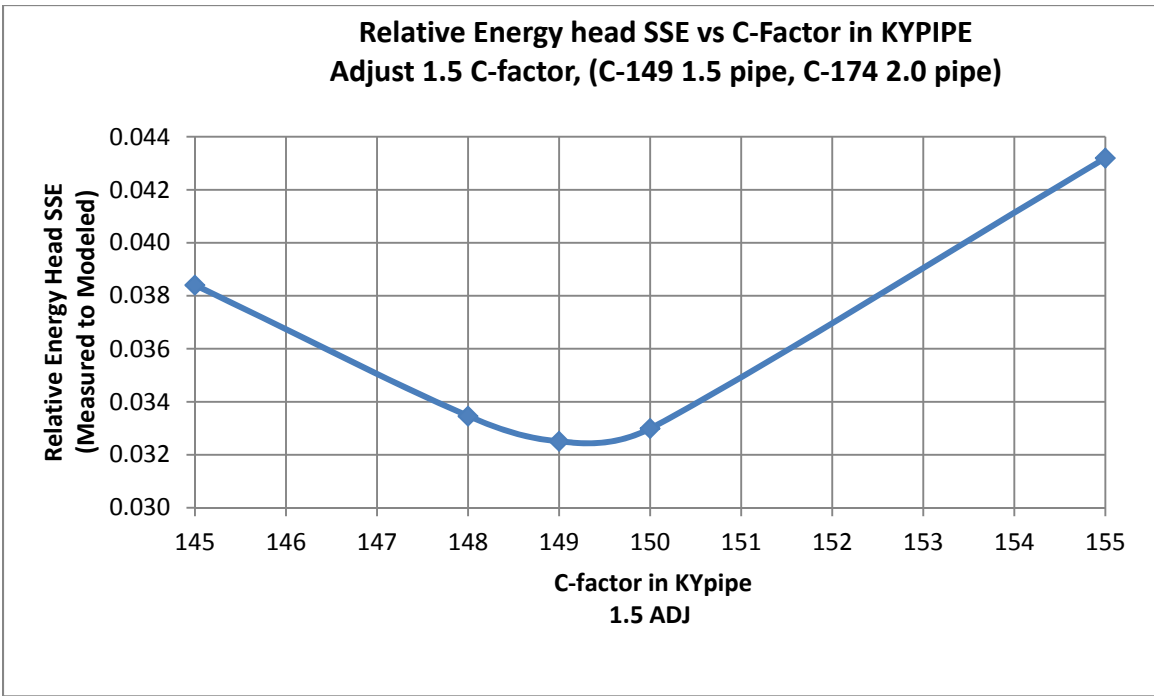Figure A.20: Case A energy head calibration, Iteration two, 1.0 pipe adjustment
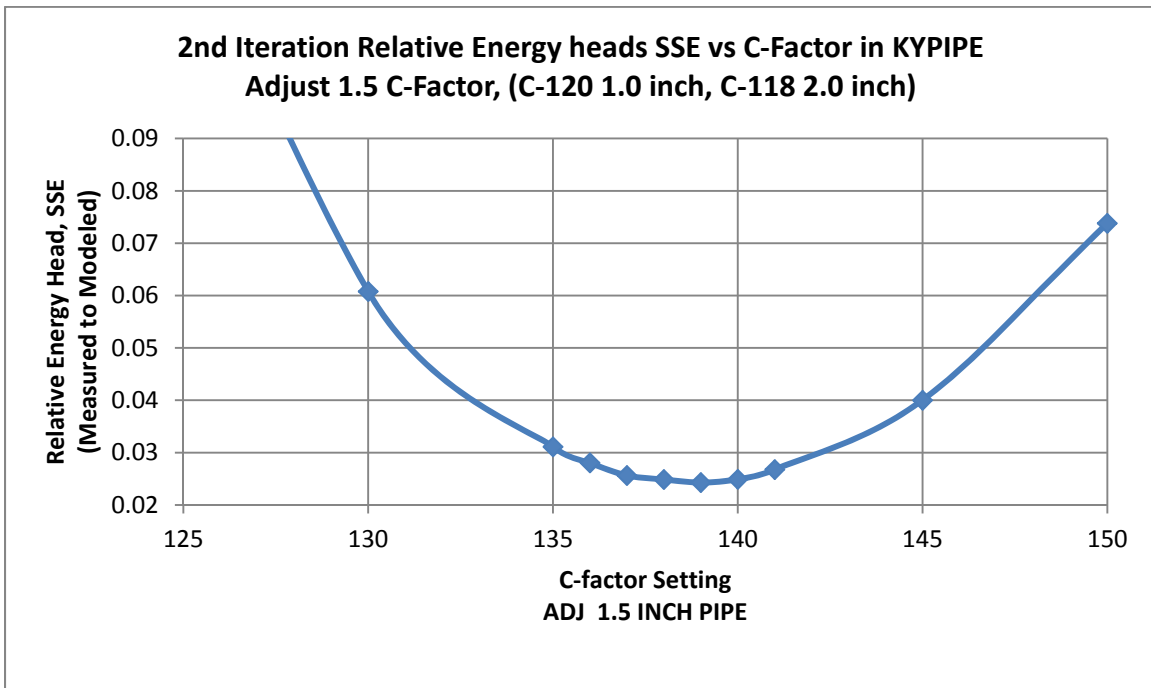
Figure A.21: Case A energy head calibration, Iteration two, 1.5 pipe adjustment"
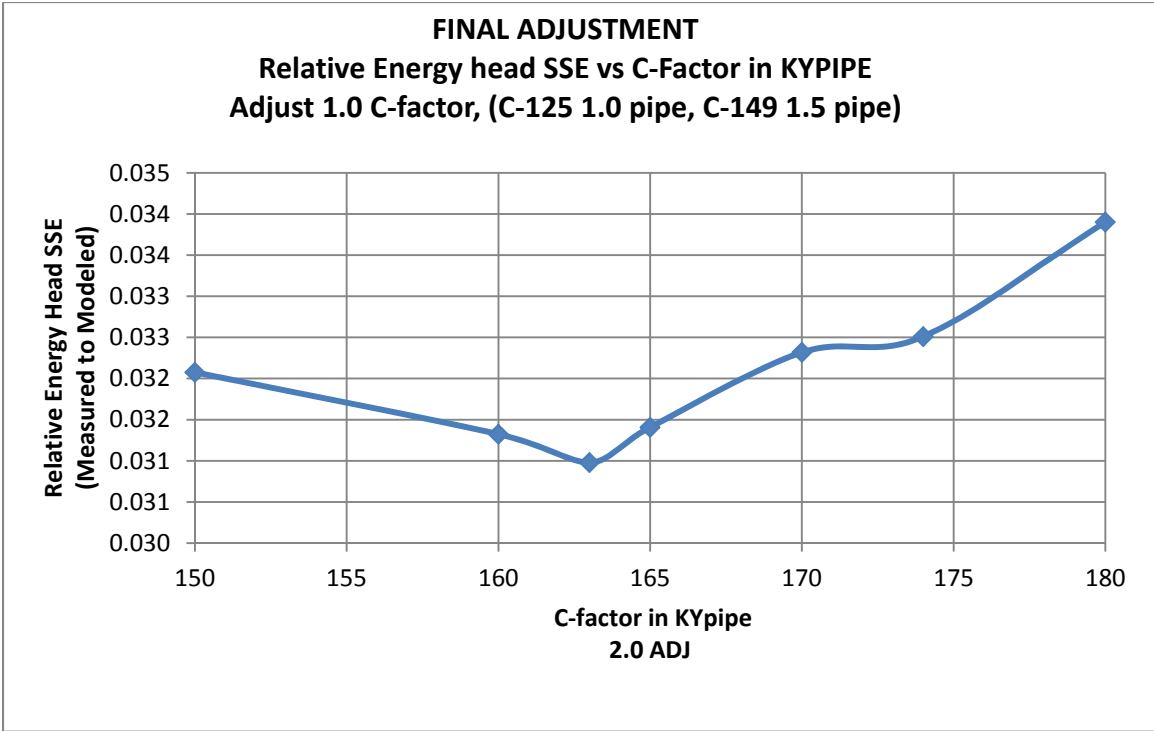
77
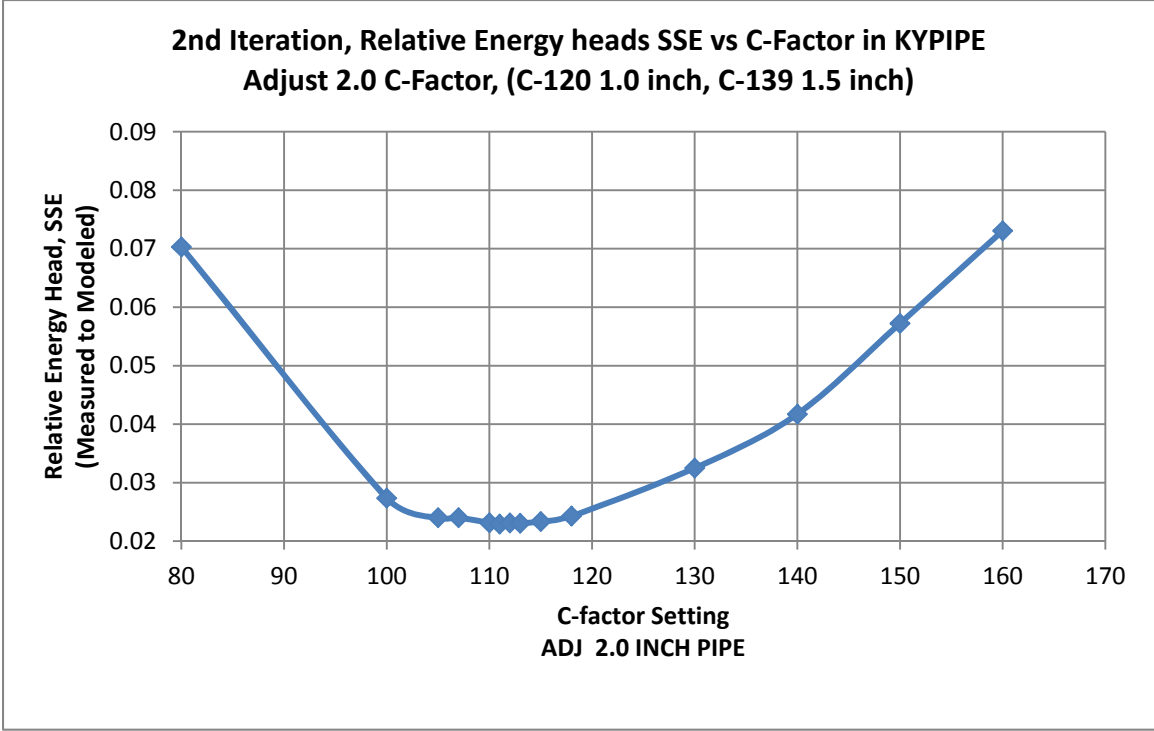
Figure A.22: Case A energy head calibration, Iteration two, 2.0 pipe adjustment

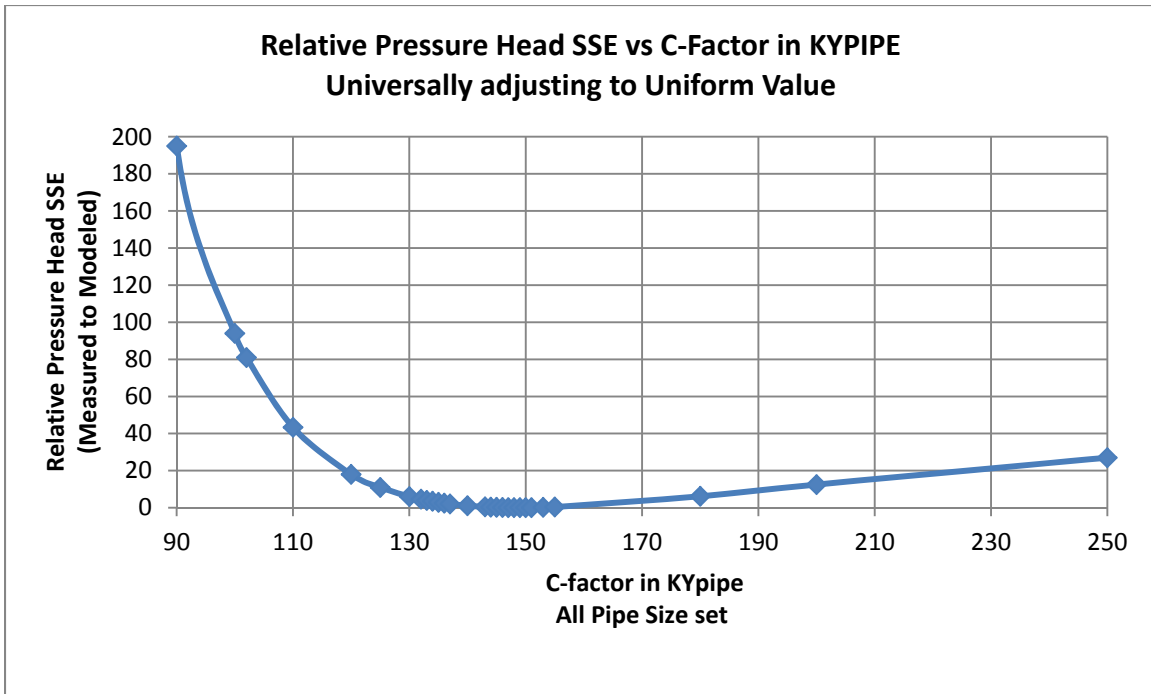# Appendix B Case B calibration plots
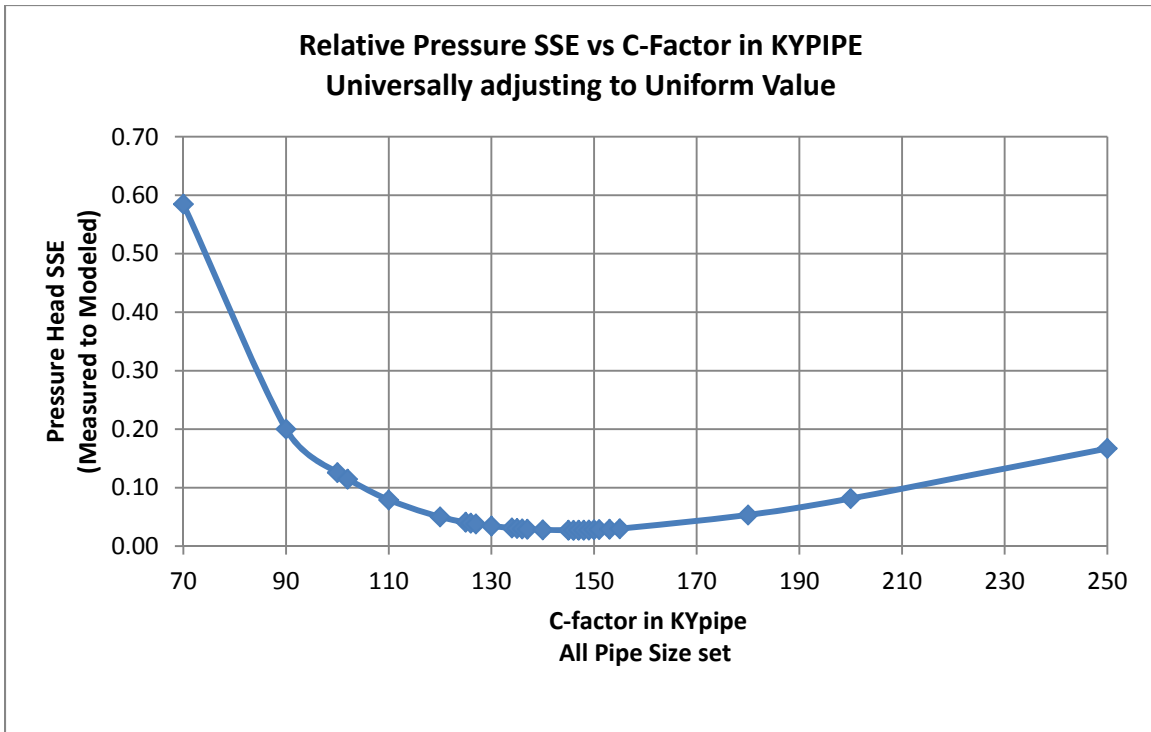
Figure B.1: Case B pressure head calibration, universal adjust of all pipe sizes
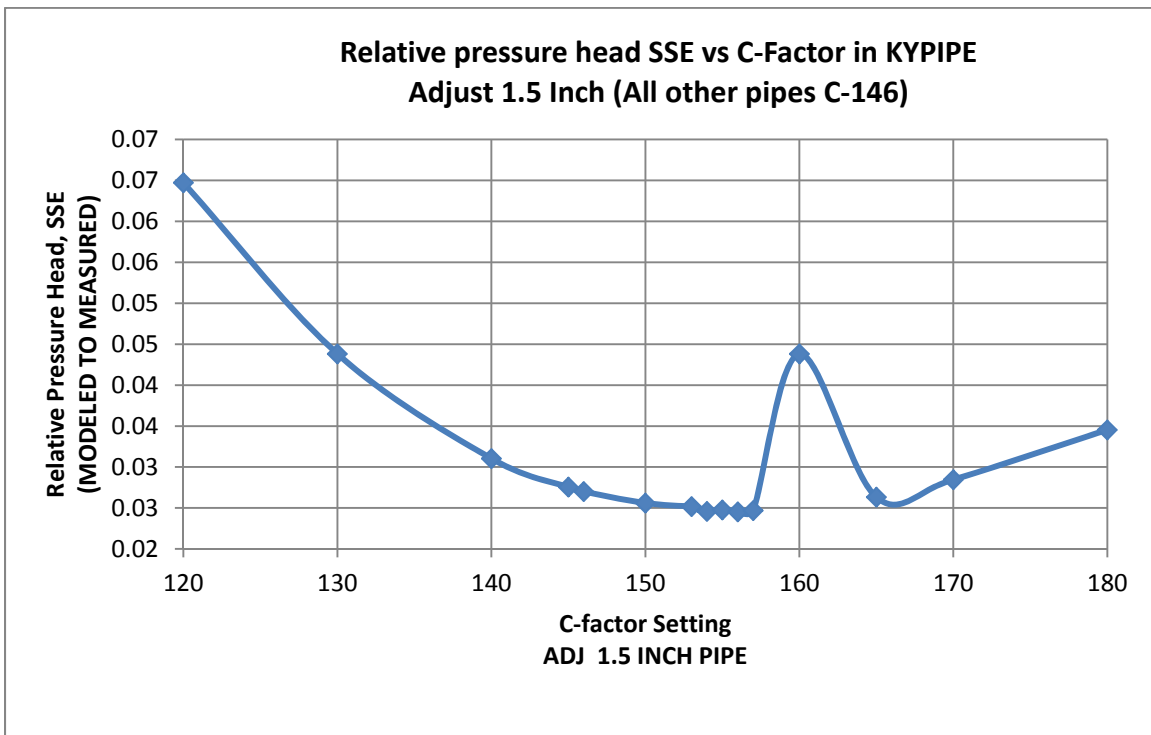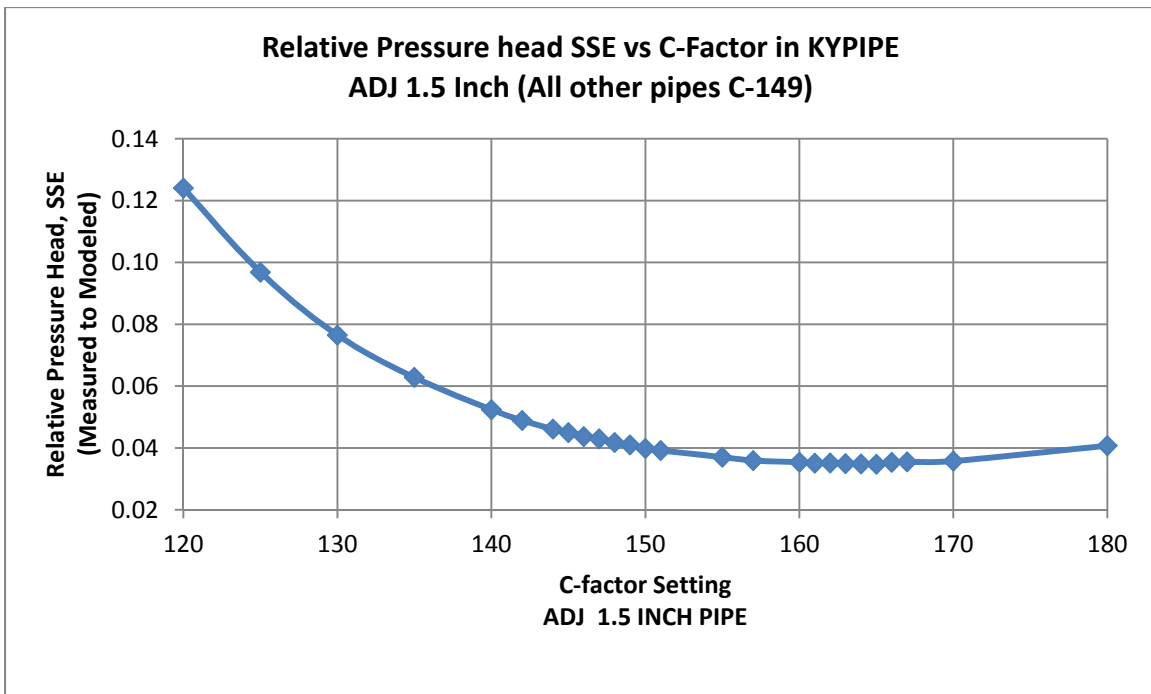

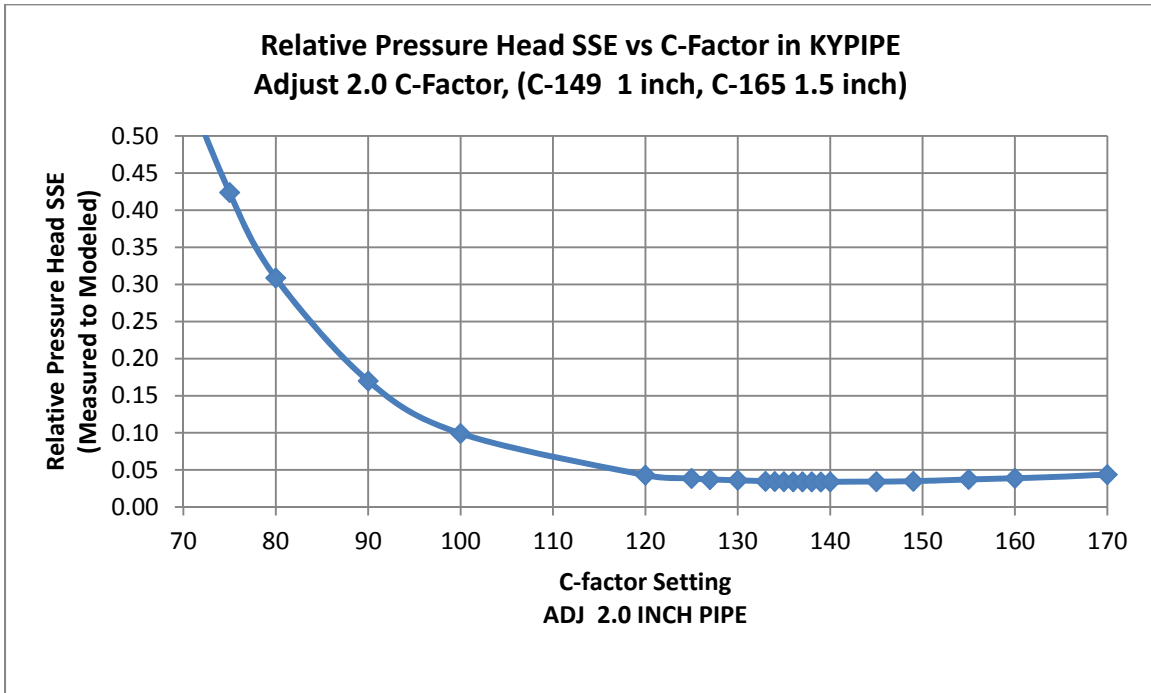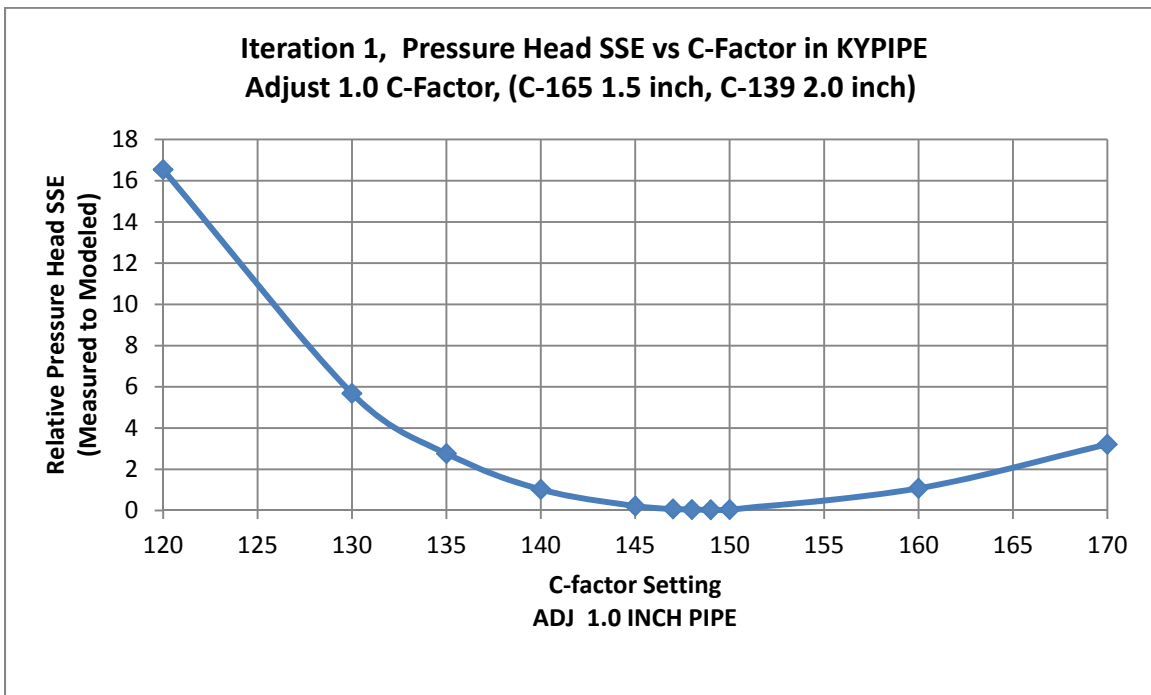Figure B.2: Case B pressure head calibration, 1.5 pipe adjustment
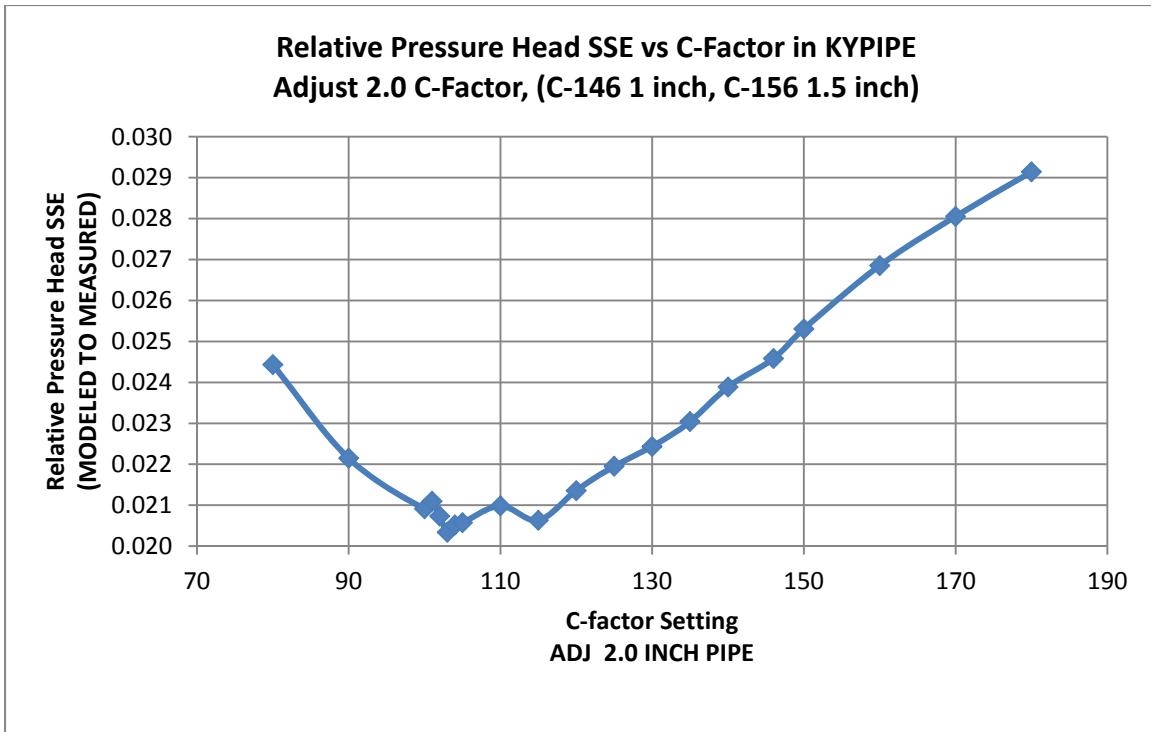
Figure B.3: Case B pressure head calibration, 2.0 pipe adjustment
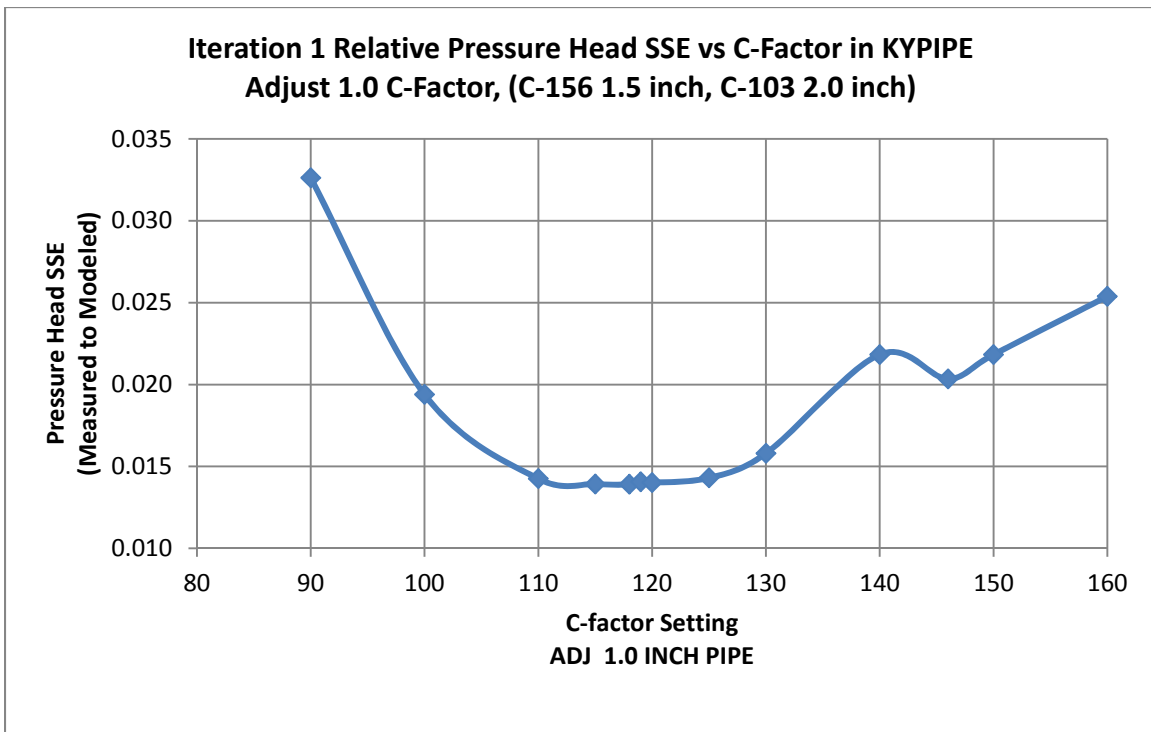
Figure B.4: Case B pressure head calibration, Iteration one, 1.0 pipe
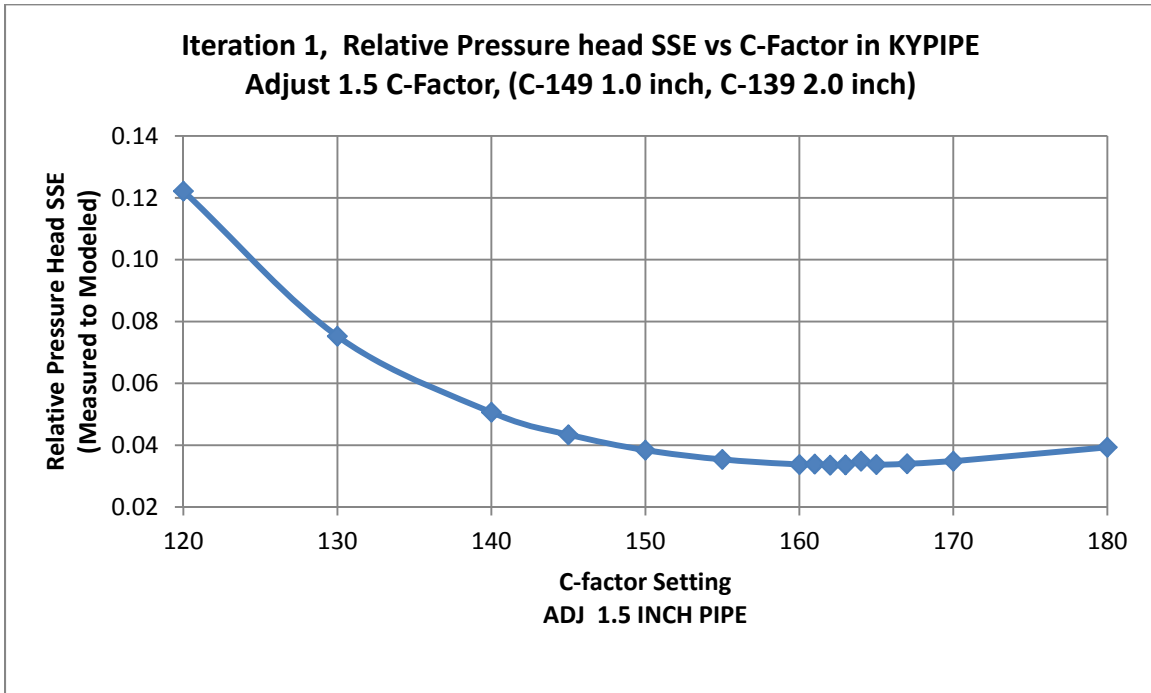adjustment

81
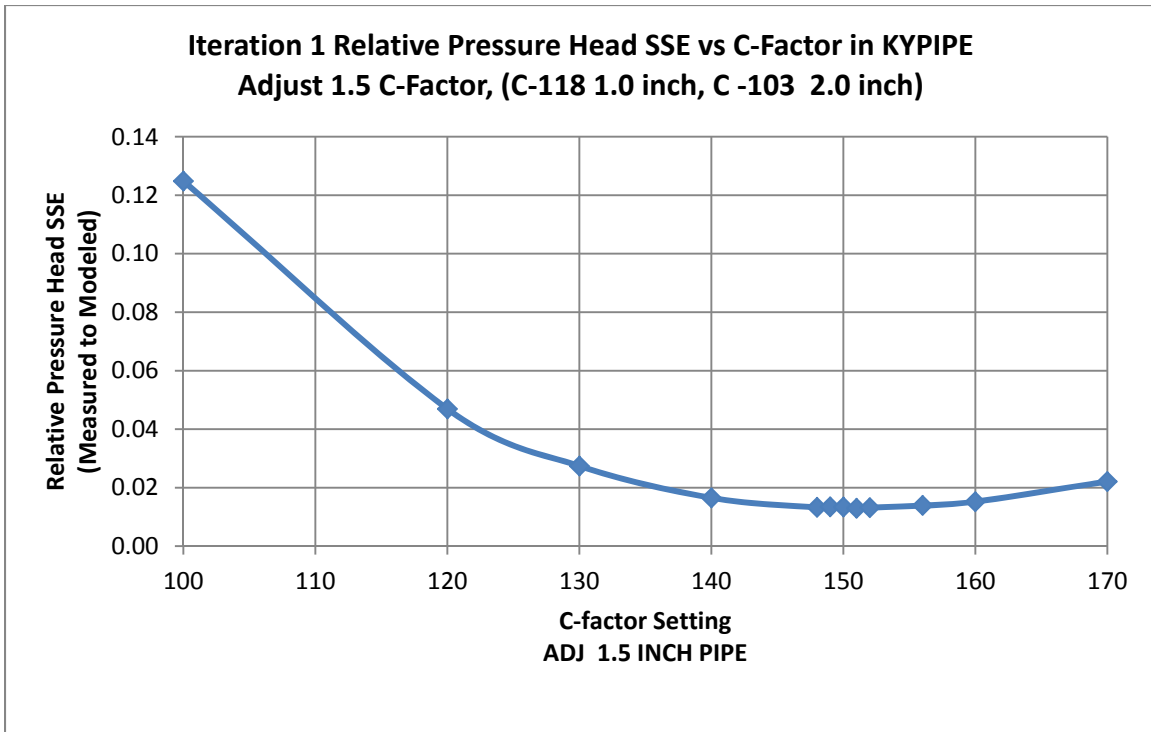
Figure B.5: Case B pressure head calibration, Iteration one, 1.5 pipe adjustment
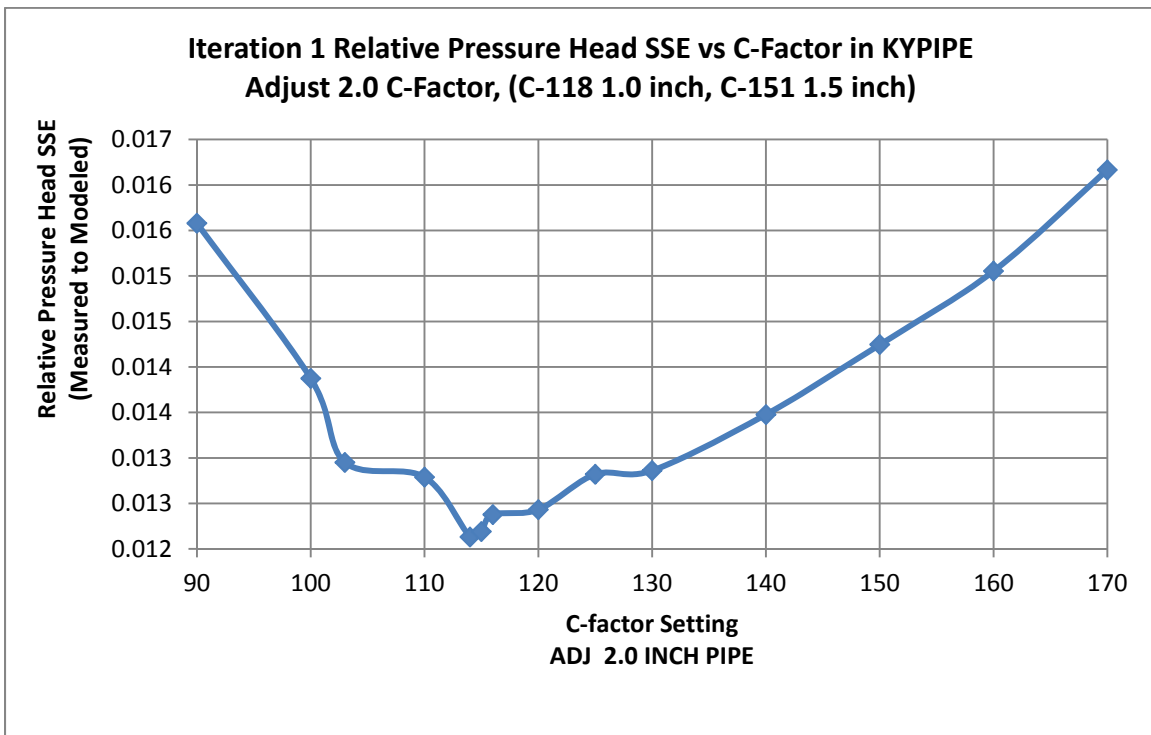
Figure B.6: Case B pressure head calibration, Iteration one, 2.0 pipe adjustment
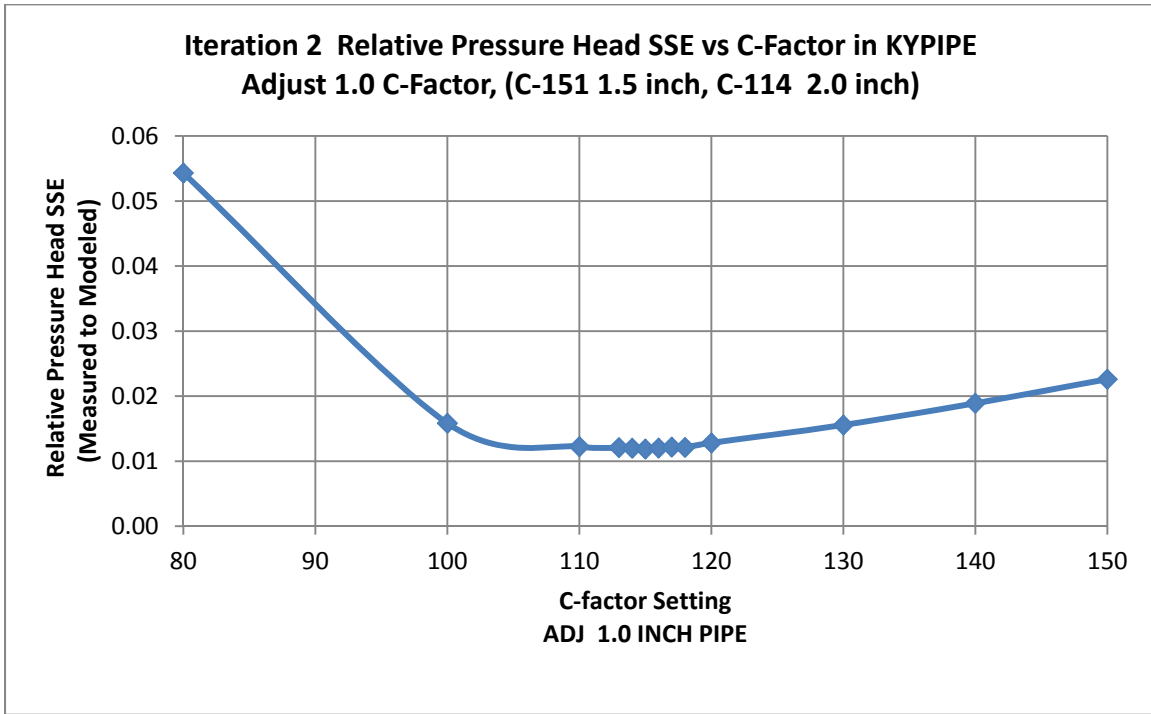
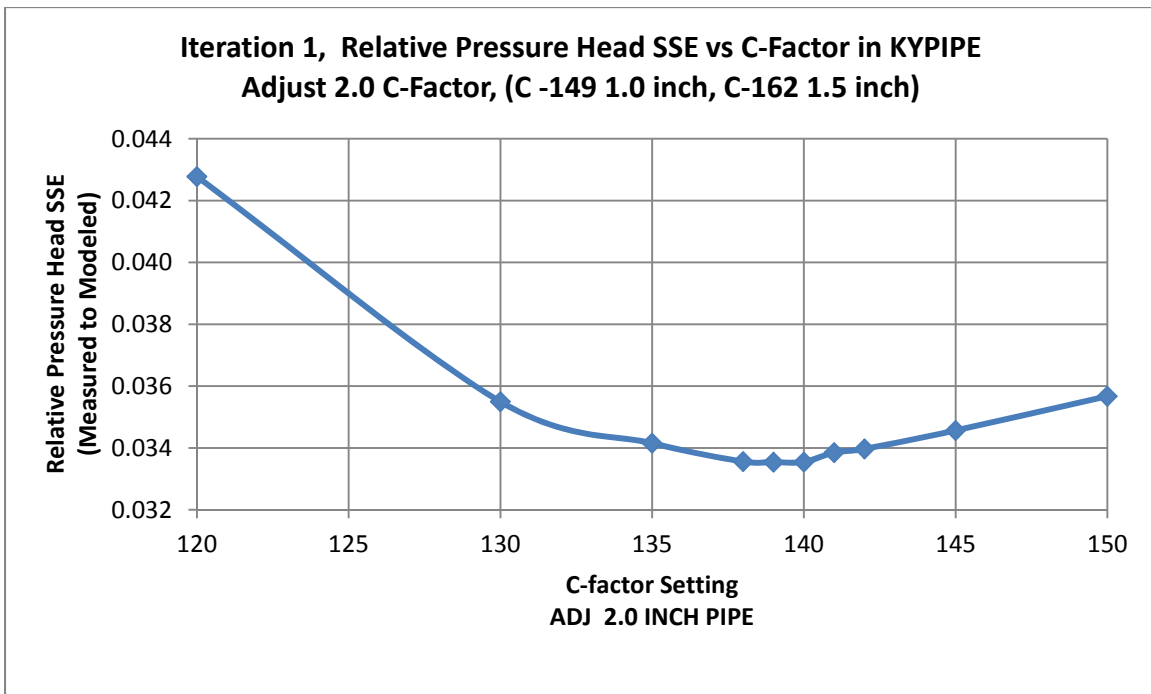Figure B.7: Case B pressure head calibration, Iteration two, 1.0 pipe adjustment
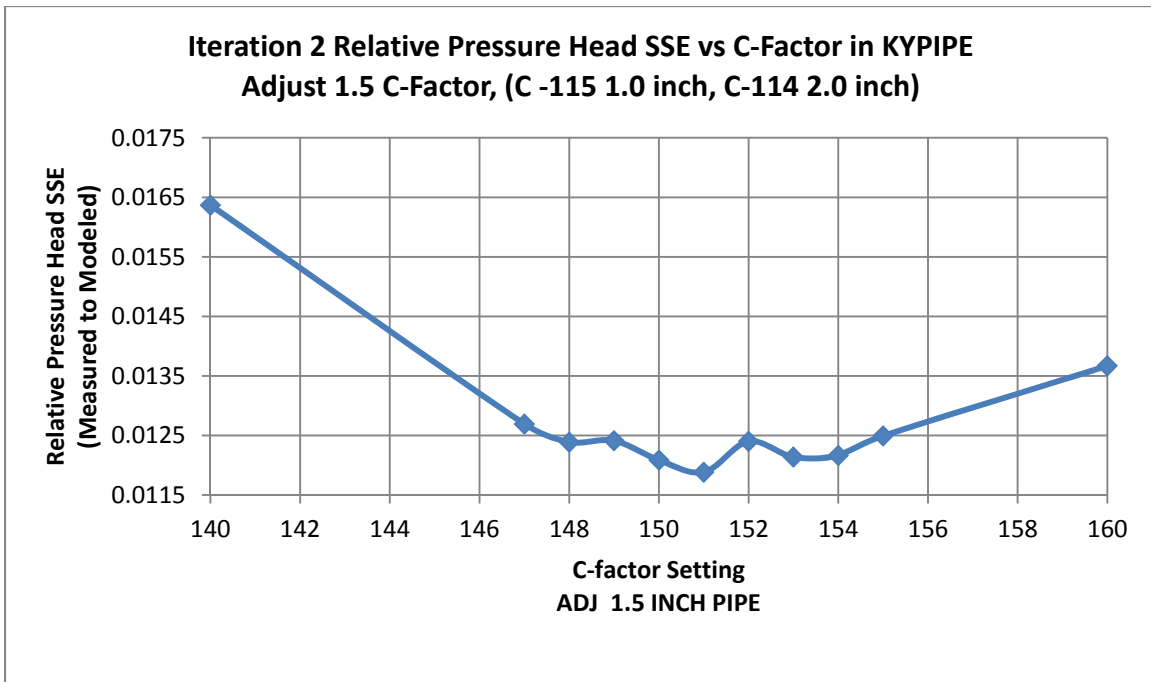
Figure B.8: Case B pressure head calibration, Iteration two, 1.5 pipe adjustment
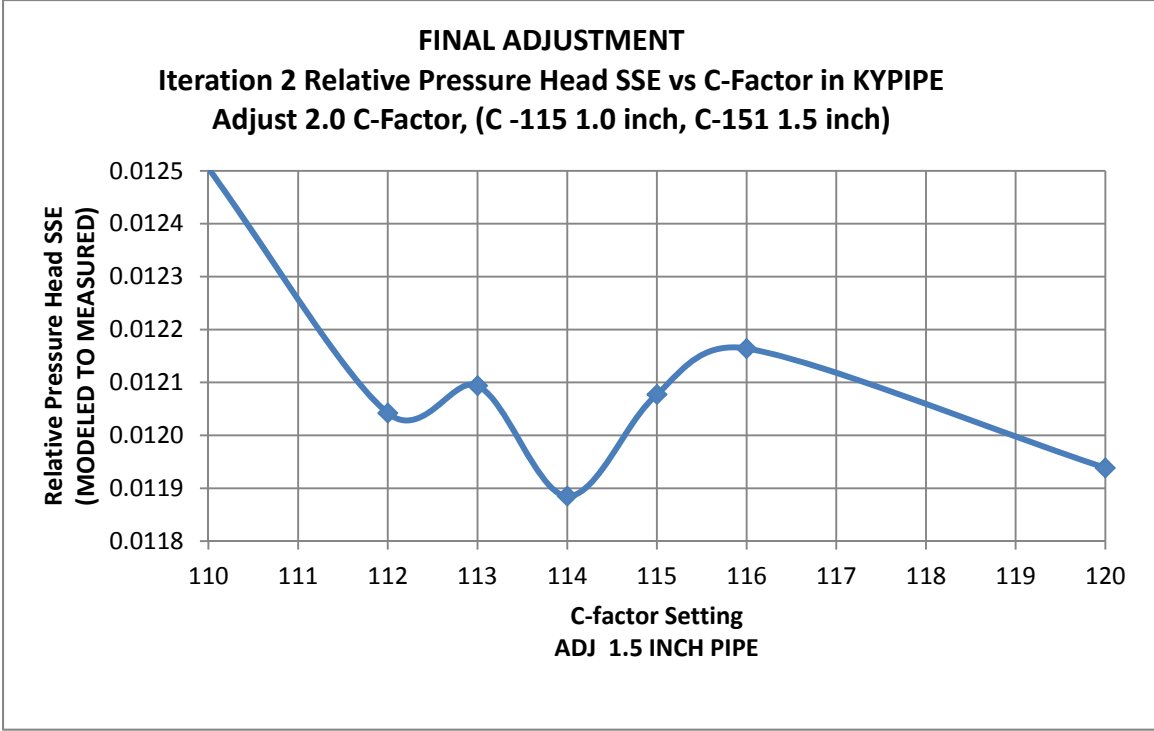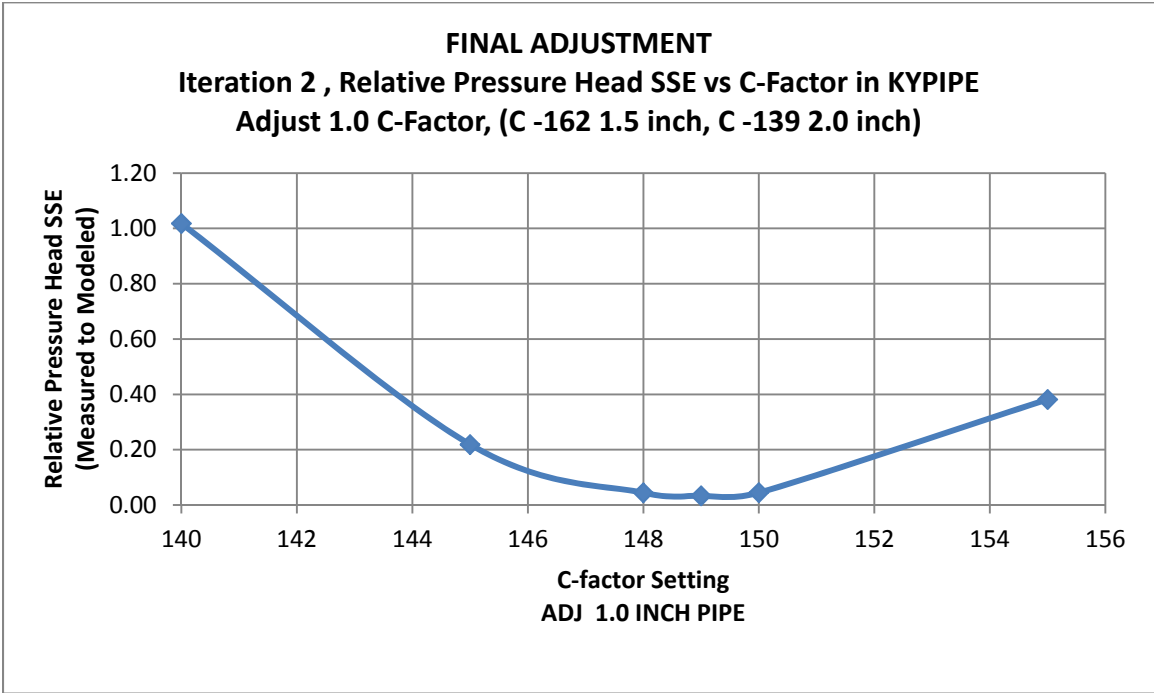
Figure B.9: Case B pressure head calibration, Iteration two, 2.0 pipe adjustment
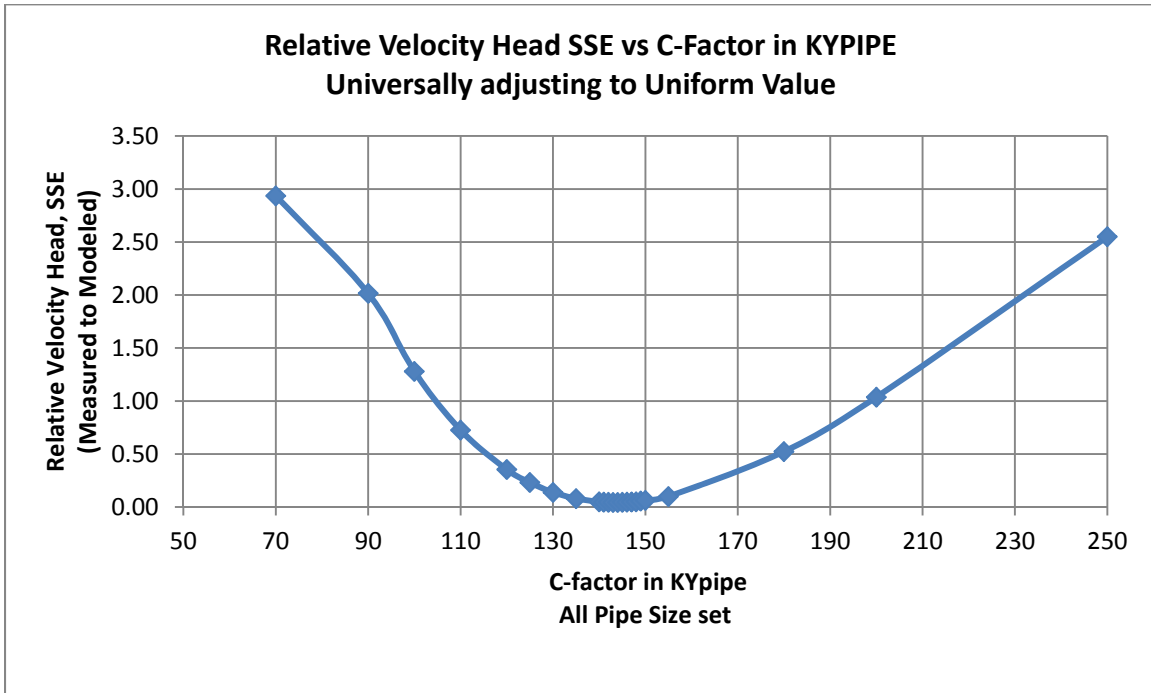
Figure B.10: Case B velocity head calibration, universal adjust of all pipe sizes
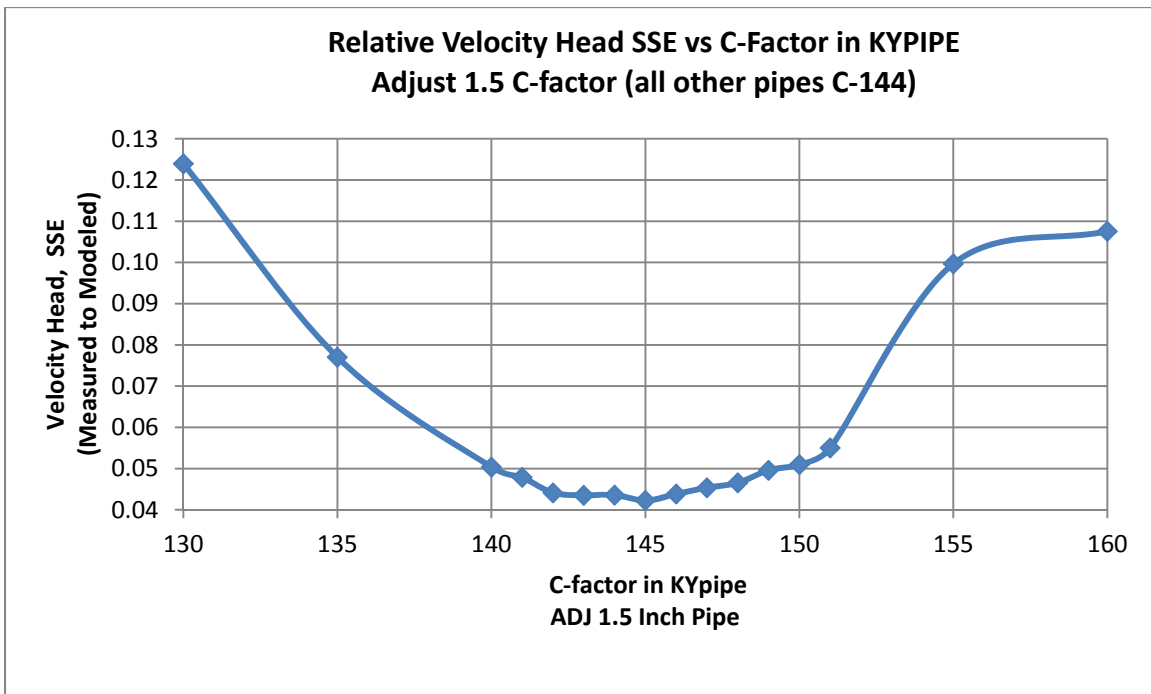
Figure B.11: Case B velocity head calibration, 1.5 pipe adjustment
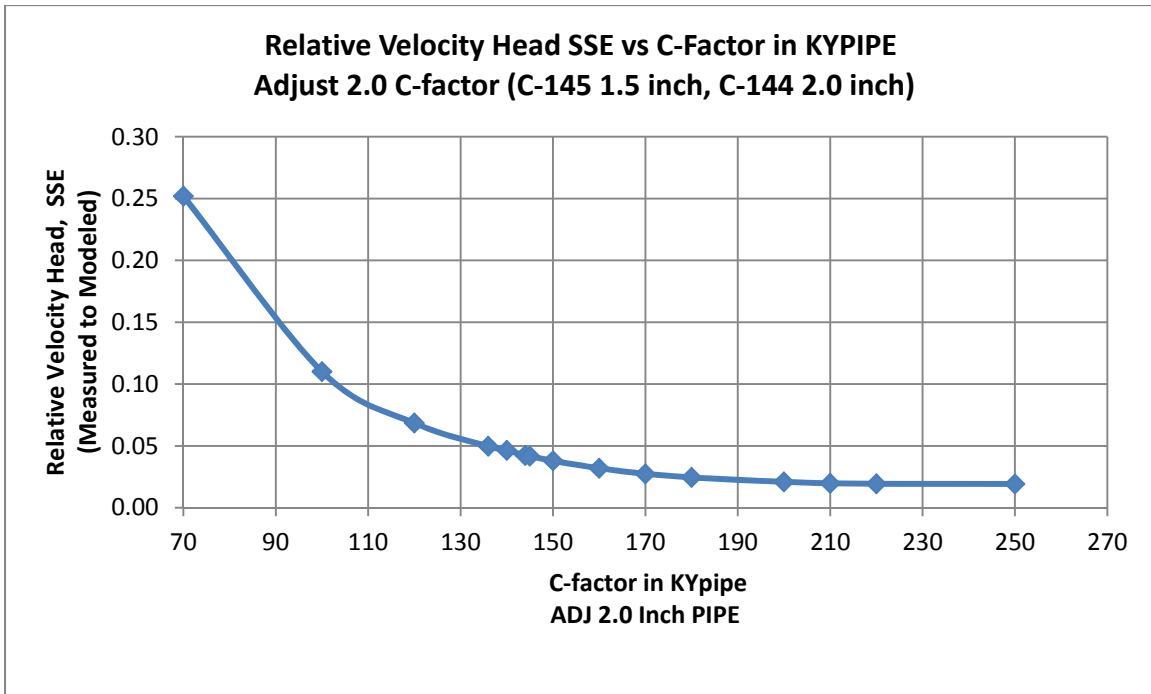
Figure B.12: Case B velocity head calibration, 2.0 pipe adjustment
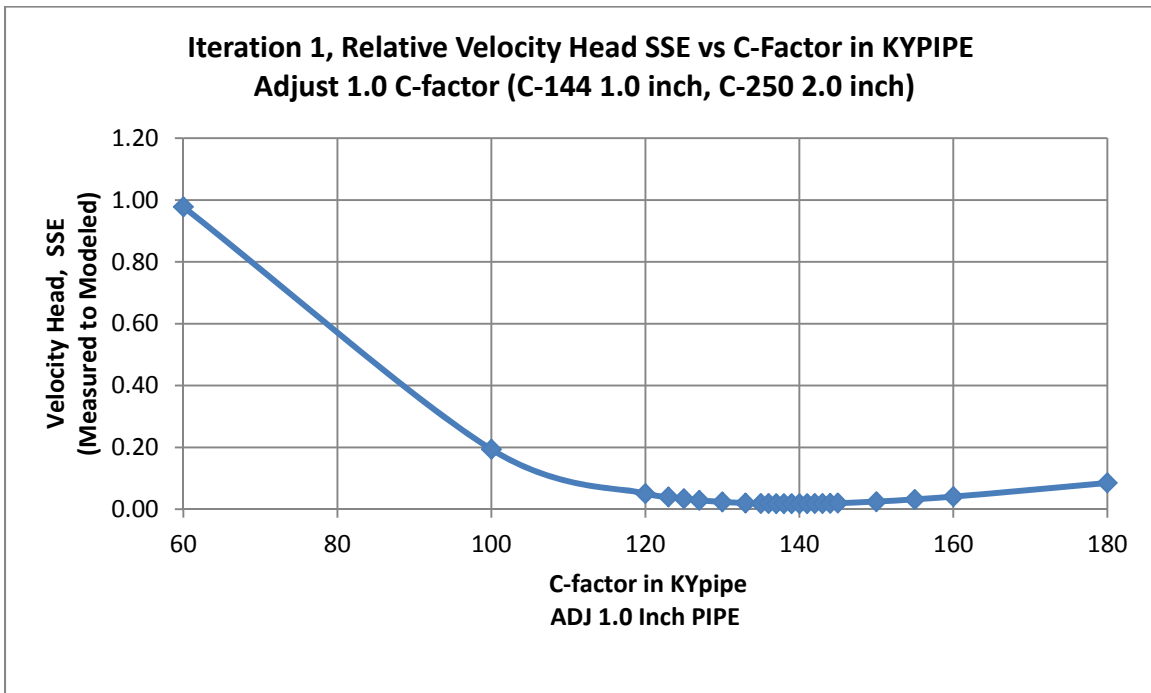
Figure B.13: Case B velocity head calibration, Iteration one, 1.0 pipe
adjustment
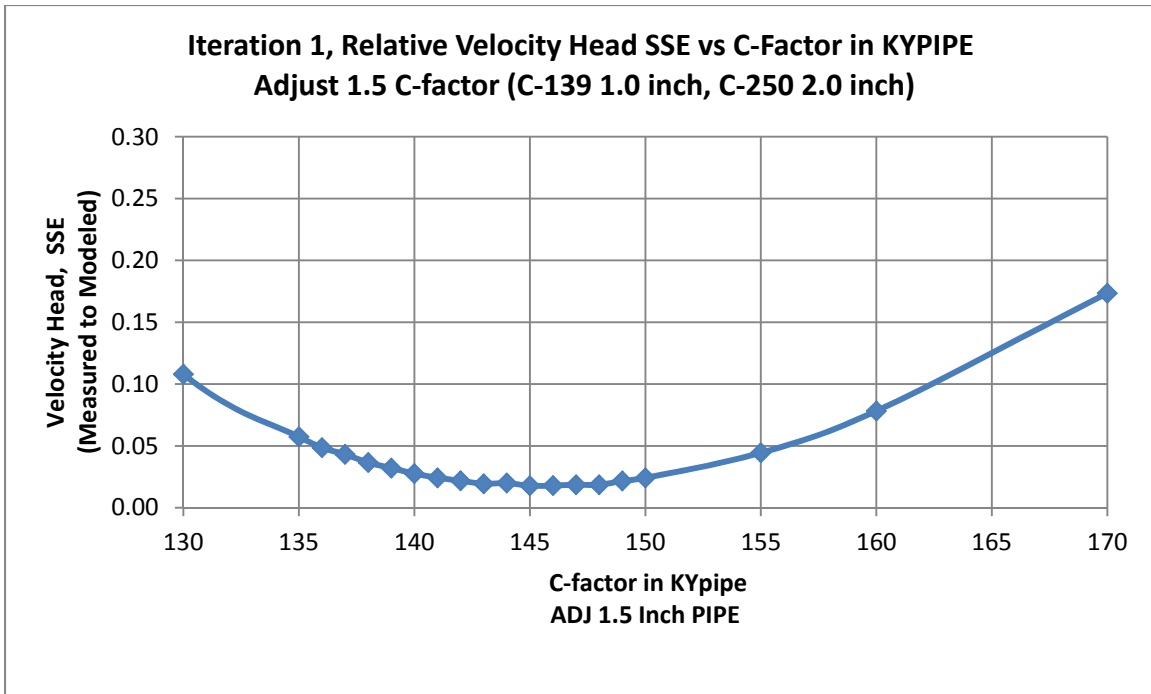
Figure B.14: Case B velocity head calibration, Iteration one, 1.5 pipe adjustment
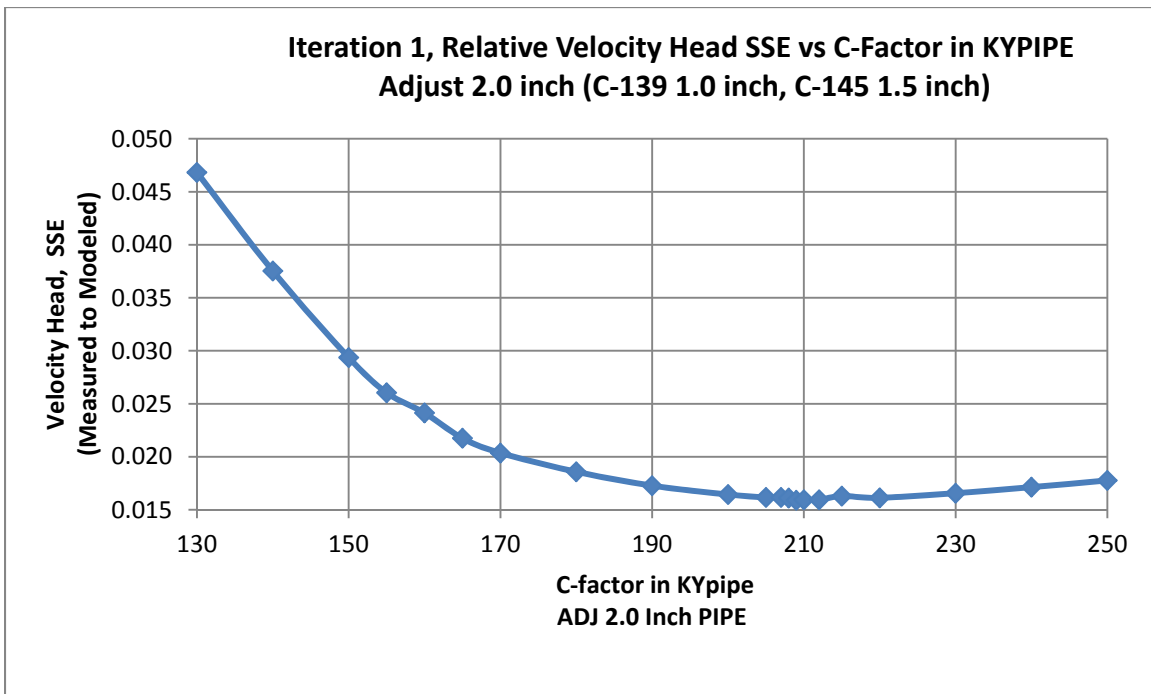
Figure B.15: Case B velocity head calibration, Iteration one, 2.0 pipe adjustment
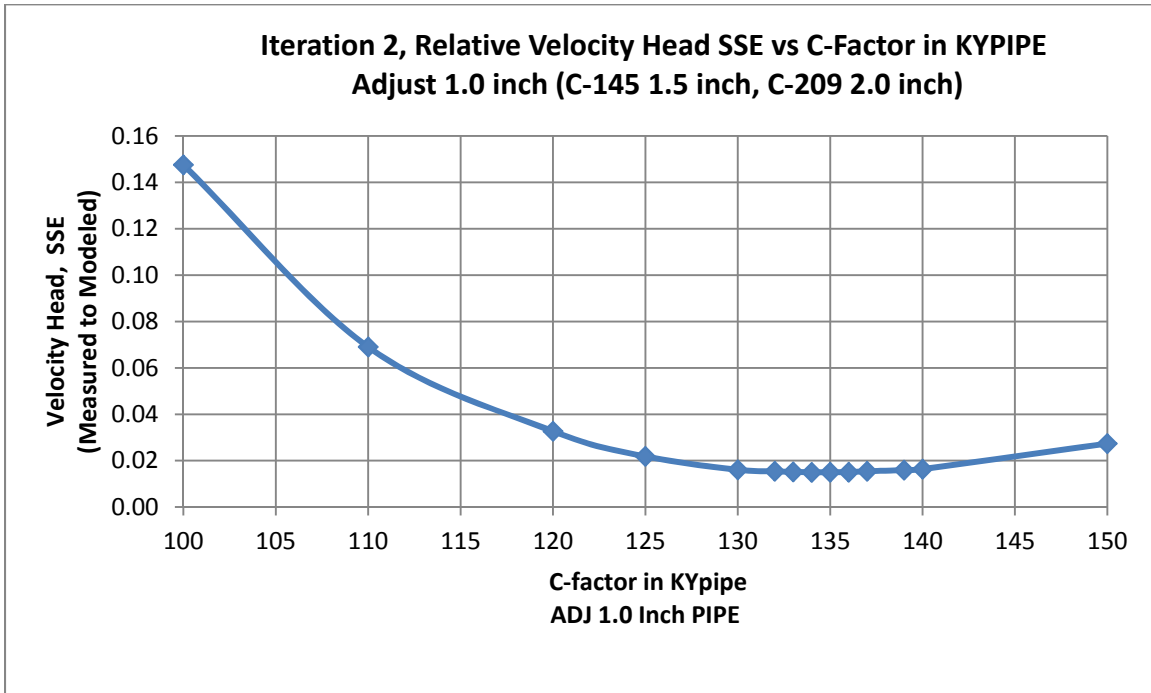
Figure B.16: Case B velocity head calibration, Iteration two, 1.0 pipe adjustment
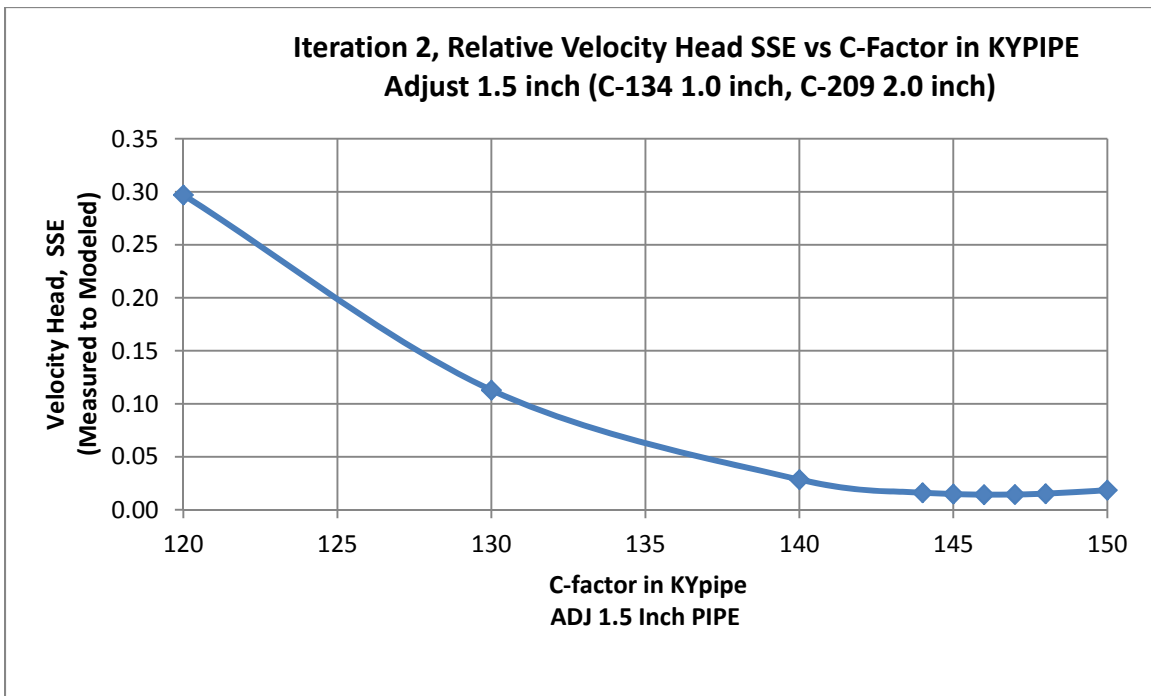
Figure B.17: Case B velocity head calibration, Iteration two, 1.5 pipe adjustment
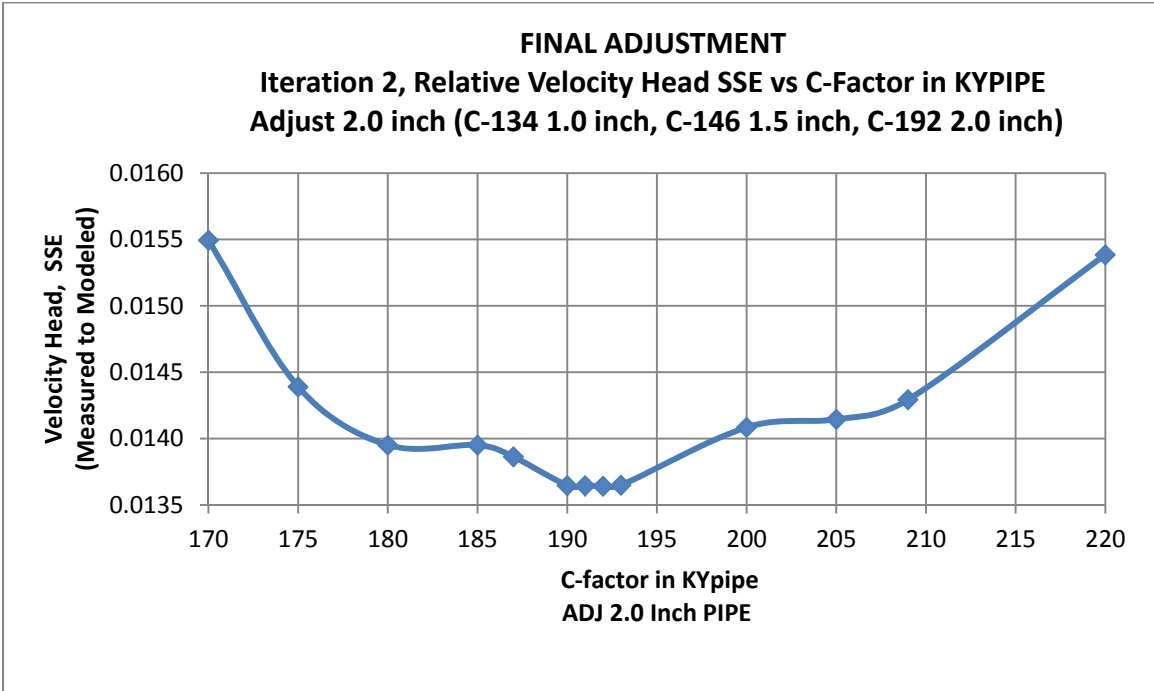
Figure B.18: Case B velocity head calibration, Iteration two, 2.0 pipe final adjustment
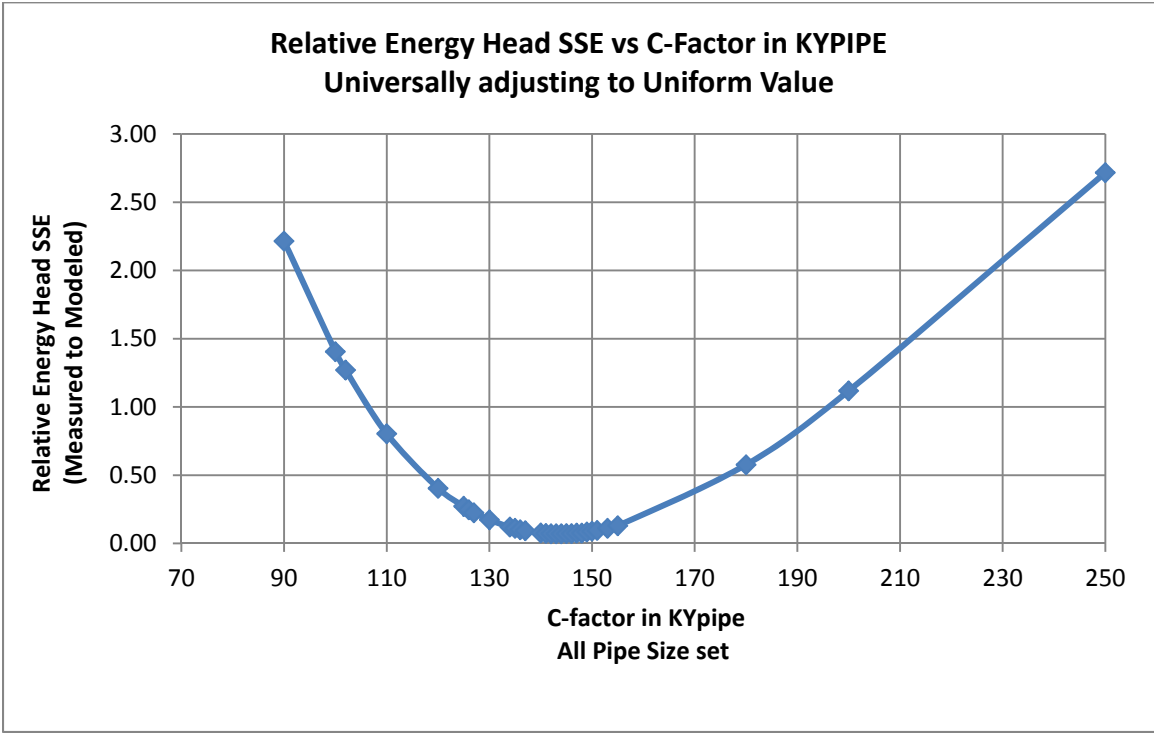
Figure B.19: Case B energy head calibration, universal adjust of all pipe sizes
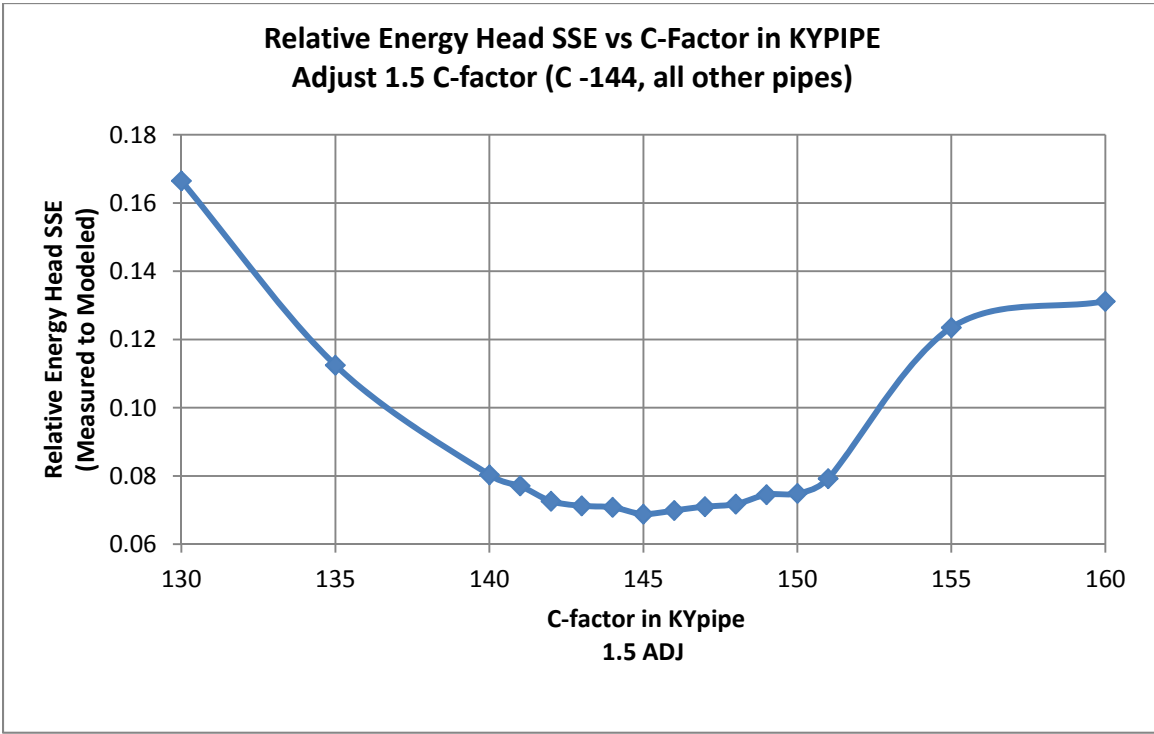
Figure B.20: Case B energy head calibration, 1.5 pipe adjustment
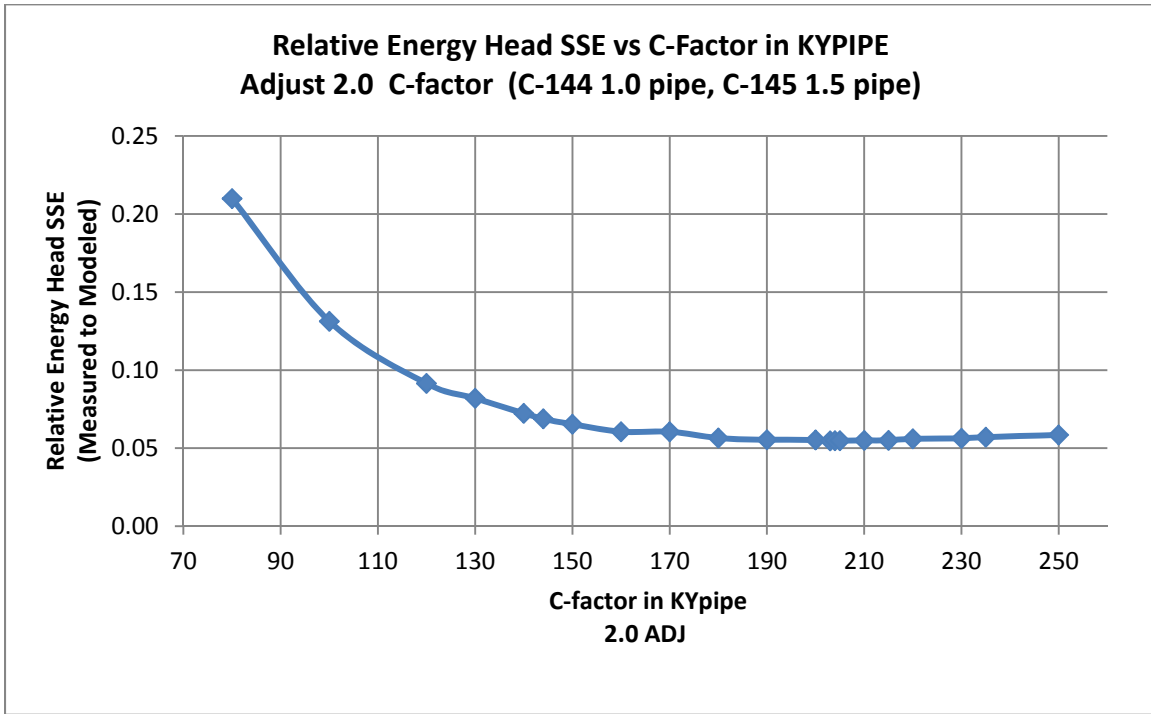
Figure B.21: Case B energy head calibration, 2.0 pipe adjustment
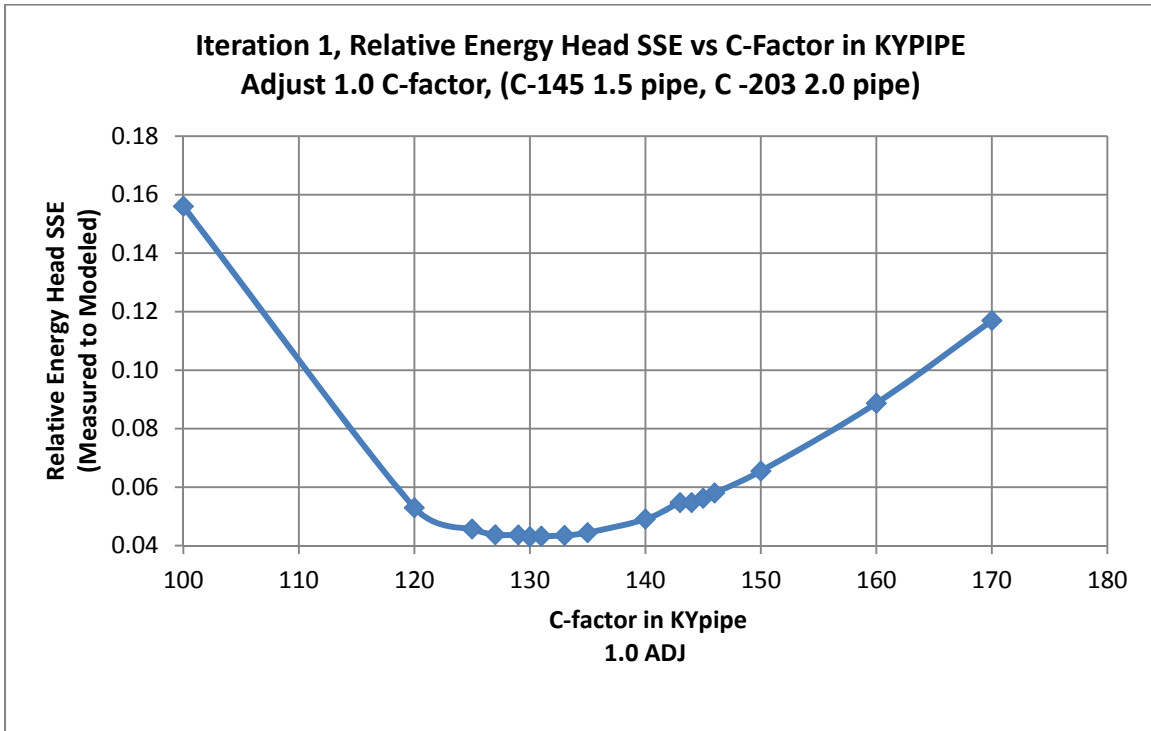
Figure B.22: Case B energy head calibration, Iteration one, 1.0 pipe adjustment
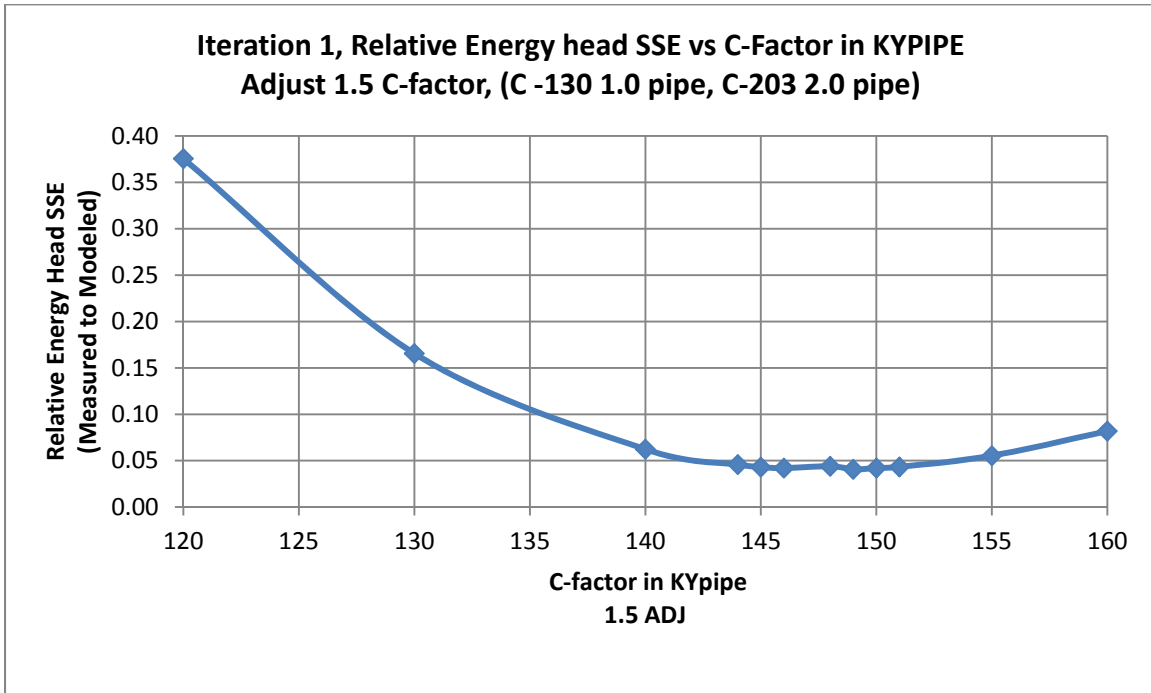
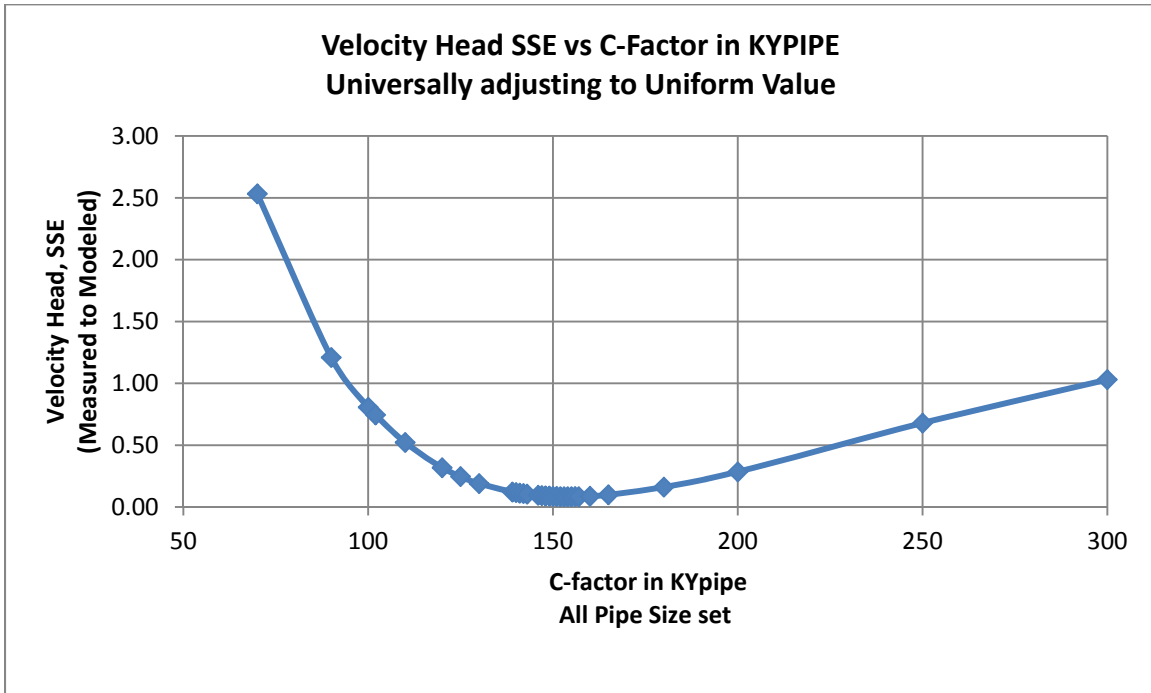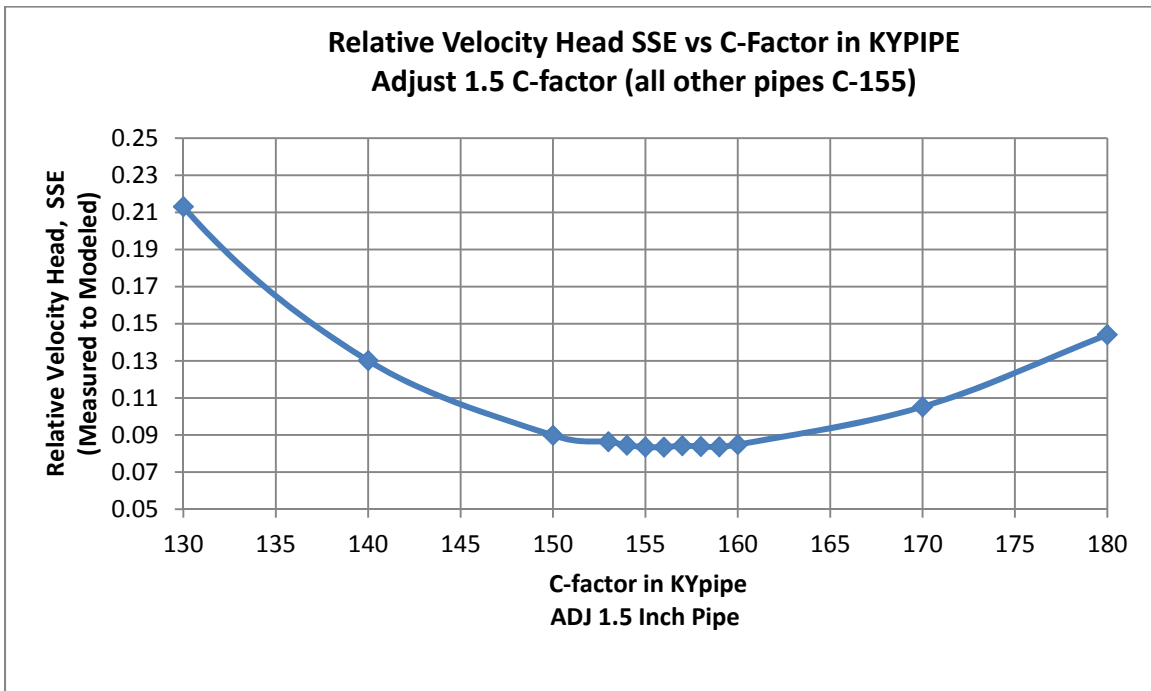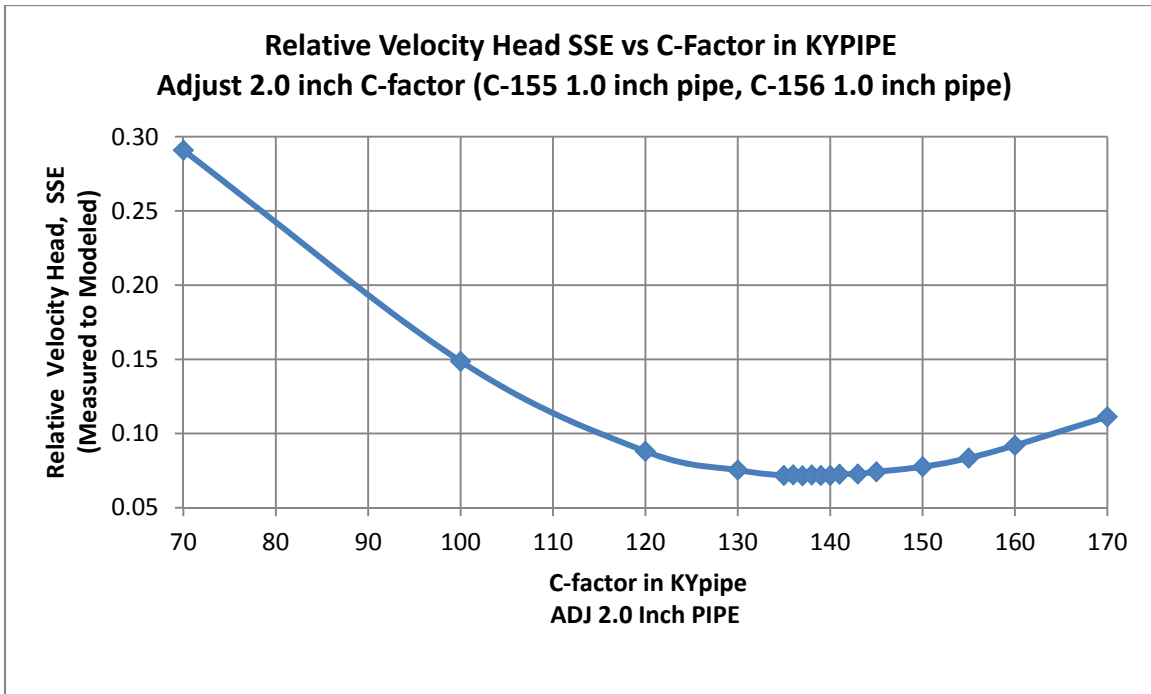Figure B.23: Case B energy head calibration, Iteration one, 1.5 pipe adjustment
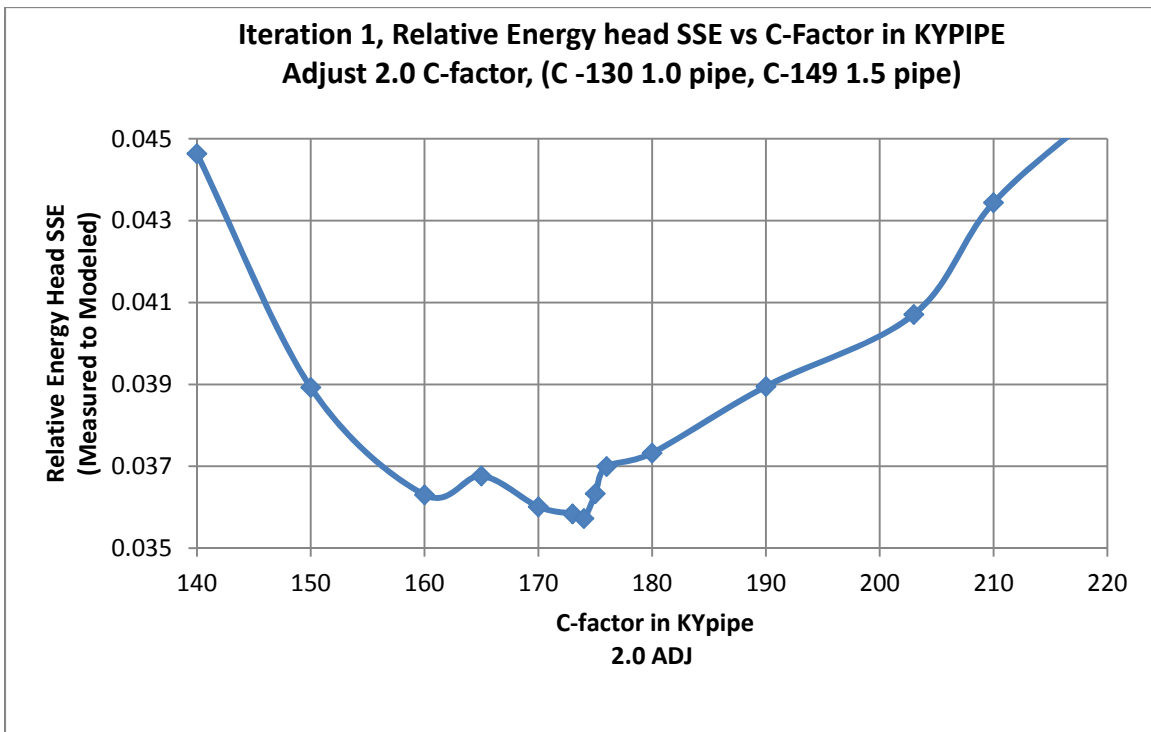
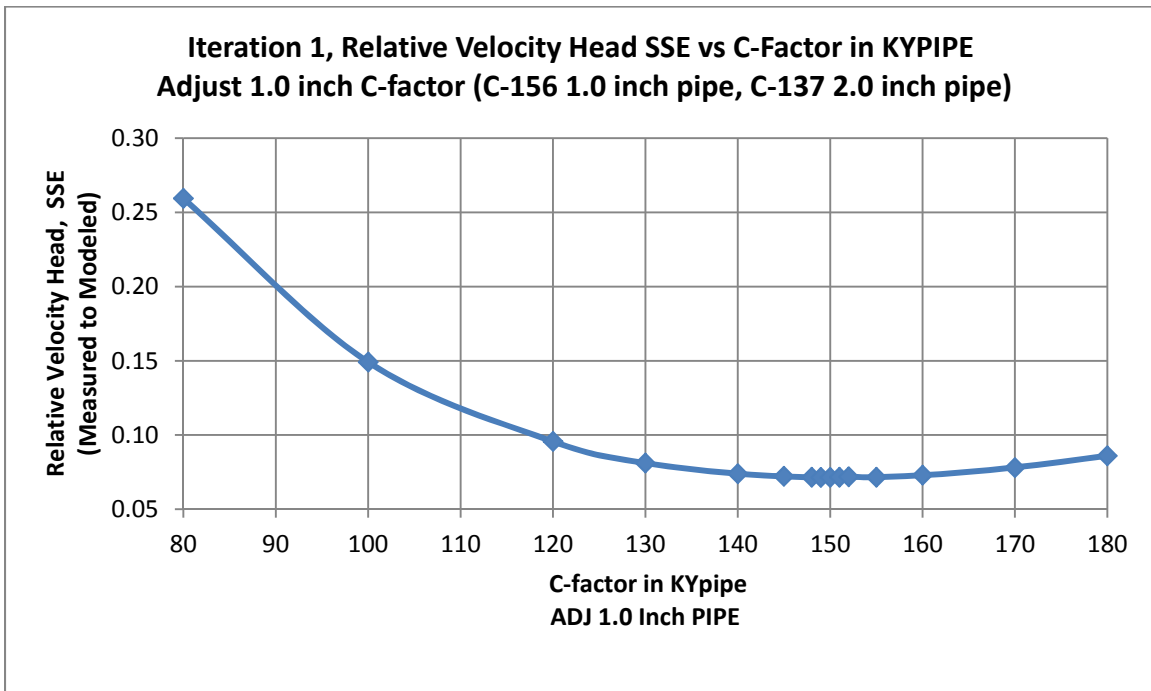Figure B.24: Case B energy head calibration, Iteration one, 2.0 pipe adjustment

Figure B.25: Case B energy head calibration, Iteration two, 1.0 pipe adjustment

Figure B.26: Case B energy head calibration, Iteration two, 1.5 pipe adjustment

Figure B.27: Case B energy head calibration, Iteration two, 2.0 pipe adjustment

Appendix C Case C calibration plots

Figure C.1: Case C pressure head calibration, universal adjust of all pipe sizes

Figure C.2: Case C pressure head calibration, 1.5 pipe adjustment

Figure C.3: Case C pressure head calibration, 2.0 pipe adjustment

Figure C.4: Case C pressure head calibration, 1.0 pipe adjustment
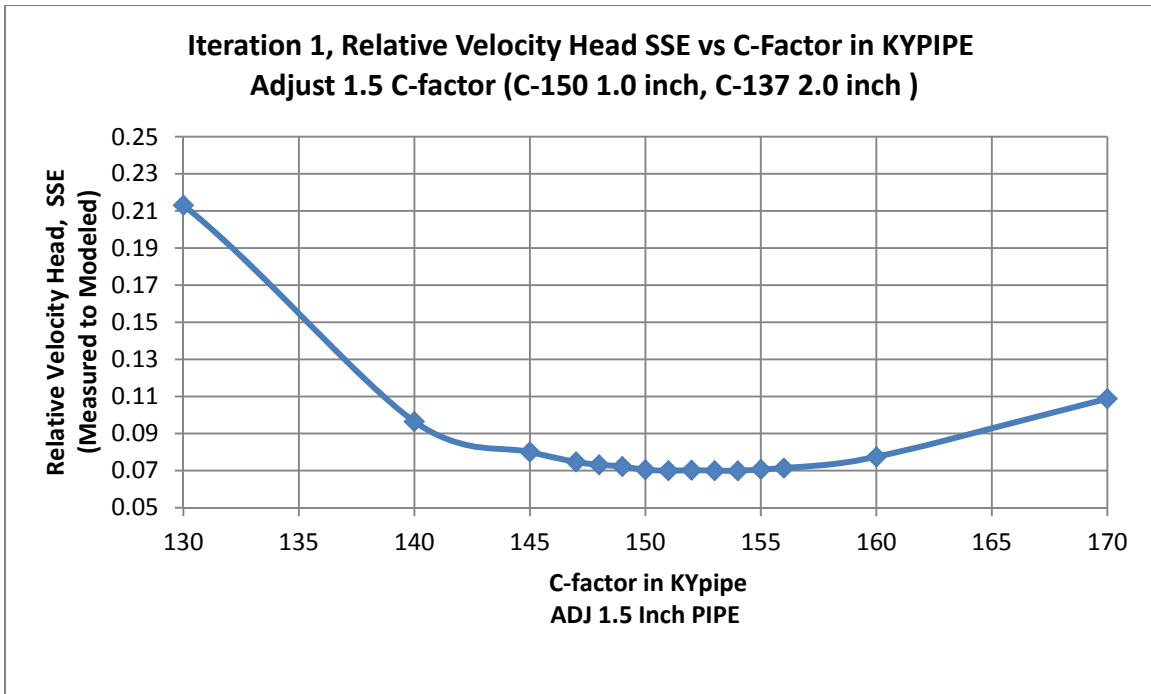
Figure C.5: Case C pressure head calibration, Iteration one, 1.5 pipe adjustment

Figure C.6: Case C pressure head calibration, Iteration one, 2.0 pipe adjustment

Figure C.7: Case C pressure head calibration, Iteration two, 1.0 pipe adjustment

Figure C.8: Case C velocity head calibration, universal pipe size adjustment

Figure C.9: Case C velocity head calibration, 1.5 pipe adjustment

100

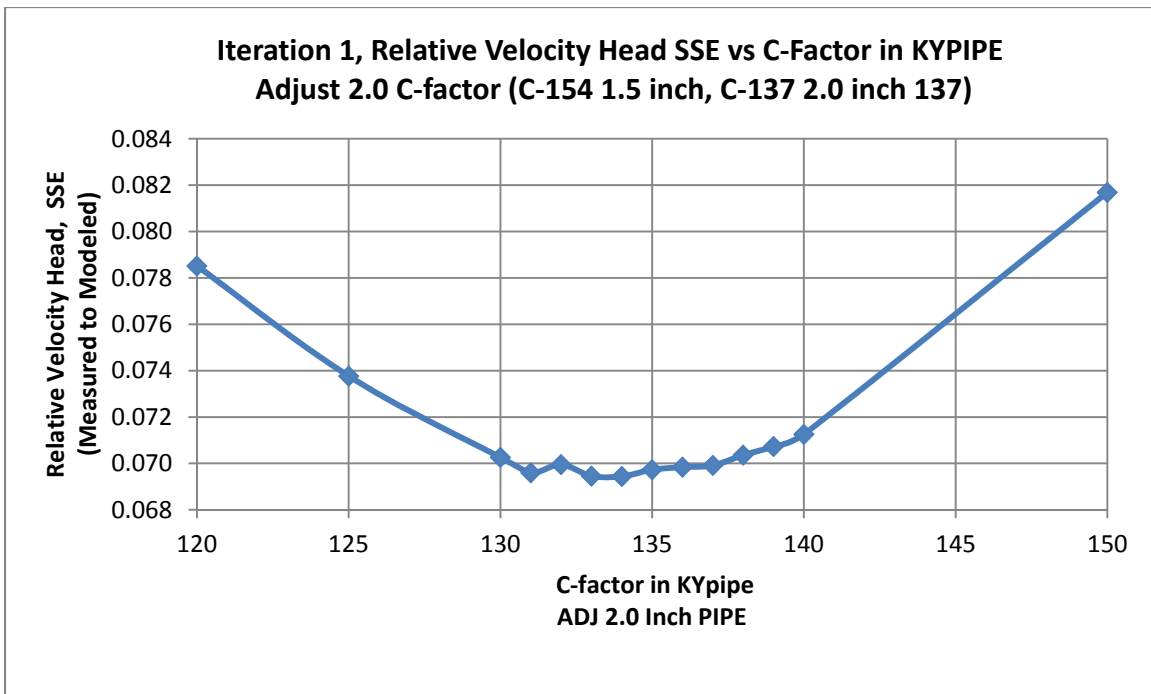Figure C.10: Case C velocity head calibration, 2.0 pipe adjustment

Figure C.11: Case C velocity head calibration, Iteration one, 1.0 pipe adjustment

101

Figure C.12: Case C velocity head calibration, Iteration one, 1.5 pipe adjustment

Figure C.13: Case C velocity head calibration, Iteration one, 2.0 pipe adjustment
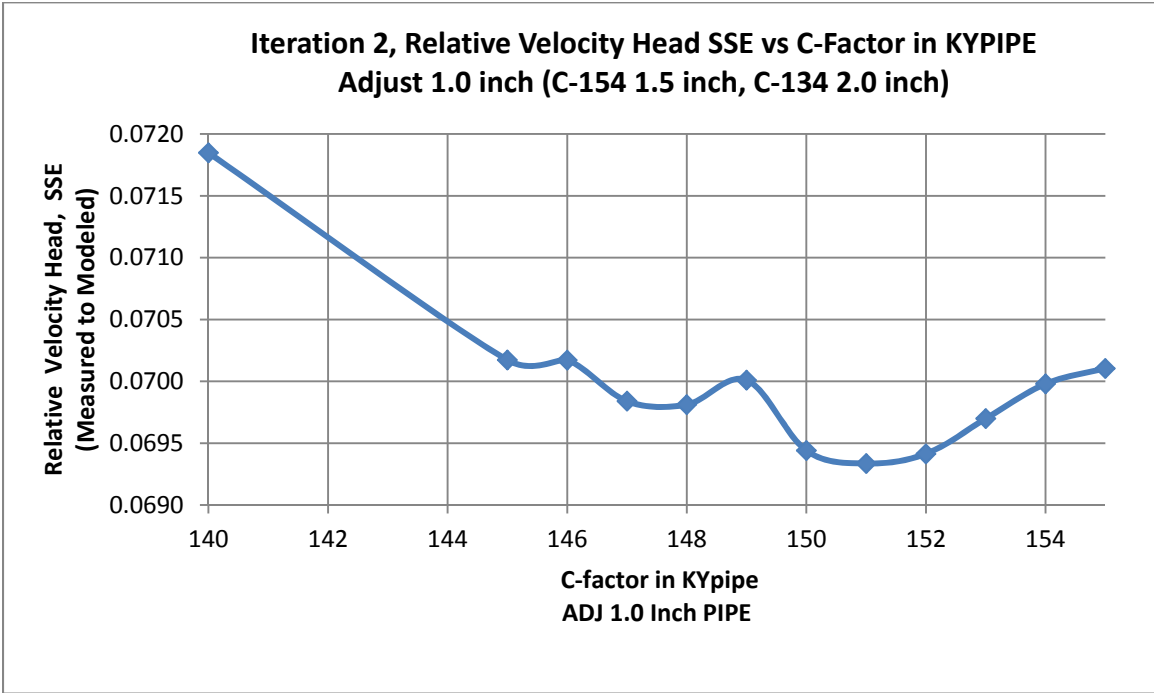
102

Figure C.14: Case C velocity head calibration, Iteration two, 1.0 pipe adjustment
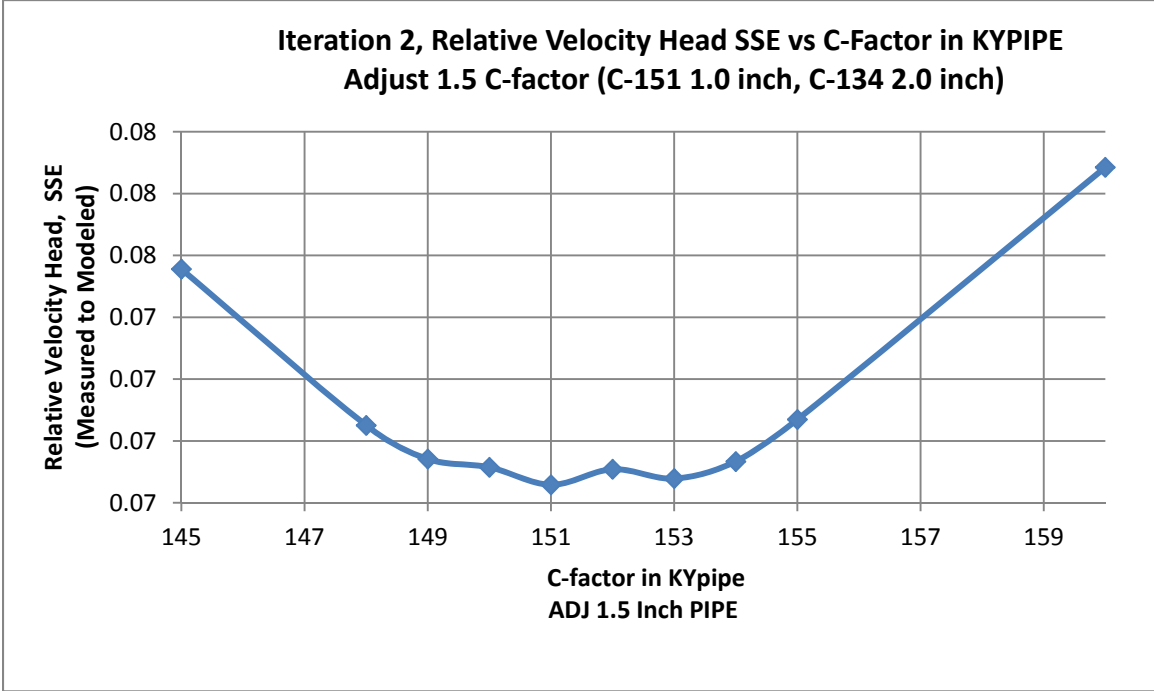

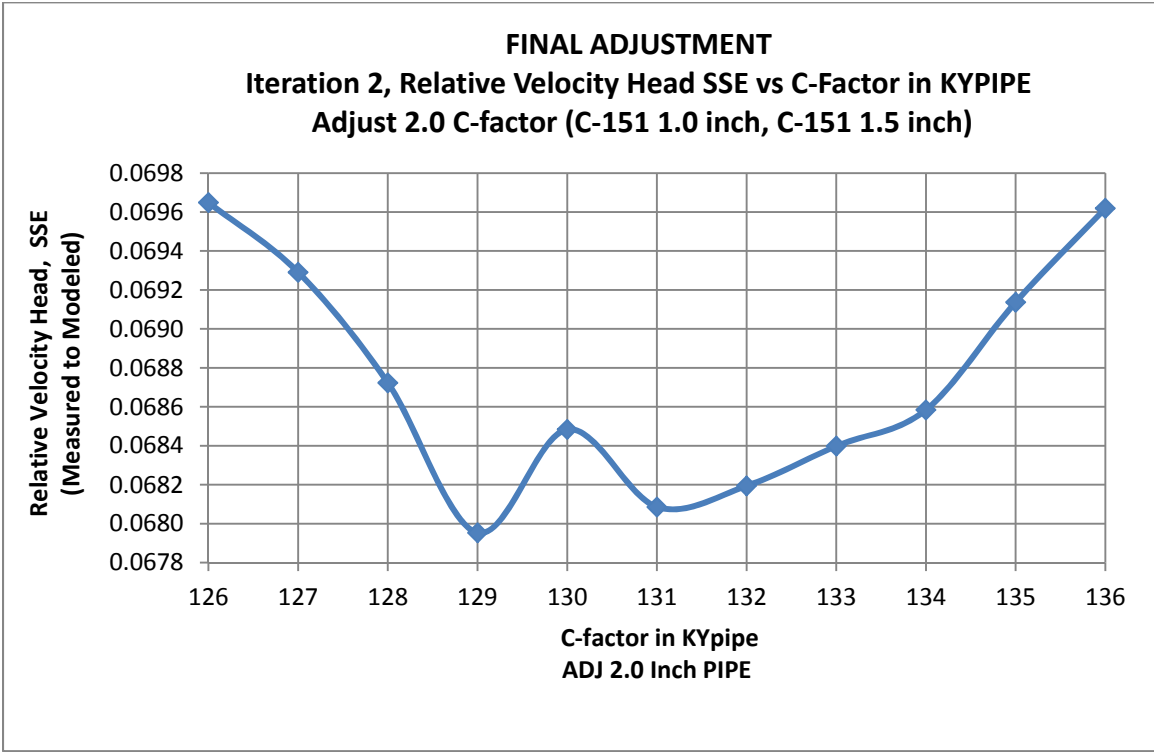Figure C.15: Case C velocity head calibration, Iteration two, 1.5 pipe adjustment

Figure C.16: Case C velocity head calibration, Iteration two, 2.0 pipe final adjustment
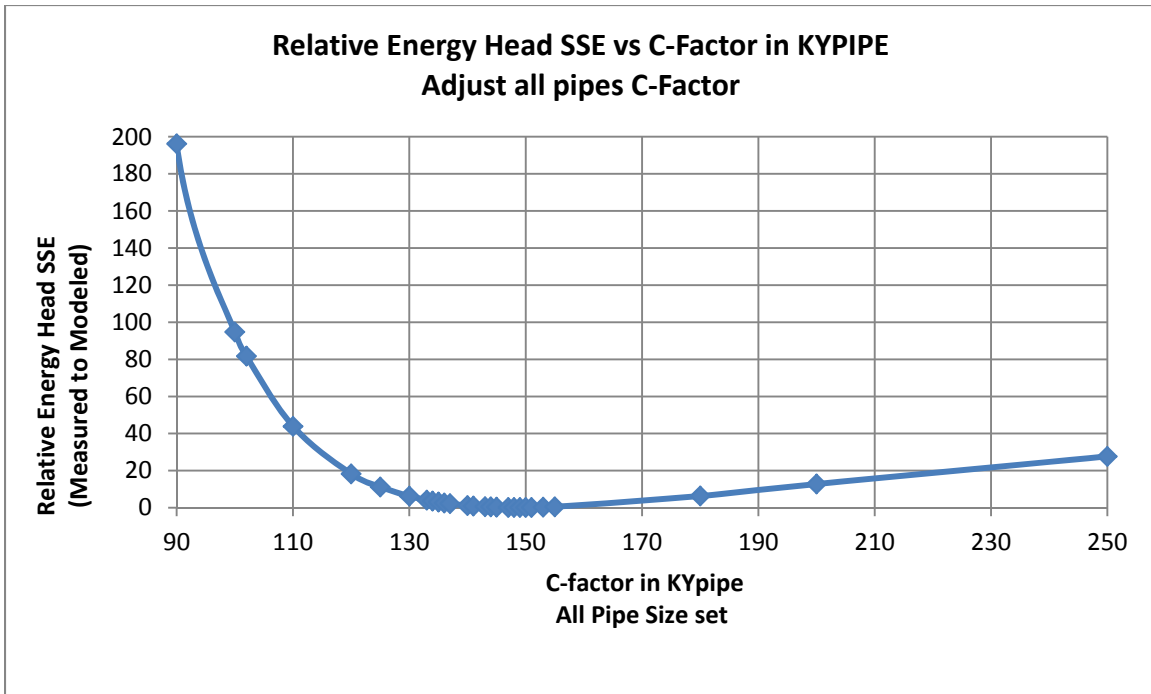
Figure C.17: Case C energy head calibration, universal pipe adjustment
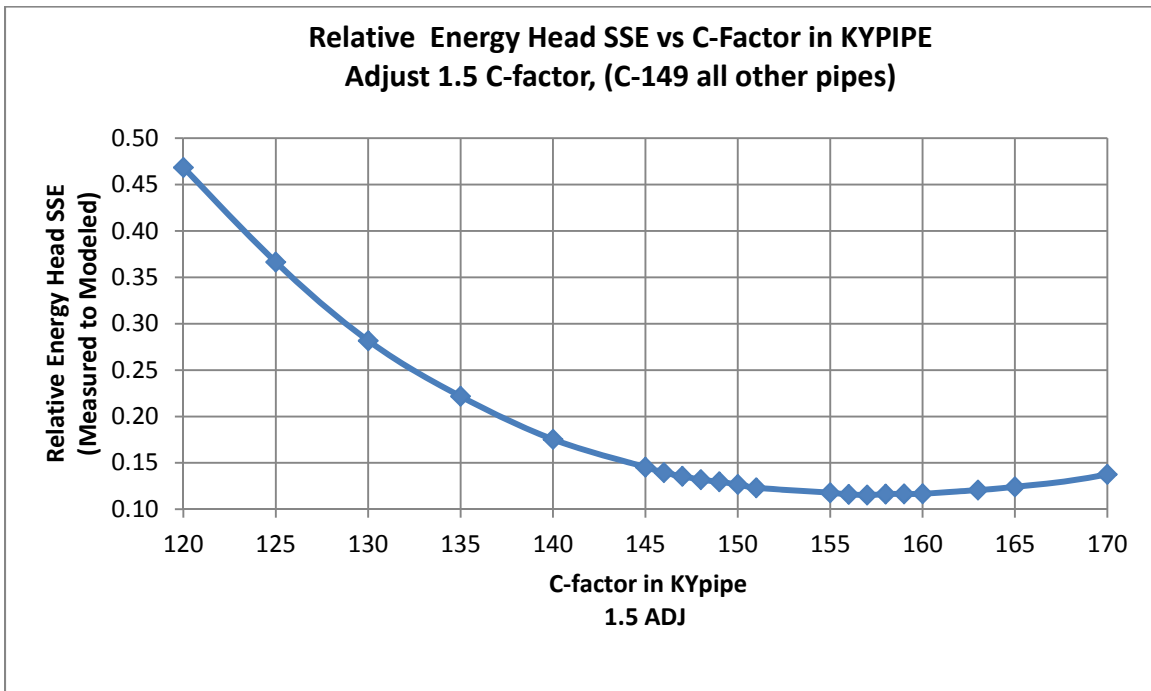

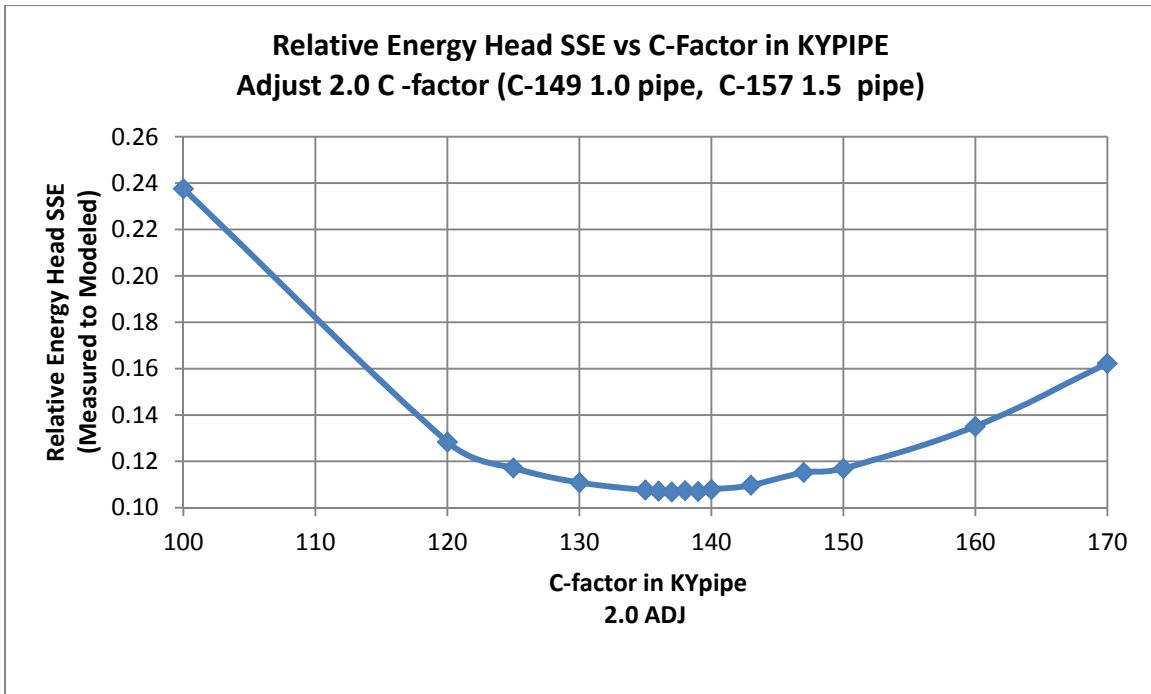Figure C.18: Case C energy head calibration, 1.5 pipe adjustment

Figure C.19: Case C energy head calibration, 2.0 pipe adjustment
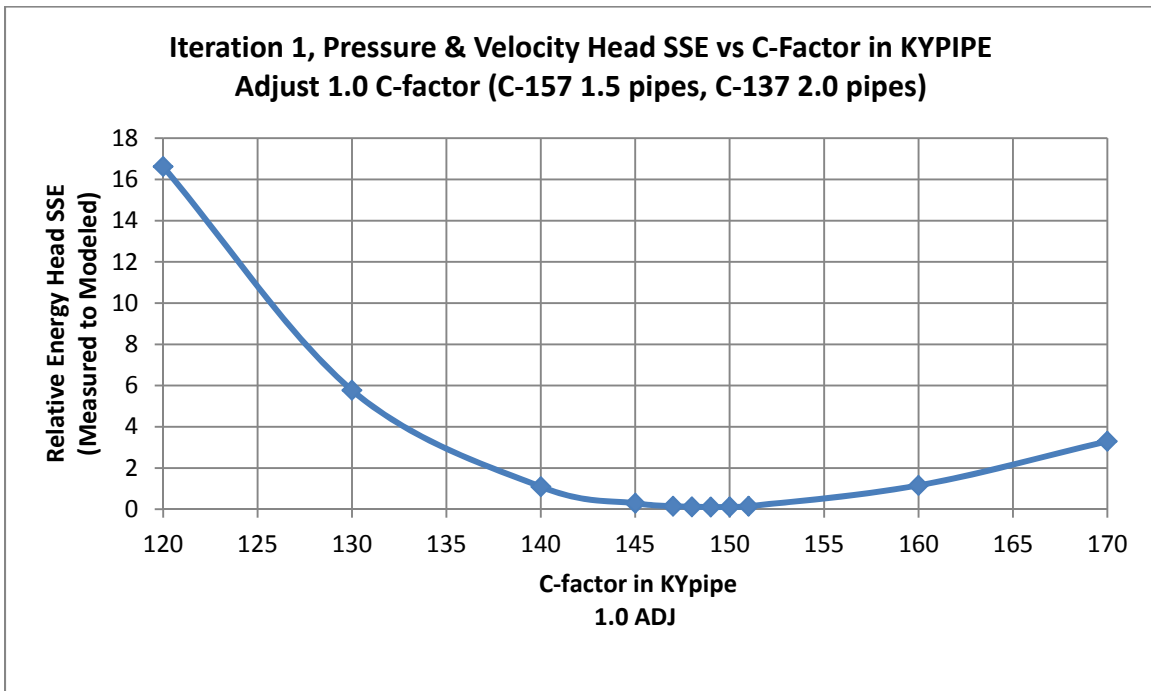

Figure C.20: Case C energy head calibration, Iteration one, 1.0 pipe
adjustment

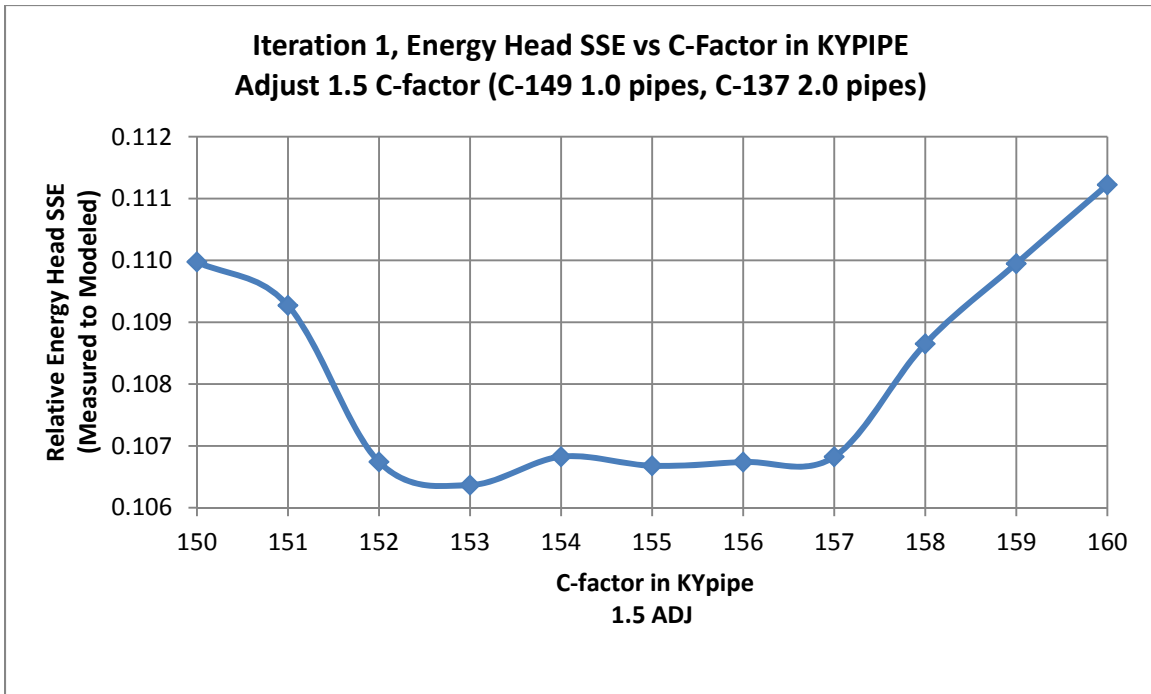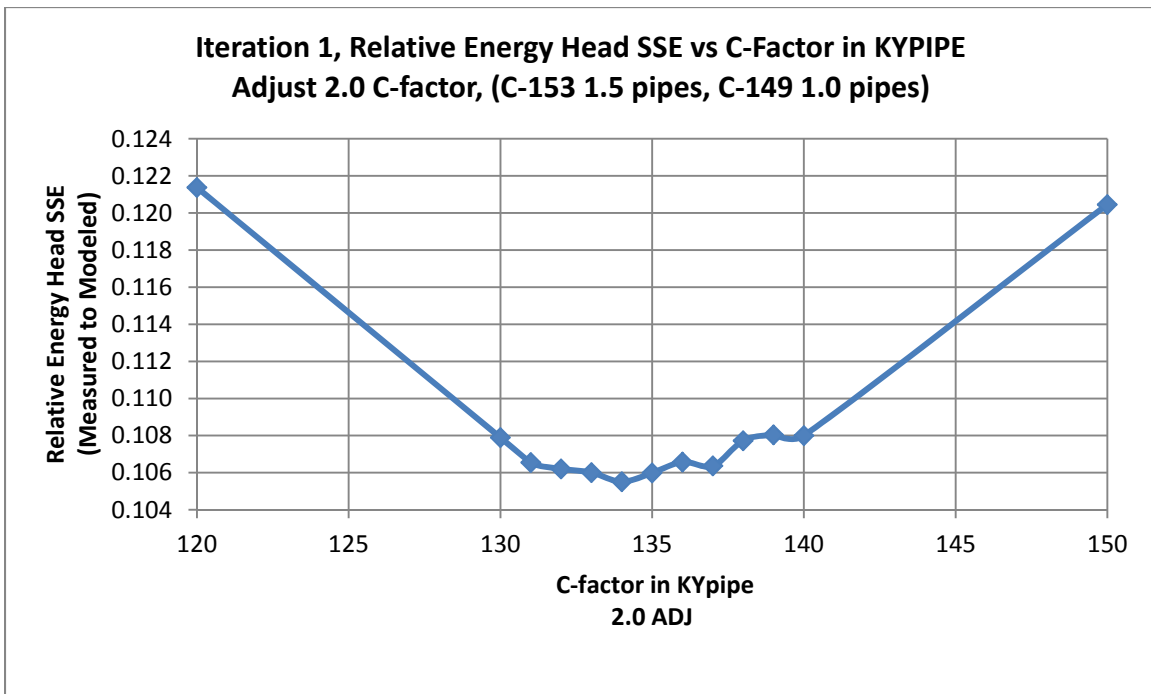Figure C.21: Case C energy head calibration, Iteration one, 1.5 pipe adjustment

Figure C.22: Case C energy head calibration, Iteration one, 2.0 pipe adjustment
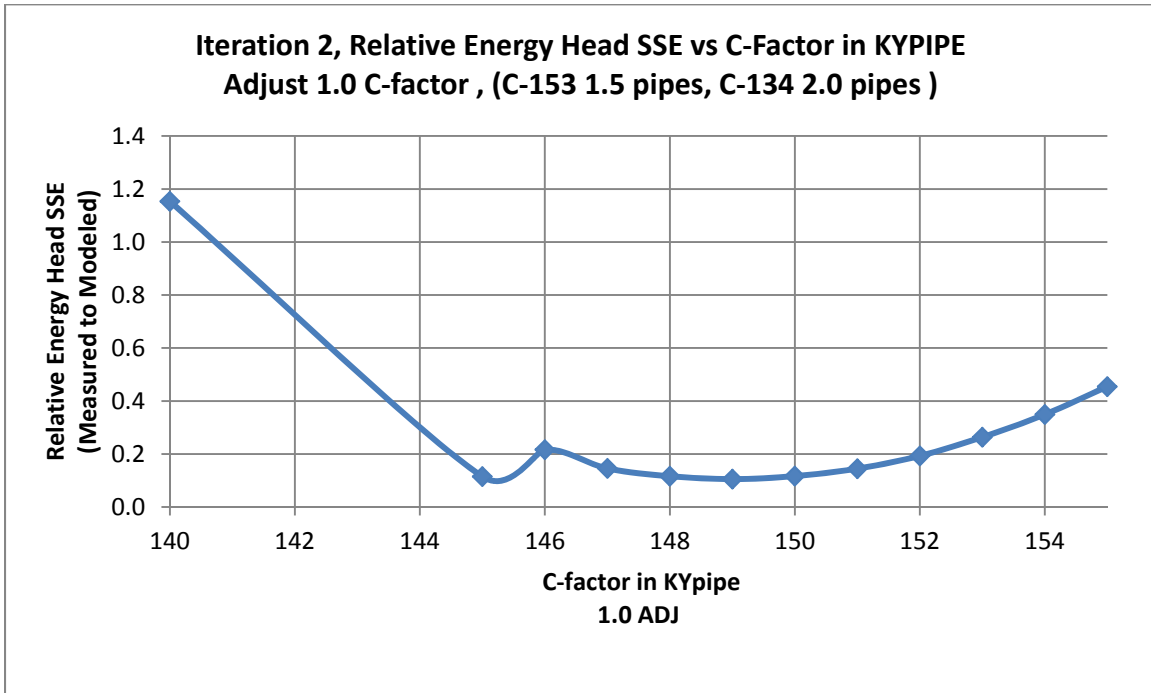
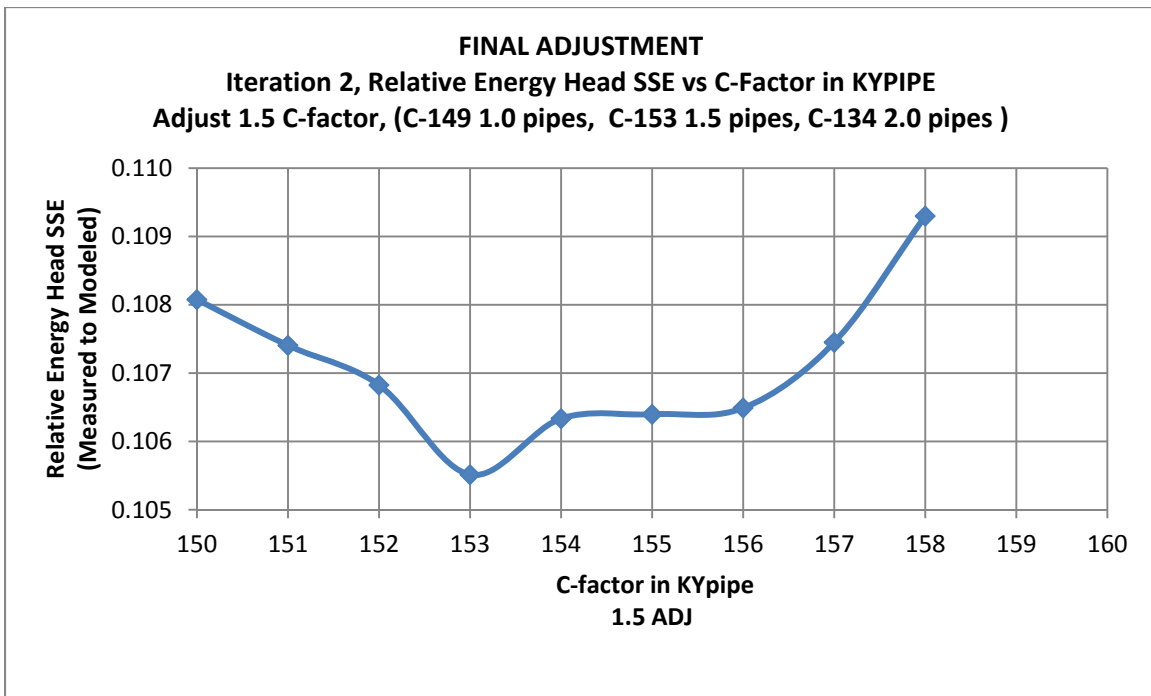Figure C.23: Case C energy head calibration, Iteration two, 1.0 pipe adjustment

Figure C.24: Case C energy head calibration, Iteration two, 1.5 pipe adjustment

108

Appendix D Measurement Average vs. Std Deviation Statistical testing

SUMMARY OUTPUT (IS Pressure STD DEV A FUNCTION OF PRESSURE Average, Test Hypothesis: Slope equal to zero?)

Regression Statistics	
Multiple R	0.794356497
R Square	0.631002244
Adjusted R Square	0.628590494
Standard Error	0.043479627
Observations	155

(IS STD DEV A FUNCTION OF PRESSURE, Test Hypothesis of Slope equal to zero?
No, using Fisher test   There is almost 0% significance that the slope between STD DEV of pressure measurement time series and the Average pressure measurement is zero. Therefore STD DEV of a pressure time series of measurement is a function of measured pressure average.

ANOVA

	df	SS	MS	F	Significance F
Regression	1	0.494618355	0.494618355	261.6366683	6.08921E-35
Residual	153	0.289243128	0.001890478		
Total	154	0.783861483			

	Coefficients	Standard Error	t Stat	P-value	Lower 95%	Upper 95%	Lower 95.0%	Upper 95.0%
Intercept	0.012621216	0.005589835	2.257887062	0.025367207	0.001577992	0.02366444	0.001577992	0.02366444
X Variable 1	0.013886704	0.000858519	16.17518681	6.08921E-35	0.012190623	0.015582786	0.012190623	0.015582786

SUMMARY OUTPUT	Test Hypothesis of Slope equal to zero)

(IS STD DEV A FUNCTION OF Flow AVG, Is Slope equal to zero?)
No, using Fisher test   There is almost 0% significance that the slope between STD DEV of flow measurement time series and the Average flow measurement for time series is zero. Therefore the STD DEV of a flow time series of measurement is a function of measured flow average.

Regression Statistics	
Multiple R	0.905224578
R Square	0.819431537
Adjusted R Square	0.817901296
Standard Error	0.13608567
Observations	120

ANOVA

	df	SS	MS	F	Significance F
Regression	1	9.916937435	9.916937435	535.491746	1.12047E-45
Residual	118	2.185278534	0.01851931		
Total	119	12.10221597			

	Coefficients	Standard Error	t Stat	P-value	Lower 95%	Upper 95%	Lower 95.0%	Upper 95.0%
Intercept	0.010477698	0.015961278	0.656444819	0.512816073	-0.021129978	0.042085375	0.021129978	-0.042085375
X Variable 1	0.015831106	0.000684124	23.14069459	1.12047E-45	0.014476354	0.017185858	0.014476354	0.017185858

References

American Water Works Association. (2005). *M32, Computer Modeling of Distribution Systems* (2nd ed.). (C. Stearns, Ed.)

Basha, & al., e. (2007, October 1). Eulerian-Lagrangian Method for Constituent Transport in Water Distribution Networks. *Journal of Hydraulic Engineering, 133*(10).

Biology Online. (2008, June 17). *http://www.biology-online.org/dictionary/Diffusion*. Retrieved 4 29, 2013, from Biology Online: http://www.biology-online.org/dictionary/Diffusion

Dielman. (2005). *Applied Regression Analysis* (4th ed., Vol. 1). (A. D. al, Ed.) Mason, OH, USA: South-Western.

Farlex. (2013). *Free dictionary*. Retrieved 4 29, 2013, from Free dictionary: http://www.thefreedictionary.com/convection

Greco, & Guidice. (1999, August 1). "New Approach to Water Distribution Network Calibration". *Journal of Hydraulic Engineering, 125*(8), 849-854.

Gupta. (2008). *Hydrology and Hydraulic Systems, Third Edition* (Vol. 1). Long Grove, Illnois, United States of America: Waveland Press, Inc.

HAESTAD METHODS. (2001). *Water Distribution Modeling* (1st ed., Vol. 1). (A. Strafaci, Ed.) Waterbury, CT, U.S.A.: HAESTAD METHODS, INC.

Iglesias, Mora, Martinezr, & Fuertes. (2007). "Study of Sensitivity of the parameters of a genetic algorithm for design of water distribution networks". *Journal of Urban and Environmental Engineering, 1*(2), 61-69.

Kapelan, Savic, & Walters. (2005, March 1). "Optimal Sampling Design Methodologies for Water Distribution Model Calibration". *Journal of Hydraulic Engineering, 131*(3), 190-200.

Kapelan, Savic, & Walters. (2007, August 1). "Calibration of Water Distribution Hydraulic Models Using a Bayesian-Type Procedure". *Journal of Hydraulic Engineering, 133*(8), 927-936.

Lansey, & al, e. (1991). "Parameter Estimation for Water Distribution Networks". *Journal of Water Resources Planning & Management, 117*(1), 126-144.

Lansey, El-Shorbagy, Araujo, & Haan. (2001, April). "Calibration Assessment and Data Collection for Water Distribution Networks". *Journal of Hydraulic Engineering, 127*(4), 270-279.

Mays, L. W. (2011). *Water Resources Engineering* (2nd ed., Vol. 1). (A. S. Jenny Welter, Ed.) Hoboken, New Jersey, United States of America: John Wiley & Sons.

Munson, e. a. (2009). *Fundamentals of Fluid Mechanics* (Sixth Edition ed., Vol. 1). (M. O. Jennifer Welter, Ed.) Hoboken, New Jersey, United States of America: John Wiley & Sons, Inc.

Ormsbee, & al, e. (1989). "Implicit Network calibration". *Journal of Water Resources Planning and Management, 115*(2), 243-257.

Ormsbee, & Lingireddy. (1997). "Calibrating hydraulilc network models". *Journal of the American Water Works Association, 89*(2).

Ormsbee, & Wood. (1986). "Explicit Pipe Network Calibration". *Journal Resources Planning Management, 112*(2), 166-182.

Shanmugam, Narasimham, & et-al. (2010). "Parameter Estimation in Water Distribution Networks". *Water Resources Management, 24*, 1251-1272.

Tabesh, Jamasb, & Moeini. (2011, April). "Calibration of water distribution hydraulic models: A comparision between pressure dependent and demand driven analyses". *Urban Water Journal, 8*(2/3), 93-102.

Uber, & Bush. (1998, November/December). "Sampling Design Methods for Water Distribution Model Calibration". *Journal of Water Resources Planning and Management*, 334-344.

Walski. (1983). "Technique for calibrating network model". *Journal of Water Resources Planning & Management, 109*(4), 360-372.

Walski. (2000, January 1). "Model calibration data: the good, the bad, and the useless". (M. L. (Managing), Ed.) *Journal of the American Water Works Association, 92*(1), 94-99.

Walters, Savic, & Godfrey. (1997, 3). "Genetic Algorithims for Least-Cost Design of Water Distribution Networks". *Journal of Water Resources Planning and Management, 123*(2), 67-77.

Yoo, Chang, & Jun. (2012, January 19). "Optimization of pressure gauge locations using entropy theory". *Environmental Monitering Assessment, 184*(1), 7309-7322.

Zheng Y. Wu, C. C. (2009, April 18). "Evolving Effective Hydraulic Model for Muncipal Water Systems". *Water Resources Management, 23*, 117-136.

Vita

Place of Birth: Madisonville, KY

Education: BSCE, Dec 2002

Professional positions:

Graduate Engineering Assistant, KY Transportation Cabinet, (1/07/2003 to 6/30/2003)

Engineer in Training I, KY Transportation Cabinet, (6/30/2003 to 3/15/2005)

Engineer in Training II, KY Transportation Cabinet, (3/15/2005 to 3/15/2008)

Transportation Engineer I, KY Transportation Cabinet, (03/15/2008 to 05/15/2010)

Research Assistant/Teaching Assistant, University of Kentucky, (05/01/2011 to 05/01/2013)

Professional & Scholastic Honors:

Raymond Fellowship (8/15/2011 to 05/01/2012)

Research Assistantship (08/15/2011 to 05/01/2013)

Engineering in Training certification, Commonwealth of Kentucky

Professional Publications:

Presentation at 05/2012 EWRI Water Resources Conference, Albuquerque NM

Presentation at 05/2013 EWRI Water Resources Conference, Cincinnati OH

Typed name of Student: Robert "Craig" Ashby